From stable isotopes in the environment to process understanding:

Exploring nitrate sinks and sources in the Baltic Sea

Dissertation

zur

Erlangung des akademischen Grades

doctor rerum naturalium (Dr. rer. nat)

der Mathematisch-Naturwissenschaftlichen Fakultät

der Universität Rostock

vorgelegt von

Claudia Frey,

geb. am 17.04.1985 in Leipzig

Rostock 2014

Universität Rostock Traditio et Innovatio

Leibniz Institute for Baltic Sea Research Warnemünde

urn:nbn:de:gbv:28-diss2015-0073-7

Day of submission: 15.12.2014
Day of public defense: 17.04.2015

Doctoral committee:

1. Referee: PD Dr. Maren Voss
   Leibniz Institute for Baltic Sea Research Warnemuende
2. Referee: Prof. Dr. Heide Schulz-Vogt
   Leibniz Institute for Baltic Sea Research Warnemuende

Table of contents

Summary

The increase in anthropogenic nitrogen (N) emissions into the environment has led to serious eutrophication in marine ecosystems, with increasing oxygen-deficient zones and the frequent occurrence of harmful algal blooms. The Baltic Sea, one of the world's largest brackish water bodies, has been subject to intense eutrophication and oxygen deficiency (Hypoxia) in the central basins. Hypoxia is also spreading in coastal zones and leads to death ofmarine life but also to a reduced capacity to remove N which may even intensify eutrophication. The Baltic Sea receives large N loads by rivers from its drainage area, but to which extent they influences different regions is unclear. Hence, my first aim was to identify major nitrate source in different regions of the Baltic Sea by analyzing dual stable isotopes in nitrate in the winter surface waters in combination with a Bayesian mixing model. In winter, at very low temperatures, internal turnover processes play a minor role and the isotopic signature in nitrate can be used to identify nitrate sources. While rivers and the coastal regions of the Baltic Sea are exposed to anthropogenic N, in the sea's central basins the main N source is N_2 fixation. The central Baltic Sea also contains hot spots for the development of hypoxia, which drives N loss, this process is investigated in the second part of this thesis. Because no N is removed during anoxia and ammonium accumulates, the oxic-anoxic interface (redoxcline) is characterized by high microbial turnover and by N loss. Rates of N loss processes, like denitrification were identified using the natural dual stable isotope composition of nitrate together with a numerical reaction-diffusion model. Isotopes can be used to estimate N loss because they provide a signal that integrates processes both in time and in space. In the hypoxic zone occurs not only N loss by denitrification but also internal recycling processes, such as nitrification. Half of the denitrified nitrate comes from nitrification, and the other half is from diffusion along the concentration gradient into the denitrifying zone. Previous studies identified a key microbial player, *Sulfurimonas gotlandica*, belonging to the *Epsilonproteobacteria*, as a major denitrifier. Hence, identifying the impact of *S. gotlandica*on the isotopic signature in nitrate in laboratory studies will facilitate the interpretation of field data. Denitrification in the Baltic Sea is driven by hydrogen sulfide (chemolithoautotrophic denitrification) rather than by organic matter as in oxygen-deficient zonesin the open ocean. The third aim of this thesis was to identify the isotope fractionation of N and O in nitrate that arises by chemolithoautotrophic denitrification. The results revealed that N isotope fractionation was consistentwith heterotrophic denitrification, but the 1:1 ratio of $\delta^{18}O$ to $\delta^{15}N$ typical for heterotrophic denitrification was not confirmed. This difference can be attributed to the different enzymes used; in our study bacterial nitrate reduction was carried out by the periplasmic nitrate reductase and not by the membrane bound nitrate reductase. The enzyme dependence of the baseline ratio for denitrification may have profound consequences for interpreting dual stable isotope values in nitrate, particularly in stratified systems where chemolithoautotrophic denitrification is the dominat N loss

pathway. Given the global expansion of oxygen-deficient zones a better understanding of N loss, such as provided herein, is needed.

Zusammenfassung

Eutrophierung in küstennahen, aquatischen Ökosystemen führt immer häufiger zum Auftreten von Algenblüten und zu Sauerstoffmangel im bodennahen Wasser durch den Abbau des organischen Materials. Auch die Ostsee, eines der größten Brackwassermeere der Welt, leidet unter Eutrophierung und der zunehmenden Sauerstoffarmut in den tiefen Becken. Dieses sich nun auch küstennah ausbreitende Phänomen führt nicht nur zum Absterben der Fauna,sondern auch zur verringerten Kapazität des Ökosystems Stickstoff zu entfernen, wodurch Eutrophierung noch verstärkt werden könnte. Durch die dichte Besiedlung des Einzuggebietes und dessen starke landwirtschaftliche Nutzung gelangen großen Stickstofffrachten in die Ostee. Inwieweit diese Frachten verschiedene Regionen beeinflussen, ist schwierig zu bestimmen.Deshalb befasst sich die erste Studie dieser Arbeit mit der Identifizierung von Stickstoffquellen in die Ostsee, anhand der natürlichen Isotopenverhältnissen von Stickstoff und Sauerstoff im Nitrat in Verbindung mit einem Bayesian Mischungsmodel. Aufgrund der niedrigen Temperaturen im Winter spielen interne Stoffumsetzungsprozesse keine Rolle und die Isotopensignatur im Nitrat kann dazu genutzt werden verschiedene Quellen zu identifizieren. Dabei konnte gezeigt werden, dass hauptsächlich die Küsten unter dem anthropogen eingetragenen Stickstoff leiden und dass die Hauptstickstoffquelle in der zentralen Ostsee die Stickstofffixierung darstellt. In diesen zentralen Bereichen der Ostsee,mit Sauerstoffarmut in den tiefen Becken, ist der Stickstoffumsatz entscheidend beeinflusst, welches Gegenstand des zweiten Kapitels ist. Während in anoxischen Wassersschichten keinerlei Stickstoff entfernt werden kann und sich Ammonium als Abbauprodukt akkumuliert, findet in der oxisch-anoxischen Grenzschicht ein vermehrter Stickstoffverlust statt. Um die Prozesse zu identifizieren und Raten der Stickstoffentfernung zu bestimmen, wurden die stabilen Isotope im Nitrat zur Hilfe genommen und ein numerisches Reaktion-Diffusions Modell angewendet. Stabile Isotope sind ein zeitlich integriertes Signal verschiedener Umwandlungsprozesse,wodurch Abschätzungen über Stickstoffverluste, wie Denitrifizierung angestellt werden können. Meine Studie zeigte, dass nicht nur reduktive Prozesse, die zur Entfernung von Stickstoff führen, an der Grenzschicht eine Rolle spielen sondern gleichzeitig interne Recycling- Prozesse, vorallem Nitrifizierung. Dies führt dazu, dass die Hälfte des denitrifizerten Nitrats aus der Nitrifzierung und die andere Hälfte des Nitrats aus der Diffusion entlang des Nitratgradienten stammt. In der oxisch-anoxischen Grenzschichtist die Diversität der Organsimen gering und der Hauptdenitrifizierer ist das*EpsilonproteobacteriumSulfurimonas gotlandica*. Mit der Bestimmung seines Einflusses auf die Isotopensignatur im Nitrat ist es möglich die natürlichen Isotopensignaturen zu charakterisieren. Die Besonderheit in der Ostsee liegt darin, dass Denitrifizierung nicht wie im offenen Ozean durch organisches Material angetrieben wird, sondern anorganisch durch Schwefelwasserstoff (chemolithoautotrophe Denitrifizierung). In dieser Arbeit konnte gezeigt werden, dass

sich die Stickstofffraktionierung im Nitrat nicht von der Fraktionierung der heterotrophen Denitrifizierung unterscheiden lässt.Allerdings konnte das für heterotrophe Denitrifizierung typische Verhältnis zwischen Sauerstoff- und Stickstoffisotopen von 1:1nicht bestätigt werden. Ursache hierfür ist, dass die Denitrifizierung von einer periplasmatischen Nitratreduktase und nicht von einer membrangebunden Nitratereduktase durchgeführt wird. Nicht nur in der Ostsee ist es von Bedeutung den Einfluss der chemolithoautotrophen Denitrifizierung auf die Isotopensignatur im Nitrat identifizieren zu können, sondern auch in anderen stratifizierten Gewässern. Besonders in Hinblick auf die Ausbreitung von Sausteroffmangelzonen ist es wichtig deren Einfluss auf den Stickstoffkreislauf zu verstehen.

Introduction

Framework

This PhD thesis was part of the EU BONUS+ project HYPER (HYPoxia mitigation for Baltic Sea Ecosystem Restoration). The project joins seven institutes from seven different countries around the Baltic Sea exploring the concept "understanding the past to model the present and predict the future". Hypoxia has been present in the Baltic Sea since its formation ca. 8000 cal yr BP (Conley et al., 2009), but the spatial extent and the intensity of hypoxia in the water column increased tremendously during the twentieth century due to intense anthropogenic nutrient loading(Osterblom et al., 2007; Gustafsson, 2012). Hypoxia has resulted in the elimination of benthic fauna and, by acting as an internal feedback that increases the P flux from sediments into overlying water (Conley et al., 2002), has enhanced the effects of eutrophication (Conley et al., 2009). Although excessive nutrient inputs are the direct cause of the reduced health of the Baltic Sea ecosytsem, understanding is the key to its recovery from eutrophication. Hence, HYPER investigates the causes and impacts of hypoxia in the Baltic Sea to establish a sound scientific basis for nutrient management and thereby achieve a reduction in hypoxia. The results thus far have provided quantitative knowledge of the changes in sediment function, specially, that with worsening hypoxia N removal is replaced by nitrogen release as ammonium (Jäntti and Hietanen, 2012), and important ecosystem services carried out by benthic fauna are lost (Carstensen et al., 2014).

The focus of this PhD thesis reserach within HYPER was the influence of hypoxia on the nitrogen cycle in the water column. N turnover in the hypoxic zone of the Baltic Sea is investigated in the second chapter. The role of denitrification carried out by a key microbial player on N loss from the Baltic Sea redoxcline is examined in the third chapter.

Human alteration of the N cycle

Over the past several decades humans have created more reactive nitrogen than generated by natural processes, which has caused considerable alterations in nitrogen cycling in marine environments (Canfield, 2010; Gruber and Galloway, 2008). Today,

40% of the world's oceans are strongly impacted by human activities (Halpern et al., 2008). The production of synthetic nitrogen fertilizers from N_2 (Haber Bosch process) and the burning of fossil fuels have dramatically increased the amount of reactive nitrogen in the environment(Galloway et al., 2003). Most of the nitrogen applied to the terrestrial ecosystem enters coastal zones and oceans via rivers (Gruber and Galloway, 2008). Increased nutrient runoffs lead to the accumulation of reactive nitrogen in the marine environment and cause severe environmental disturbances. The consequences are a series of ecosystem changes, including eutrophication, an increase in the occurrence of harmful algal blooms, hypoxia (low oxygen) or anoxia (no oxygen), changes in food-web structure, and habitat degradation (Galloway et al., 2003; Diaz and Rosenberg, 2008; Conley et al., 2011). Coastal regions and enclosed or semi-enclosed seas with a high human population density and high activity in their watersheds are especially prone to eutrophication (Peierls et al., 1991; Rabalais, 2002; Selman et al., 2008).

The marine N cycle

Nitrogen is a major constituent of life and thus essential in the growth and metabolism of all organisms. Several interacting processes form the N cycle (Figure 1). Nitrate is the most highly oxidized N species in the marine environment and it plays a significant role in regulating primary production. Dinitrogen is the most abundant chemical form of N on earth (78% of air), but this N pool is only available for a specific group of bacteria, the diazotrophs, which fix atmospheric nitrogen to yield NH_3 or organic nitrogen. Diazotrophs are scattered among bacteria and archaea, with *Trichodesmium* being the most abundant filamentous diazotrophic cyanobacteria in the marine pelagic environment (Carpenter and Romans, 1991).The inorganic forms of reactive nitrogen can be assimilated into organic nitrogen. When organisms die, their organic nitrogen is remineralized to ammonium and reconverted to nitrate via nitrification. Nitrification is a two-step microbial process in which ammonium is oxidized to nitrite and nitrite then to nitrate. Most nitrification occurs aerobically. Thus,under oxic conditions, nitrate is assimilated by bacteria or phytoplankton, but under anoxic conditions nitrate becomes a favorable electron acceptor and is reduced to ammonium

(dissimilatory nitrate reduction to ammonium, DNRA) or to N_2 gas (denitrification and anammox).

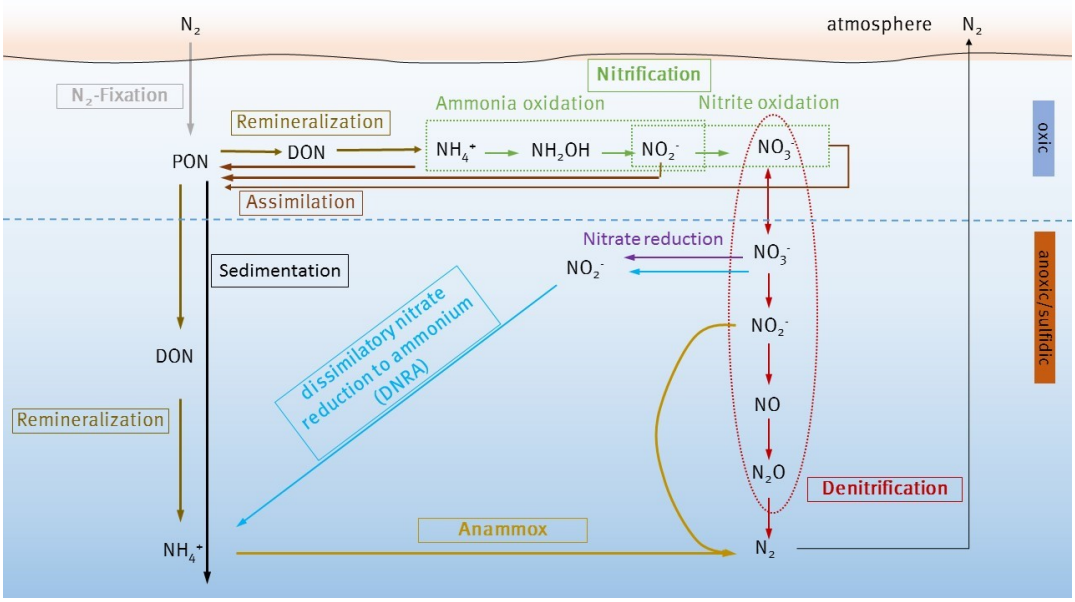

Figure 1: Microbial nitrogen transformations in the marine environment. PON- particulate organic matter, including phytoplankton; DON-dissolved organic matter.

Denitrification and anammox are oxygen sensitive. Denitrification refers to a sequence of reactions in which nitrate is reduced to gaseous products, i.e., NO, N_2O, or N_2, via NO_2^-. Each step requires a different enzyme, whose activity is tailored to the varying oxygen concentrations (Zumft, 1997). While heterotrophic denitrification uses organic matter as the substrate, its chemolithoautotrophic counterpart uses hydrogen sulfide. Anammox bacteria are sensitive to hydrogen sulfide; hence their activity is mainly found in stable redox gradients (Lam and Kuypers, 2011).

In recent years, the combined use of rate measurements, molecular analysis of active microbial groups, and model approaches has changed our understanding of the controls and pathways responsible for nitrogen loss in the ocean. While denitrification occurs patchily in time and space, depending on the supply of organic matter, anammox is slow and steady but dependent on DNRA or denitrification for the supply of dissolved inorganic nitrogen (DIN)(Dalsgaard et al., 2012; Ward, 2013). The overall N loss depends on the amount of organic matter, andthe ratio of denitrification versus anammox on the C:N ratio of the available organic matter (Ward, 2013; Babbin et al., 2014). The remineralization of organic matter with an average C:N ratio of 6.6 can support ~30%

anammox from total N loss. A lower C:N ratio (more N relative to C content) results in higher proportions of anammox from total N loss (Babbin et al., 2014).

The discovery of a link between the N cycle and the sulfur cycle, also known as the "cryptic sulfur cycle", complicates the view of organic matter as the sole driver of N-loss in the open ocean (Canfield et al., 2010). The same applies to sulfidic water columns, where a link between hydrogen sulfide oxidation and denitrification was suggested in 1991 (Brettar and Rheinheimer, 1991) and eventually confirmed(Fuchsman et al., 2012; Bruckner et al., 2013; Wenk et al., 2014). This unique N loss pathway may play a more important role in marine nitrogen balance than previously thought.

The marine N balance

N enters the ocean by nitrogen fixation and is removed from the marine ecosystem by denitrification and anammox. The balance of the oceanic nitrogen budget is unclear (Table 1) but clearly acts as a crucial control of the ocean's potential to sequester atmospheric CO_2 via the marine biological pump.

Table 1: Sources and sinks in the global marine nitrogen budget

Process	Tg N year^{-1}	Process	Tg N year^{-1}
sources		*sinks*	
Pelagic N_2 fixation	110[a] – 170[f]	Water column denitrification	80[a] – 240[e]/400[g]
Benthic N_2 fixation	15[c]	Sedimentary denitrification	95[a] - 285[d]
River input	25[b] - 76[a]/80[e, 1]	Sedimentation	25[a,e]
Atmospheric deposition	10[e] - 30[a]/50[e, 1]	N_2O loss	4[e]
Total sources	160 - 475	*Total sinks*	204 - 389

[a] Gruber and Sarmiento, (1997), [b] Brandes and Devol, (2002), [c] Capone (1988), [d] Middelburg et al., (2010), [e] Gruber and Galloway, (2008) – [1]with human impact, [f] Großkopf et al., 2012, [g]Codispoti 2007

Estimates for the global oceanic N budget range from arough balance between sources and sinks (Gruber et al., 1997; Eugster and Gruber, 2012) to a rather large net deficit of between 140 and 234 Tg N yr^{-1}(Galloway et al., 2004; Codispoti, 2007). In marine

systems, cyanobacteria are capable of fixing 110 – 177 Tg N yr^{-1}(Gruber et al., 1997; Großkopf et al., 2012), an amount that is currently exceeded by inputs of agricultural and industrial N (Galloway et al., 2003). To counteract those large inputs, a major loss of fixed nitrogen is taking place in the sediments via denitrification (200 – 280 Tg N yr^{-1}) and burial (25 Tg N yr^{-1}) (Brandes and Devol, 2002). One of the main uncertainties in the global marine nitrogen budget is the amount of nitrogen loss in oxygen-deficient zones (ODZs), whose spread in the coming decades due to climate change has been predicted (Stramma et al., 2008).

Role of ODZs in N loss

An ODZs is commonly defined as a water body with an oxygen concentration below 20 µmol L^{-1}(Paulmier and Ruiz-Pino, 2009). The formation of ODZs is favored by high levels of oxygen consumption in subsurface waters due to high surface primary production (up to 1g C m^{-2} d^{-1}) and subsequent remineralization of sinking organic matter combined with the poor ventilation of oxygen-rich waters. The three major open-ocean ODZs are the Eastern Tropical North Pacific (ETNP), the Eastern Tropical South Pacific (ETSP), and the Arabian Sea, which currently make up 8% of the global ocean area (Paulmier and Ruiz-Pino, 2009). So far, the lower limit of detection of the method for the determination of oxygen concentrations (Winkler method, 1 µmol L^{-1}) does not allow true anoxia to bedistinguishing from hypoxia. However, new analytical technologies have revealed that ODZs can be truly anoxic marine zones (AMZs) (Revsbech et al., 2011) and related to an intermediate state between fully oxic and fully sulfidic systems (Ulloa et al., 2012) (Figure 2). The development of different ecosystem states is determined by the rate of primary production, the rate of N_2-fixation, and oxygen availability,which together result in different chemical profiles in the water column (Figure 2). In sulfidic systems, ecosystem state is mainly determined by oxygen availability. Sulfidic bottom waters are found in semi-enclosed seas with restricted water circulation, such asthe Black Sea, the Baltic Sea, and the Cariaco Basin (Figure 2). The accumulation of toxic hydrogen sulfide in bottom waters has lethal consequences on higher life forms. These so called“dead zones”are currently increasing in number and size in open oceans and coastal zones (Diaz and Rosenberg, 2008; Stramma et al., 2008; Conley et al., 2011).

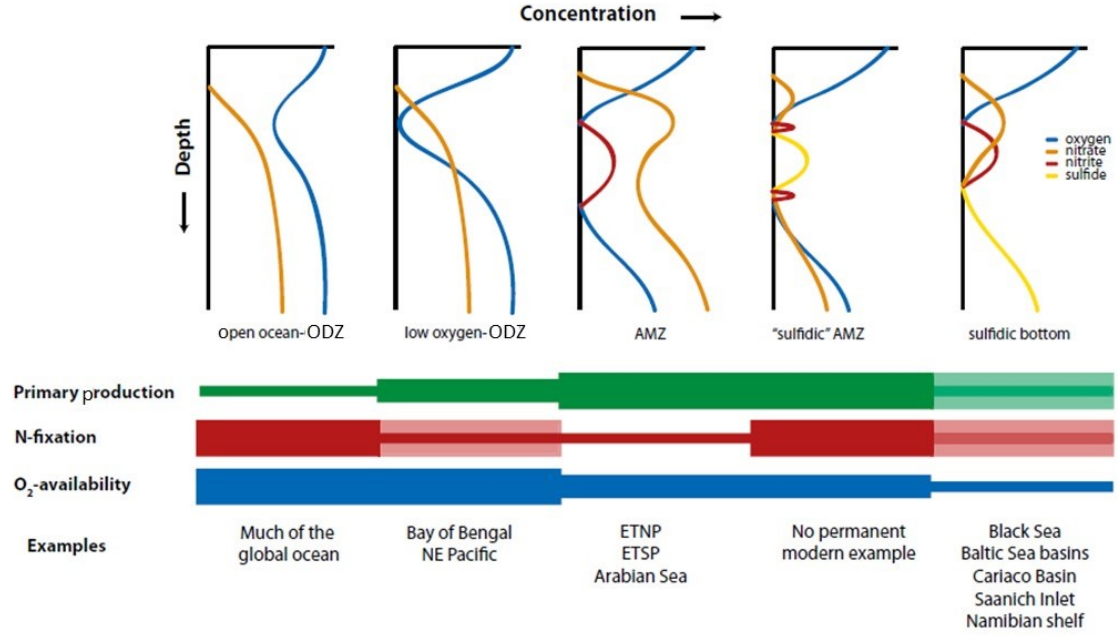

Figure 2: Development of different ecosystem states depending on drivers, such as primary production, N_2 fixation, and the availability of oxygen. (from Ulloa et al. 2012)

In the transition zone between oxidizing and reducing conditions, termed the redoxcline, diverse microbial communities contribute to major losses of fixed nitrogen (Gruber et al., 1997; Codispoti et al., 2001). In fact, these zones account for 30-50% of the total fixed-N loss from the ocean (Codispoti et al., 2001; Gruber and Galloway, 2008), but they also support 25- 50% of the oceanic production ofN_2O, which is a highly potent greenhouse gas (Codispoti, 2010; Santoro et al., 2011).

Identifying sources and processes by means of stable isotopes

Nitrogen has two stable isotopes ^{14}N and ^{15}N. The latter possesses one additional stable neutron and accounts for a small fraction of total N (0.3765 %). The stable isotopes of nitrogen have been particularly useful in shedding light on N processes in the ocean, because fixed nitrogen species are chemically dynamic on temporal and spatial scales that may not be appreciated even by comprehensive *in situ* sampling. The isotope ratio of ^{15}N to ^{14}N is 0.00378 and is expressed in delta notation in units per mil (‰):

$$\delta^{15}\mathrm{N}_{\mathrm{sample}} = \left(\left[\frac{^{15}N}{^{14}N}\right]_{sample} \Big/ \left[\frac{^{15}N}{^{14}N}\right]_{reference} - 1\right) \times 1000 \qquad (1)$$

The standard is atmospheric N_2, with a $\delta^{15}N = 0$ ‰. Chemically, the two isotopes have the same properties but the lighter molecule has a higher molecular velocity due to its lighter mass. In biological reactions, mass-dependent differences result in isotopic fractionation, in which molecules with lighter isotopes react more quickly than those with heavier isotopes. Consequently, consumed substrates become enriched with the heavier isotope and their reaction products with the lighter isotope. The isotope effect, or fractionation factor ε, quantifies the relative magnitude of isotopic enrichment in the reactant pool:

$$\delta^{15}\mathrm{N} \;=\; \delta^{15}\mathrm{N}_{\mathrm{initial}} + {}^{15}\varepsilon(\ln(f)) \qquad (2)$$

where *f* is the remaining nitrate fraction, $\delta^{15}N_{initial}$ is the $\delta^{15}N$ of the initial substrate pool, and ε is the kinetic isotope effect of the transformation.This Rayleigh model for isotope fractionation applies to reactions occurring in closed systems(Mariotti et al., 1981). Fractionation factors are process- specific and vary as a function of environmental conditions (Table 2). While N_2 fixation lacks an apparent N isotope effect, both in laboratory studies and in the field (Carpenter et al., 1997; Waser et al., 1998), a large isotope effect (20- 30 ‰) is associated with its counterpart, denitrification (Mariotti et al., 1981; Brandes et al., 1998; Barford et al., 1999; Voss et al., 2001)(Table 2). Recent studies have challenged the view of very high *in situ* isotope fractionation during denitrification, instead finding relatively low values of ε under diverse natural conditions, such as nutrient availability, the presence of different carbon sources or inputs of oxygen (Kritee et al., 2012; Ryabenko et al., 2012; Casciotti et al., 2013).Sediment denitrification was initially considered to leave no or little imprint on nitrate in the water column (Lehmann et al., 2007); however, a high rate of isotope fractionation during denitrification in shallow coastal sediments was indeed determined(Dähnke and Thamdrup, 2013).The effect of inorganic electron donors, such as hydrogen sulfide, on the isotope fractionation of nitrate during chemolithoautotrophic denitrification is unknown. The internal cycling of nitrogen, including nitrate and ammonium assimilation and nitrification, are also associated with a large fractionation factor (Table 2).Nonetheless, for all processes, there is no fractionation if the entire substrate pool is consumed.

Table 2: Isotope effects for microbial nitrogen processes

Process	N fractionation factor ε (‰)	Details
in pure cultures		
Nitrification		
Ammonium oxidation	14- 38	bacteria*, e.g., Nitrosomonas europaea*[a], *Nitrospira tenuis*[b]
	13- 41	archaea, e.g., CN25, CN75, CN150[c]
Nitrite oxidation	-12.8	*Nitrococcus mobilis*[d]
heterotrophic denitrification	13- 30	*Paracoccus denitrificans*[e], *Pseudomonas stutzeri*[f], *P. denitrificans*[g]
chemolithoautotrophic denitrification	?	unknown
Anammox (on NH_4^+ pool)	23- 29	*Kuenenia stuttgartiensis*[l]
Nitrogen fixation	0	*Trichodesmium sp.*[h], *Azotobacter vinlandi*[i]
Ammonium Assimilation	15- 25	*Emiliana huxlei, Chaetoceros debilis*[j]
Nitrate assimilation	4- 20	*Emiliana huxlei*[j], *Thalassiosira weissflogii*[k]
in situ		
Denitrification		
water-column	20- 40	ETNP, Arabian Sea, ETSP[m,n,o]
	1- 5	Santa Barbra Basin, Cariaco Basin[p,q]
	15-20	Lake Lugano[r]
sediments	0- 3	deep sea sediments, Bering Sea[w]
	18-19	coastal sediments, Baltic Sea[x]
Nitrogen fixation	-0.4	Trichodesmium colonies [h]
Ammonium assimilation	5- 20	bacterial assemblage, Chesapeake Bay[s,t]
Nitrate assimilation	4- 6	southern Ocean, subarctic Pazific[u,v]
Nitrification	15	Chesapeake Bay [s]

[a]Mariotti et al. (1981); [b]Casciotti et al. (2010); [c]Santoro and Casciotti, (2011); [d]Casciotti (2009); [e]Barford et al. (1999), [f]Wellman et al. (1968), [g]Delwiche and Steyne (1970), [h]Carpenter et al. (1997), [l]Waser et al. (1999), [j]Waser et al. (1998), [k]Granger et al. (2010), [l]Brunner et al.(2013),[m]Voss et al. (2001), [n]Brandes et al. (1998), [o]Naqvi et al.(1998), [p]Sigman et al. (2003), [q]Thunell et al. (2004), [r]Wenck et al. (2014), [s]Horrigan et

al. (1990), [t]Hoch et al. (1994), [u]Sigman et al (1999), [v]Wu et al. (1997), [w]Lehmann et al. (2007), [x]Dähnke et al. (2013)

The coupled measurement of the N and O isotopes of nitrate is an established method to trace biogeochemical transformations of nitrogen and to identify different nitrate sources (Kendall, 1998; Sigman et al., 2001, 2005; Casciotti et al., 2002; Wankel et al., 2006, 2007; Kendall et al., 2007). Oxygen has three stable isotopes, ^{16}O, ^{17}O, and ^{18}O. ^{17}O is very rare and is usually not considered in natural abundance studies. The pathways of ^{18}O contrast with those of its nitrogenous partners and the input and output processes of oxygen are distinct from those of nitrogen. Nitrification represents a source process for the entry of oxygen into the N cycle via ammonium and nitrite oxidation. Denitrification (nitrate and nitrite reduction) removes oxygen, as a water molecule. The different fates of $\delta^{18}O$ and $\delta^{15}N$ can be exploited to gain insights into the N cycle. The ratio of the O and N isotope effect for marine denitrification and assimilation is 1. This ratio and deviations from it can be used to predict biological N transformations. Thus, the potential role of N_2 fixation relative to nitrate assimilation (Bourbonnais et al., 2009) and the relative magnitude of assimilation to nitrification in surface mixed layers (Wankel et al., 2006; Dähnke et al., 2010) have been determined by analyzing the deviations from the 1:1 ratio of $\delta^{18}O$ to $\delta^{15}N$ in nitrate. The isotope systematics of nitrification are complicated because nitrification is carried out through two microbial processes with distinct and large, but also opposing isotope effects (Table 2, Figure 3).

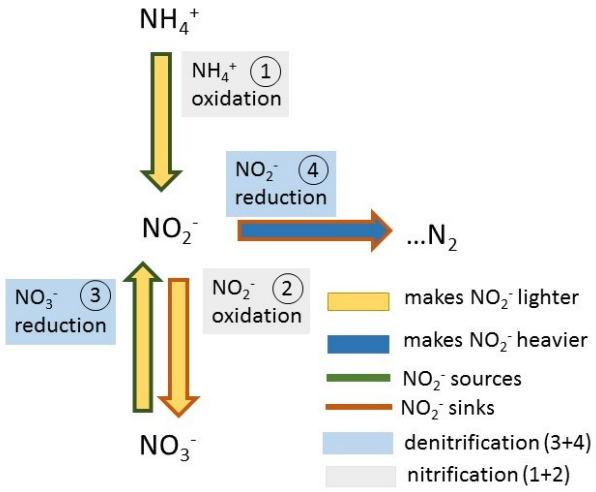

Figure 3: Overview of the N isotope effects of nitrification and denitrification on nitrite.

While nitrogen isotope fractionation factors for ammonium oxidation are in the range of 14 – 38 ‰ for ammonium- oxidizing bacteria or archaea, the isotope effect for oxygen is dependent on three factors: the source (H_2O or O_2), isotope fractionation during incorporation, and the exchange of oxygen atoms between water and nitrite (Casciotti et al., 2010). During nitrite oxidation, there is an inverse isotope effect for N such that residual nitrite is depleted in ^{15}N whereas the product nitrate becomes heavier in ^{15}N (Casciotti, 2009). Oxygen isotope fractionation in nitrite oxidation depends on: the fractionation factor for nitrite oxidation, the fractionation factor for water incorporation, and the exchange of oxygen atoms between nitrite and water(Casciotti, 2009).In regions where ammonium and nitrite oxidation are tightly coupled, oxygen isotope exchange is low, but when they become decoupled, such as in primary or secondary nitrite maxima, oxygen isotope exchange plays a role (Buchwald et al., 2012; Casciotti and Buchwald, 2012). These recent findings have improved interpretations of the dual stable isotope values of nitrate in ODZs, where reduction and oxidation processes are tightly coupled (Casciotti et al., 2013).

The combined use of $\delta^{15}N$ with $\delta^{18}O$ also provides a tool to distinguish between major nitrate sources (Figure 4).

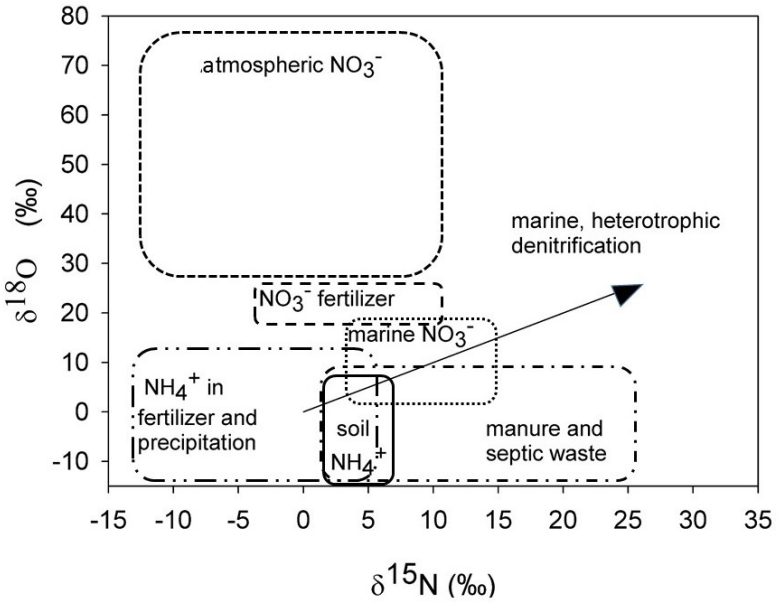

Figure 4: Isotopic composition of nitrate from different sources and its change during denitrification. (redrawn after Kendall et al. 2007)

With respect to N, nitrate from atmospheric deposition (-10- 8 ‰) is distinct from that in manure and sewage (7-20 ‰) (Mayer et al., 2002; Kendall et al., 2007). Synthetic

fertilizers (0 ± 3 ‰), natural organic N in soils (-3- 5 ‰) and nitrate from nitrification cannot be distinguished based on $\delta^{15}N$ alone. Rather, by also using the $\delta^{18}O$ value of nitrate, four major nitrate sources can be distinguished: atmospheric deposition, with a relatively high $\delta^{18}O$ value (25 -70 ‰); nitrate-containing fertilizers, with a $\delta^{18}O$ value of approximately 22 ± 3 ‰; nitrate in manure and/or sewage, with a low $\delta^{18}O$ (< 15‰); and nitrate derived from nitrification in soils,where $\delta^{18}O$ values vary depending on the oxygen isotope ratios in water and dissolved oxygen (-15 – 15 ‰) (Mayer et al., 2002; Kendall et al., 2007).

The Baltic Sea and its nitrogen cycle

The Baltic Sea is a nutrient rich system, reflecting its strong river- mediated terrestrial inputs from a drainage area that is over three times larger than the area of the sea itself. Strong freshwater inputs and precipitation, which are not balanced by evaporation, lead to a net outflow of lower saline water into the North Sea (Reissmann et al., 2009). Because the Baltic Sea is land-locked, with only a narrow, shallow connection to the North Sea (Danish straits), water exchange is severely restricted. The Baltic Sea has a horizontal salinity gradient of 25 in its south-western part but only 2-3 in the Gulf of Bothnia. This low salinity makes the Baltic Sea one of the largest brackish water masses in the world. It consists of a series of basinsthat were formed by ice movements during and after the last glaciation (Grasshoff, 1975). The deepest basin is the Landsort Deep (459 m), and the largest is the Gotland Deep (249 m). In addition to the horizontal salinity gradient, there is also a vertical gradient. A permanent halocline, at a depth of 60- 80 m in the Gotland basin, separates less saline water in the upper layer from lower-laying, highly saline, and therefore denser water. Consequently, vertical mixing is limited (Reissmann et al., 2009). The restricted vertical and horizontal exchange results in the stagnation of water masses in the Baltic Sea. Water renewal by major inflows is controlled by strong storm events, which can lead to inputs of high-salinity, oxygenated North Sea water, and thus the renewal of Baltic Sea bottom water. Prior to 1983 these inflow events occurred at least once a year, but since then only two major inflow events have taken place, in 1993 and 2003 (Matthäus et al., 2008). After a decade without major Baltic inflows, a deep- water renewal in the Gotland Basin was

registered in the summer of 2014(Nausch et al., 2014). The lack of vertical mixing combined with oxygen consumption during the remineralization of organic matter gradually leads to anoxia. The result is the replacement of the aerobic remineralization of organic matter by fermentation, which in turn produces H_2S and thus expands sulfidic bottom waters (Piker et al., 1998).

The Baltic Sea has suffered from eutrophication since the start of industrialization in the beginning of the 20th century (Elmgren, 2001). Phytoplankton growth and bloom formation are triggered by nitrogen and phosphorus inputs, which increased several fold in the 1970s and 1980s (Larsson et al., 1985; Conley et al., 2009). Each year, 970 kt of N enters the Baltic Sea (status 2007), of which approximately 25% is from atmospheric deposition and 75% from rivers (HELCOM, 2013, Table 3). Despite an annual 16% decrease in N load (333 t year^{-1}) (HELCOM, 2013) in a recent study 176 out of the 189 studied areas were affected by eutrophication (Andersen et al., 2010) and an increasing trend of coastal hypoxia driven by anthropogenic nutrient input was apparent (Conley et al., 2011). Nutrient loads in rivers that empty into the Baltic Sea correlate with the population density along its coast (HELCOM, 2013; Humborg et al., 2007; Voss et al., 2011). The region north of the Baltic is less densely populated (<10 inhabitants/km²) and the land cover is dominated by boreal forest, while the south is densely populated (>500 inhabitants/km²) and heavily cultivated (Lääne et al., 2005; HELCOM, 2013). The five major rivers, Neva, Vistula, Daugava, Nemunas and Oder that drain into the Baltic make up 50 % of the total DIN load. Moreover, all of these rivers, except Neva,empty into the southern Baltic, further increasing eutrophication pressure (HELCOM, 2013). Strategies for nutrient load reduction have focused mostly on P rather than on N, because a lower N:P ratio in the central Baltic Sea triggers algal blooms (Saaltink et al., 2014). In summer, the N limitation, that occurs after the diatom- and dinoflagellate- dominated spring blooms, favors cyanobacterial blooms (Wasmund et al., 1998; Ploug, 2008; Suikkanen et al., 2011). Estimates for annual inputs from N_2 fixation vary from 370 kt of N (Wasmund et al., 2001) up to 855 kt of N (Voss et al., 2005), with an increasing trend due to eutrophication (Vahtera et al., 2007) and to the increased phosphorus supply from sediments of the anoxic basins (Mort et al., 2010; Jilbert et al., 2011). The additional phosphorus release intensifies an internal feedback loop by

triggering cyanobacterial blooms, which in turn increase N inputs into the central basin (Vahtera et al., 2007).

Different methods to estimate N loss in the Baltic Sea (models, isotope signature in sediment, budget calculations, nutrient profiles, and ^{15}N incubations) have been used to evaluate the balance of the Baltic Sea N budget (Table 3). While N sinks roughly balance N sources (Voss et al., 2005), an overall higher N input has been identified (HELCOM, 2013). N loss takes place in low- oxygen environments in the water column or in sediments. Removal of N along the coastline mainly takes place in sediments, whereas in the central Baltic Sea most N removal occurs in the redoxcline of the water column. The variation in N removal in the water column reflects interannual variations in the size of the hypoxic area but also in denitrification rates (Hietanen et al., 2012; Dalsgaard et al., 2013).

Table 3: Nitrogen budget of the Baltic Sea

Process	kt year^{-1}	Process	kt year^{-1}
sources		*sinks*	
riverine	737[b]	burial (in the Baltic Proper)	113[g]- 300[i]
atmospheric	196[a] -232[b,c]	water column denitrification	89- 547[j]; 206[g]
N_2 fixation	180[d] – 855[e, f]	sedimentary denitrification	426- 652[g]; 729[h]; 855[e]
input from the North Sea	419[c]		
total	1532 - 2243	*total*	628- 1702

[a]Bartnicki et al. (2008); [b]HELCOM (2013); [c]Savchuk et al. (2008); [d]Rolff et al. (2008); [e]Voss et al. (2005); [f]Wasmund et al. (2005); [g]Deutsch et al. (2010); [h]Savchuk(2005); [i]Dalsgaard et al. (2013)

The pelagic redoxcline of the central Baltic Sea is situated in the aphotic zone. It ranges over several meters in depth and is marked by a strong chemical gradient (Figure 5). The highly active prokaryotic communities within this depth horizon (Labrenz et al., 2005, 2007; Brettar et al., 2006; Jost et al., 2008)include key groups that make up significant percentages of the total cell abundance and perform important biogeochemical processes. Two prominent groups are the ammonium- oxidizing

Thaumarchaeota subcluster GD2 (Labrenz et al., 2010) and the sulfur- oxidizing *Gammaproteobacteria* SUP05 (Glaubitz et al., 2013), which make up 25% and 10-30%, respectively, of the total prokaryotic community. The *Sulfurimonas* subgroup GD17 uses sulfide as an electron donor and is the main chemolithoautotrophic denitrifer, accounting for up to 30% of total prokaryotes (Grote et al., 2008, 2012; Grote, 2009).

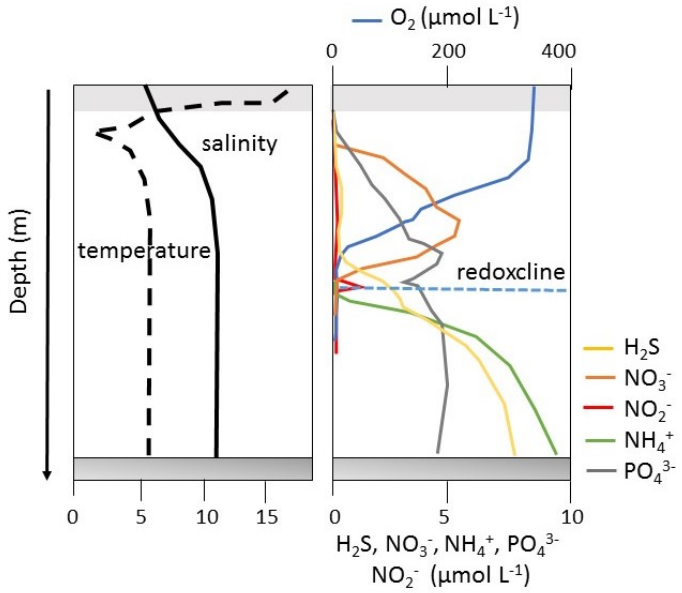

Figure 5: Typical profile of the central Baltic Sea, showing the strong chemical gradients (measured in the Landsort Deep, May 2011). The oxygen concentration begins to decrease below the halocline. Nitrate peaks and decreases to zero in the same depth where oxygen reaches zero. Ammonium and hydrogen sulfide concentration start to increase once oxygen and nitrate are depleted.

So far, little is known about the nitrate isotope dynamics of the redoxcline in the Baltic Sea. A first study found little enrichment of $\delta^{15}N$ (Eichner, 2000), but the $\delta^{18}O$ in nitrate has not been used to study N cycling in the Baltic Sea redoxcline.

Aims of the dissertation

The aims of this thesis were: (1) to obtain a better-constrained nitrogen budget, with clearly characterized sources and fluxes of nitrogen in the modern Baltic Sea and (2) to improve our current understanding of the mechanisms that underlie biological nitrogen transformations. Ultimately, greater knowledge of the Baltic Sea nitrogen cycle will provide insights into its links to eutrophication.

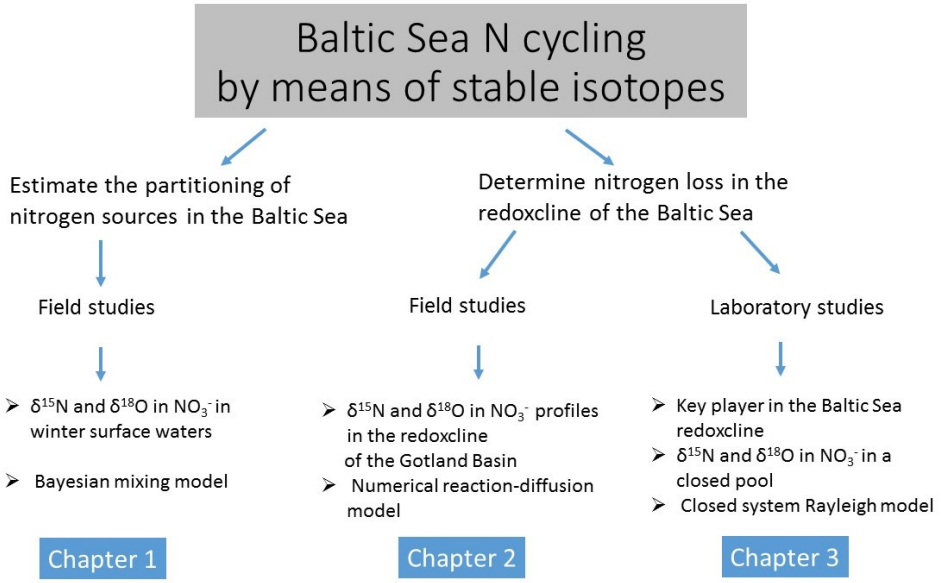

Figure 6: Scheme summarizing the research performed for this thesis.

1) Estimate the partitioning of nitrogen sources in the Baltic Sea

Maps of the distribution of particular stable isotopes (called isoscapes) have been used to evaluate local differences in the contributions of distinct sources. Thus far, the $\delta^{15}N$ of the surface sediment in the Baltic Sea is the only spatially well- described component that has been used to study source allocation in different regions (Voss et al., 2005). Research carried out as part of this thesis was directed at closing the gaps in our knowledge regarding $\delta^{15}N$ and $\delta^{18}O$ isotope distribution in nitrate, by establishing a method to determine the contribution of nitrogen sources to the Baltic Sea. The method combines determination of the dual stable isotope values of nitrate with a Bayesian mixing model. The results provide a basis for further studies on the reduction and management of nutrient inputs in the Baltic Sea. The combined approach provides a new tool that can be applied in identifying nitrogen source allocation in other eutrophied basins, enclosed seas, or coastal areas.

Chapter 1 of this thesis makes use of the nitrogen and oxygen isotopes in nitrate from the winter surface water of the Baltic Sea to determine how different areas of the Baltic are impacted by different nitrate sources.A Bayesian mixing model was used to identify four different sources: nitrogen fixation, atmospheric deposition, nitrate from

natural run-off (pristine soils), and agricultural runoff. The potential implications of the results and comparisons of the method with other methods estimating sources in the Baltic Sea are discussed herein.

2) Determination of nitrogen loss in the redoxcline of the Baltic Sea

Insights into nitrogen turnover processes were gained by using the stable isotope signature of nitrate within the redoxcline of the central Baltic Sea. Due to the scarcity of information on the impact of chemolithoautotrophic denitrification on nitrate fractionation, a multi-step approach was used:

1) Identify the isotopic signatures of N and O in nitrate in the oxic-anoxic gradient in the Baltic Sea redoxcline.
2) Develop a numerical model for N-cycling within the Baltic Sea redoxcline including nitrate sources and sinks, to estimate an integrated denitrification rate
3) Determine the isotope fractionation factor and the sensitivity towards oxygen of chemolithoautotrophic denitrification by the key microbial player of the Baltic Sea redoxcline.

Chapter 2 of this thesis describes the *in situ* isotopic signature of nitrate in the Baltic Sea redoxcline and applies both a closed system Rayleigh model and a numerical reaction-diffusion model to the data to identify the impact of major N turnover processes on the nitrate signature. Finally, the numerical model is used to determine denitrification rates on the basis of the isotopic values in nitrate.

Chapter 3 presents the results of a laboratory experiment with the key denitrifier *Sulfurimonas gotlandica*strain GD1^{T},in which the isotopic fractionation factors of N and O in nitrate during chemolithoautotrophic denitrification were determined under varying environmental conditions. Additionally, the sensitivity of the process towards oxygen was investigated by tracer addition techniques.

This thesis provides the first estimate of N sources and processes based on the isotopic signature of nitrate in the Baltic Sea. It also includes the first study of isotope fractionation in nitrate by chemolithoautotrophic denitrification.

Chapter 1

Nitrate source identification in the Baltic Sea using its isotopic ratios in combination with a Bayesian isotope mixing model

Korth, F., Deutsch, B., Frey, C., Moros, C., and Voss, M.

Biogeosciences **11**: 4913-4924.

doi:10.5194/bg-11-4913-2014

Abstract

Nitrate (NO_3^-) is the major nutrient responsible for coastal eutrophication worldwide and its production is related to intensive food production and fossil-fuel combustion. In the Baltic Sea NO_3^- inputs have increased four-fold over the last decades and now remain constantly high. NO_3^- source identification is therefore an important consideration in environmental management strategies. In this study focusing on the Baltic Sea, we used a method to estimate the proportional contributions of NO_3^- from atmospheric deposition,N_2 fixation, and runoff from pristine soils as well as from agricultural land. Our approach combines data on the dual isotopes of NO_3^- ($\delta^{15}N\text{-}NO_3^-$ and $\delta^{18}O\text{-}NO_3^-$) in winter surface waters with a Bayesian isotope mixing model (Stable Isotope Analysis in R, SIAR). Based on data gathered from 47 sampling locations over the entire Baltic Sea, the majority of the NO_3^- in the southern Baltic was shown to derive from runoff from agricultural land (33–100%), whereas in the northern Baltic, i.e., the Gulf of Bothnia, NO_3^- originates from nitrification in pristine soils (34–100%). Atmospheric deposition accounts for only a small percentage of NO_3^- levels in the Baltic Sea, except for contributions from northern rivers, where the levels of atmospheric NO_3^- are higher. An additional important source in the central Baltic Sea is N_2 fixation by diazotrophs, which contributes 49-65% of the overall NO_3^- pool at this site. The results obtained with this method are in good agreement with source estimates based upon $\delta^{15}N$ values in sediments and a three-dimensional ecosystem model, ERGOM. We suggest that this approach can be easily modified to determine NO_3^- sources in other marginal seas or larger near-coastal areas where NO_3^- is abundant in winter surface waters when fractionation processes are minor.

1.1. Introduction

Throughout the world, anthropogenic reactive N currently exceeds natural production (Galloway et al., 2003; Gruber and Galloway, 2008). Consequently, riverine nitrogen (N) fluxes have doubled in recent years, which has strongly impacted the marine N cycle and ecosystem health, both at regional and global scales. In coastal ecosystems, the adverse effects of these excess N loads include eutrophication, hypoxia, loss of biodiversity, and habitat destruction (Galloway et al., 2003; Villnäs et al., 2013). For the shallow, brackish, semi-enclosed Baltic Sea, where intense anthropogenic nutrient loadings have been

documented since the 1950s (Elmgren, 2001),riverine and atmospheric nutrient inputs are now at least four-fold higher than a century ago, when anthropogenic influence was low (Stålnacke et al., 1999; Schernewski and Neumann, 2005). Furthermore, cyanobacterial blooms, which can fix N_2, and thus add nutrients to the surface waters are regular large scale phenomenon each summer (Finni et al., 2001; Vahtera et al., 2007; Conley, Carstensen, et al., 2009; Conley et al., 2011) and the overall increase in nutrient input has supported the expansion of hypoxic zones (Finni et al., 2001; Vahtera et al., 2007; Conley, Carstensen, et al., 2009; Conley et al., 2011).

A main component of the N pool and the one most readily available is nitrate (NO_3^-) (Vitousek et al., 1997; Nestler et al., 2011), which derives from a wide variety of sources. These can be identified by analysis of the N and oxygen (O) isotopes ($\delta^{15}N\text{-}NO_3^-$ and $\delta^{18}O\text{-}NO_3^-$) since the isotopic ratios of NO_3^- from different sources fall within distinct ranges (Kendall, 1998; Kendall et al., 2007). For example, NO_3^- inputs from forested catchments can be discriminated from those coming from agricultural runoff, and the NO_3^- signature of microbial nitrification differs from that of atmospheric deposition (Kendall, 1998; Mayer et al., 2002; Kendall et al., 2007). Source attribution is, however, complicated by N-transformation processes such as denitrification, nitrification, and assimilation, each of which gives rise to significant isotope fractionation. Since heavier isotopes are sequestered more slowly than lighter ones, the reaction product will be isotopically depleted compared to the original NO_3^- source (Kendall, 1998). Alterations of isotope values because of microbial fractionation processes can be minimized by collecting the samples in winter, when low water temperatures reduce microbial activity (Pfenning and McMahon, 1997).

Nonetheless, source attribution is still complicated when there are more than three sources but only two isotopes that describe them (Fry, 2013). SIAR (Stable Isotope Analysis in R), a Bayesian isotope mixing model originally developed to infer diet composition from the stable isotope analysis of samples taken from consumers and their food sources (Moore and Semmens, 2008), was already successfully applied for NO_3^- source identification. Xue et al. (2012, 2013) were able to estimate the proportional contributions of five potential NO_3^- sources in a small watershed in Flanders (Belgium). Based on their determinations of the isotopes of nitrogen and oxygen they could show that manure and sewage were the major sources of NO_3^-.

In the Baltic Sea the NO_3^- pool present in the surface waters in spring originates from the previous growth season and is consumed during the onset of the phytoplankton spring bloom, in February/March. Stratification in summer hinders circulation down to the halocline, thus atmospheric deposition and N_2 fixation are the major N sources, whereas in coastal areas riverine discharge dominates (Voss et al., 2011; Radtke et al., 2012). Yet, to what extent the various NO_3^-sources add to the overall pool of NO_3^- in the Baltic as a whole is still a matter of debate.In this study, a source attribution for four major sources is presented. Taking the Baltic Sea as an example we will show, that the use of the isotopic composition of NO_3^-($\delta^{15}N\text{-}NO_3^-$ and $\delta^{18}O\text{-}NO_3^-$) in combination with SIAR can be used elsewhere for source identification on an ecosystem scale level.

1.2. Material and Methods

Field sampling

Surface water samples from the Baltic Sea were collected in February 2008 (n=22) and 2009 (n=17) before the onset of the phytoplankton spring bloom aboard the RV *Alko*r and in November 2011 (n=1) aboard the RV *Meteor* using a Seabird CTD system with attached water bottles. Samples from the Nemunas River (55°18`5.5 N, 21°22`53.9 E; 55°41`25.6 N, 21°7`58.4 E; n=4) and Kalix River (65°56`4.2 N, 22°53`9.2 E; n=1) (Fig.7) were taken between November 2009 and February 2010. Values for NO_3^-in which atmospheric deposition was the source were obtained from wet deposition samples collected at three stations around the Baltic Sea: Warnemünde, Germany (54°10’ N, 12°5’ E,); Majstre, Sweden (57°30’ N, 18°31’ E); and Sännen, Sweden (56°13’N, 15°17’E) from December 2009 until February 2010 (Table 4). In Warnemünde, precipitation was collected on an event basis, and retrieved daily to limit microbial degradation, using a sampler consisting of a plastic funnel (diameter: 24 cm) connected to a 1-L polyethylene bottle. At the two Swedish stations, rainwater was sampled monthly by the Swedish Environmental Research Institute (IVL) as part of the Swedish national long-term monitoring program. Here, the sampler consisted of a plastic funnel (diameter 20.3 cm) connected to an 8-L polyethylene bag. All samples were filtered through pre-combusted Whatman GF/F filters (4 h at 400°C) and stored frozen until further analysis.

Table 4: NO_3^- concentrations and $\delta^{15}N\text{-}NO_3^-$ and $\delta^{18}O\text{-}NO_3^-$ values of wet atmospheric deposition. Data are from Warnemünde (Germany), Sännen (Sweden), and Majstre (Sweden).

Location	Date	NO_3^- ($\mu mol\ L^{-1}$)	$\delta^{15}N\text{-}NO_3^-$ (‰)	$\delta^{18}O\text{-}NO_3^-$ (‰)
Warnemünde	21.12.2009	52.7	2.1	75.6
Warnemünde	04.01.2010	51.2	1.1	68.3
Warnemünde	19.01.2010	104.4	0.2	84.6
Warnemünde	01.02.2010	50.8	0.8	65.8
Warnemünde	19.02.2010	94.4	0.6	79.5
Warnemünde	22.02.2010	106.8	2.1	81.8
Sännen	Dec. 2009	12.1	-0.3	69.2
Sännen	Jan. 2010	60.4	-1.1	81.8
Sännen	Feb. 2010	69.3	-2.1	77.0
Majstre	Dec. 2009	30.7	-0.8	83.8

Nutrient concentrations and dual isotope analysis of NO_3^-

Samples were analyzed following a standard protocol for the determination of NO_3^- and nitrite (NO_2^-)(Grasshoff et al., 1983); the precision of the method is ±0.02 µmol l^{-1}. Dual isotope analysis of NO_3^- ($\delta^{15}N\text{-}NO_3^-$ and $\delta^{18}O\text{-}NO_3^-$) was carried out using the denitrifier method (Sigman et al., 2001; Casciotti et al., 2002), in which NO_3^- and NO_2^- are quantitatively converted to nitrous oxide (N_2O) by *Pseudomonas aureofaciens* (ATTC 13985), a bacterial strain that lacks N_2O reductase activity. In brief, N_2O is removed from the sample vials by purging with helium and then concentrated and purified in a GasBench II prior to analysis with a Delta Plus mass spectrometer (ThermoFinnigan). NO_2^- was not removed since its concentrations were always less than 2% (referring to the procedure described inCasciotti et al., 2007). N and O isotope measurements of roughly 30% of the samples were replicated in separate batch analyses. Two international standards, IAEA-N3 ($\delta^{15}N$=4.7‰ vs. N_2; $\delta^{18}O$

25.6‰ vs. VSMOW) and USGS 34 ($\delta^{15}N$ -1.8‰ vs. N_2; $\delta^{18}O$ -27.9‰ vs. VSMOW) (Böhlke et al., 2003), were measured with each batch of samples. Samples with NO_3^-/ NO_2^- concentrations as low as 1 µmol l^{-1}were analyzed. The sample size for the actual stable isotope measurements was 20 nmol for samples with concentrations >3.5 µmol l^{-1} and 10 nmol for those with concentrations <3.5 µmol l^{-1}. Isotope values were corrected after Sigman et al. (2009) for $\delta^{18}O$-NO_3^-;single point correction was referred to IAEA-N3 for$\delta^{15}N$-NO_3^-. The precision was <0.2 ‰ for $\delta^{15}N$ and <0.6 ‰ for $\delta^{18}O$. Together with the samples, a culture blank was analyzed to which no sample was added. The isotope ratios are reported using the delta notation in units of per mil (‰).

NO_3^- sources

To estimate the contribution of different NO_3^- sources, two isotopes $\delta^{15}N$-NO_3^- and $\delta^{18}O$-NO_3^- (j=2) from the four major NO_3^- sources: (1) atmospheric deposition, (2) runoff from pristine soils, (3) runoff from agricultural land and (4) N_2fixation were applied (Table 5). In this context, N_2 fixation was defined as NO_3^- originating from the degradation and remineralization of nitrogen fixers and therefore carried their low isotopic signal. Thus, for $NO_3^-$from N_2 fixation, $\delta^{15}N$ values of ~-2 to 0‰ were assumed, since N_2 fixation produces organic material that is only slightly N depleted against air nitrogen (Carpenter et al., 1997, 1999; Montoya et al., 2002). The $\delta^{18}O$ values were estimated to be between -3.8‰ and 2.0‰, based on measurements in the subtropical northeast Atlantic where N_2 fixation was the main source of N (Bourbonnais et al., 2009) ($\delta^{18}O$-NO_3^- = 2‰) and the estimated $\delta^{18}O$ of NO_3^- deriving from N_2 fixation by Sigman et al. (2009) ($\delta^{18}O$-NO_3^- = -0.2‰) and Bourbonnais et al. (2012) ($\delta^{18}O$-NO_3^- = -3.8‰).

To expand the dataset, we included NO_3^- isotope data from river water samples, ground water samples, and samples from tile drain outlets collected in 2003 and published in Deutsch et al. (2006). In that study, the Warnow River (n=2) was sampled twice, in January and February 2003. These sources were likewise sampled in winter, since marked seasonal shifts in the isotopic composition of NO_3^- can occur due to shifts in the origins of the sources (Knapp et al., 2005). Samples from tile drain outlets were used to represent NO_3^- from agricultural runoffand were obtained from the catchment of the Warnow River, whose waters are strongly influenced by agricultural land use (Pagenkopf, 2001). High $\delta^{15}N$-NO_3^- values of 9.9±1.5‰ and lower $\delta^{18}O$-NO_3^- values of 4.6±1.0‰ are typical for areas that are

influenced by agricultural activities and are similar to studies of Wankel et al. (2006) and Johannsen et al. (2008). Johannsen et al. (2008) found in the rivers Rhine, Elbe, Weser and Ems, with comparable high agricultural activities, $\delta^{15}N\text{-}NO_3^-$ values between 8.2 and 11.2‰ and $\delta^{18}O\text{-}NO_3^-$ values from 0.4 to 0.9‰ in winter. However, a differentiation between NO_3^- from mineral fertilizers and sewage/manure was not done; rather a mixed signal from rivers that are mainly influenced by agricultural activities was taken. Groundwater samples were used as the source of NO_3^- from pristine land (Deutsch et al., 2006). Their $\delta^{15}N\text{-}NO_3^-$ and $\delta^{18}O\text{-}NO_3^-$ values significantly differed from those of agricultural runoff ($p<0.05$) but were similar to the values of other areas, such as Biscuit Brook (Burns et al., 2009) and the San River (Koszelnik and Gruca-Rokosz, 2013), where pristine soils were sampled and reflect nitrification activity in soils unaffected by human activity.

Table 5: Means and standard deviations of the $\delta^{15}N\text{-}NO_3^-$ and $\delta^{18}O\text{-}NO_3^-$ values of the NO_3^- sources used in the SIAR mixing model. For further details, see Material and Methods, SIAR mixing model.

Source	$\delta^{15}N\text{-}NO_3^-$ (mean ± SD)	$\delta^{18}O\text{-}NO_3^-$ (mean ± SD)	n	Origin	Reference
NO_3^- from atmospheric deposition	0.3±1.4	76.7±6.8	10	Warnemünde (Germany), and Sännen and Majstre (Sweden)	This study
NO_3^- from pristine soils	1.3±1.4	1.5±0.9	5	Groundwater	Deutsch et al., (2006)
NO_3^- from agricultural runoff	9.9±1.5	4.6±1.0	21	Tile-drain outlets, Warnow River	Deutsch et al., (2006)
NO_3^- from N_2 fixation	-1.0±1.0	-0.7±2.9	0	Estimated	Carpenter et al., (1999), (1997); Bourbonnais et al., (2009), (2012); Montoya et al., (2002); Sigman et al.,(2009)

The dual isotopes of NO_3^- values presented in Deutsch et al. (2006) were analyzed according to Silva et al., (2000). In this method, NO_3^- is chemically converted via anion exchange resins to $AgNO_3^-$ and the $\delta^{15}N\text{-}NO_3^-$ and $\delta^{18}O\text{-}NO_3^-$ values are measured via pyrolysis and isotopic ratio mass spectrometry (for a detailed description, see Deutsch et al. 2006). A normal distribution of the isotopic data from the four sources was confirmed by applying the Shapiro-Wilk normality test. $\delta^{15}N\text{-}NO_3^-$ and $\delta^{18}O\text{-}NO_3^-$ values from NO_3^- from atmospheric deposition of 0.3±1.4‰ and 76.7±6.8‰, respectively, are also in line with literature values. The $\delta^{15}N$ values of atmospheric NO_3^- are usually between -15 to +15‰ and the $\delta^{18}O$ between 63 and 94‰ (Kendall et al., 2007).

Six regions within the catchment of the Baltic Sea were investigated for their potential NO_3^- sources (Fig. 7). According to the topography of the Baltic Sea, the samples were assigned to four major areas: Western Baltic Sea, Baltic Proper, Gulf of Finland, and Gulf of Bothnia. Additionally, three rivers differing in their degree of anthropogenic impact were included in this study and divided into two groups: northern and southern rivers. Rivers with high nutrient loads drain mainly into the southern Baltic Proper and were represented here by the Nemunas and Warnow Rivers, whose NO_3^- concentrations in winter can be as high as 260 µmol l^{-1}(Deutsch et al., 2006; Pilkaitytė and Razinkovas, 2006). The Gulf of Bothnia receives large amounts of fresh water from rivers represented by the Kalix River. These rivers drain mainly pristine, forested land and have maximum NO_3^- concentrations of around 20 µmol l^{-1} (Sferratore et al., 2008).

SIAR mixing model

The applied mixing model is described by the following equations:

$$X_{ij} = \sum_{k=1}^{K} p_k \left(s_{jk} + c_{jk}\right) + \varepsilon_{ij} \quad (3)$$

$$s_{jk} \sim \mathrm{N}(\mu_{\mathrm{jk}}, \omega_{\mathrm{jk}}^2) \quad (4)$$

$$c_{jk} \sim \mathrm{N}(\lambda_{\mathrm{jk}}, \tau_{\mathrm{jk}}^2) \quad (5)$$

$$\varepsilon_{ij} \sim \mathrm{N}(0, \sigma_{\mathrm{j}}^2) \quad (6)$$

where X_{ij} is the observed isotope value j of the mixture i; i=1,2,3,…,I are individual observations; and j=1,2,3,…,J are isotopes. s_{jk} is the source value k of isotope j (k = 1,2,3,…, K) and is normally distributed, with a mean of μ_{jk} and a standard deviation of ω_{jk}. p_k is the proportion of source k that needs to be estimated by the model. c_{jk} is the fractionation factor

for isotope j on source k and is normally distributed, with a mean of λ_{jk} and a standard deviation of τ_{jk}. ε_{ij} is the residual error representing additional unquantified variations between mixtures and is normally distributed, with a mean of 0 and a standard deviation of σ_j. Detailed descriptions of the model can be found in Jackson et al., (2009), Moore and Semmens, (2008), and Parnell et al., (2010). As noted above, by collecting samples between November and February we minimized the influence of fractionation processes such as assimilation and denitrification that can alter the isotopic signal of NO_3^-.Therefore in Eq. (3) we assumed that $c_{jk} = 0$.

Two different runs of the SIAR model were performed. In the first, for the Western Baltic Sea, Baltic Proper, and Gulf of Finland, all four sources were included in the calculation. In the second, for the Gulf of Bothnia, the southern rivers, and the northern rivers, N_2 fixation as a potential NO_3^- source was excluded since in these areas there is no N_2 fixation by diazotrophs because the Gulf of Bothnia is phosphorus limited, in contrast to the Baltic Proper (Graneli et al., 1990).

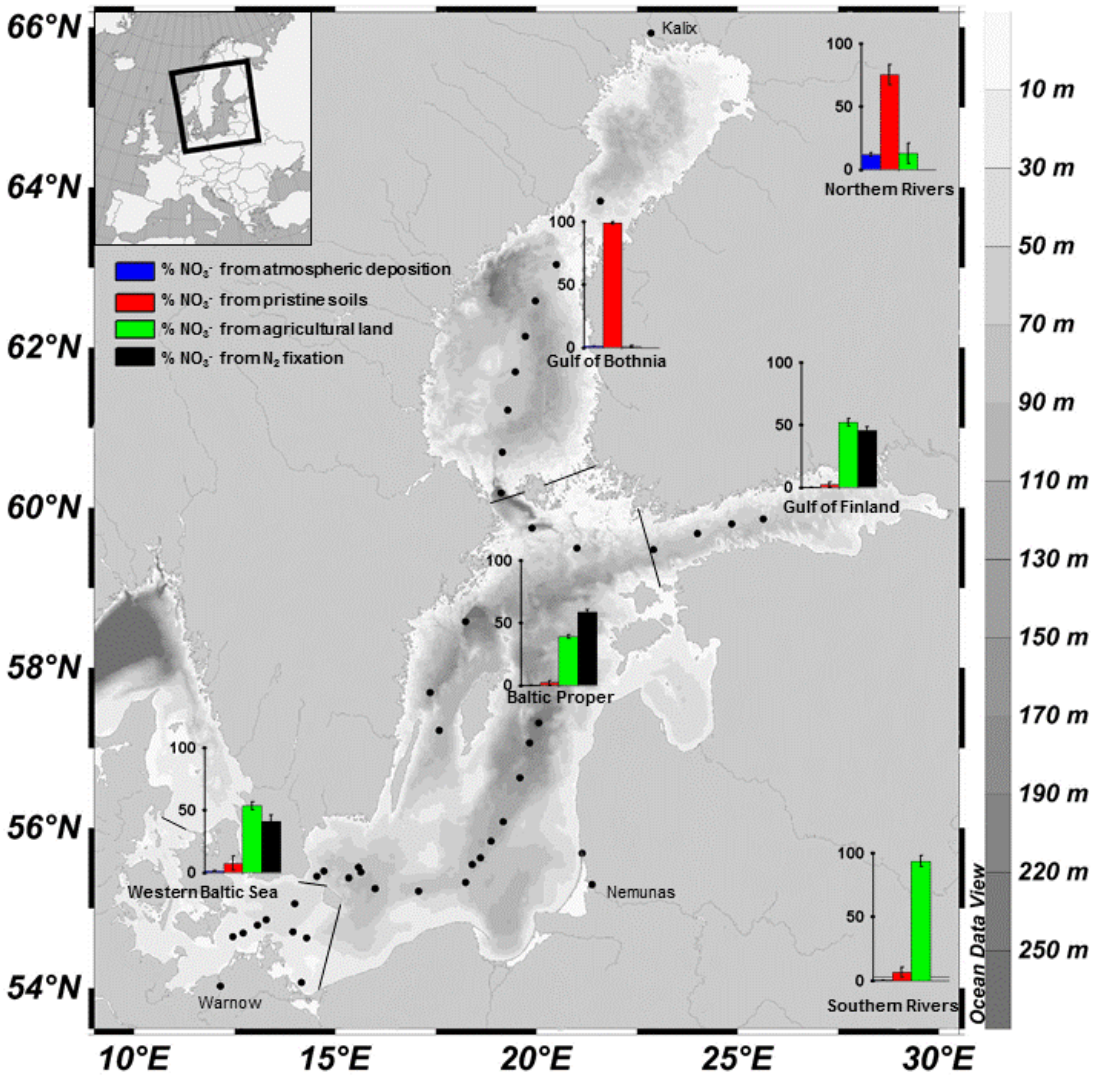

Figure 7: Station Map of the Baltic Sea and percent contribution of the four nitrate sources, NO_3^- from atmospheric deposition (blue), pristine soils (red), agricultural runoff (green), and N_2 fixation (black), for the Western Baltic Sea, Baltic Proper, Gulf of Finland, Gulf of Bothnia, southern rivers, and northern rivers. Stations are indicated as black dots. For more details see Suppl. Table S1.

1.3. Results

NO_3^- concentrations and isotopes

Winter (Nov.-Feb.) surface NO_3^- concentrations ranged from a minimum of 2.6 µmol l^{-1} in the open Baltic Sea to a maximum of 259 µmol l^{-1} close to the estuaries of the most nutrient-rich rivers, i.e., the Nemunas and Warnow Rivers (Fig. 8, supplemental Table S1). In most basins of the Baltic Sea, the NO_3^- concentrations in winter were almost identical, with the exception of the Gulf of Finland, where concentrations were about two-fold higher (7.6±0.9 µmol l^{-1}; Fig. 8). In the western Baltic Sea, the Baltic Proper, and the Gulf of Bothnia NO_3^- concentrations were similar with 3.3±0.6, 3.4±0.8, and 3.7±0.4 µmol l^{-1}, respectively.

Highest nitrate concentrations in the Nemunas River also corresponded to the highest δ^{15}N-NO_3^- with 10.0 ‰ and vice versa, with lowest concentrations and nitrogen isotope values in the Baltic Proper (1.5 ‰). The δ^{18}O-NO_3^- values ranged from -2.8 ‰ in the Gulf of Bothnia to 10.6 ‰ in the Northern River, Kalix (Fig. 8, Table S1).

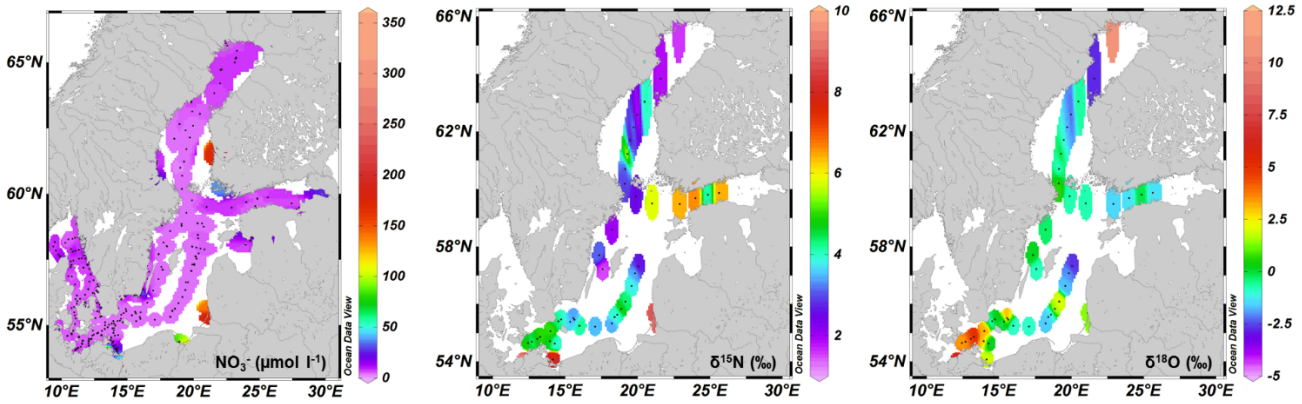

Figure 8: Surface water column NO_3^- concentrations (A), δ^{15}N-NO_3^- values (B), and δ^{18}O-NO_3^- values (C) for the Baltic Sea. Stations are indicated as black dots. Additional NO_3^- concentrations were obtained from the Data Assimilation System (DAS) (http://nest.su. se/das/) in winter (Nov.–Feb.) of the years 2000 to 2012.

Sources of NO_3^-

SIAR calculated that in the southern Baltic Sea, agricultural runoff was the main NO_3^- source with the highest contribution in the western Baltic Sea with up to 67 % (mean 53.5±3.2%) and in the southern rivers with up to 100% (mean 93.5±4.1%) (Table 6, Fig. 7). NO_3^- from atmospheric deposition was negligible with 3.5% (mean 1.1±0.5%) and NO_3^- from pristine soils lower with up to 42% (mean 7.5±5.9%) in the western Baltic Sea (Table 6, Fig. 7). In the Baltic Proper, NO_3^- from N_2 fixation was the dominant NO_3^- source with up to 65.3% (mean 58.8±2.0%) (Table 6, Fig. 7). In the northern Baltic Sea NO_3^- from atmospheric deposition is only important in the northern rivers with a contribution of up to 23.4% (mean 11.8±1.5%) (Table 6, Fig. 7). NO_3^- from pristine soils is mainly transported by the northern rivers (75.3±7.9%) to the Gulf of Bothnia where SIAR calculated that 99.0±0.9% stems from the runoff from pristine soils (Table 6, Fig. 7).

Table 6: Source attribution results: Mean, standard deviation, and minimum and maximum values for the potential contributions of four potential NO_3^- sources for the areas Western Baltic Sea, Baltic Proper, Gulf of Finland, Gulf of Bothnia, southern rivers, and northern rivers.

Area	NO_3^- from atmospheric deposition		NO_3^- from pristine soils		NO_3^- from agricultural runoff		NO_3^- from N_2 fixation	
	Mean±SD	Min-Max	Mean±SD	Min-Max	Mean±SD	Min-Max	Mean±SD	Min-Max
Western Baltic Sea	1.1±0.5	0.0–3.5	7.5±5.9	0.0–42.0	53.5±3.2	41.0–66.5	37.9±5.1	11.0–51.9
Baltic Proper	0.1±0.1	0.0–0.9	2.1±1.9	0.0–14.7	39.0 ±1.6	32.8–45.5	58.8±2.0	49.3–65.3
Gulf of Finland	0.2±0.2	0.0–2.0	2.4±2.1	0.0–24.3	51.9±3.0	40.9–63.4	45.5±3.2	32.7–59.0
Gulf of Bothnia	0.1±0.1	0.0–0.5	99.0±0.9	91.7–100.0	1.0±0.9	0.0–8.2	-	-
Southern rivers	0.2±0.1	0.0–1.3	6.4±4.2	0.0–24.5	93.5±4.2	75.2–100.0	-	-
Northern rivers	11.8±1.5	6.6–23.4	75.3±7.9	33.8–92.8	12.9±8.1	0.0–57.2	-	-

Comparison of isotope patterns in the water column and sediments

The$\delta^{15}N$ values from surface water correlated significantly with those from surface sediments, as reported in Voss et al. (2005) ($p<0.001$) (Fig. 9). Stations for sediment sampling were in close vicinity to stations from water column sampling (Fig 10). In the Baltic Proper, the $\delta^{15}N$ of the surface water NO_3^- was indistinguishable from the $\delta^{15}N$ of the sediment surface (3.6±1.0‰ and 3.5±0.6‰, respectively; Table 7). In the near-coastal areas of the Baltic Proper and the Gulf of Finland, the $\delta^{15}N$of surface water NO_3^- was 7.9±1.8‰, slightly higher than the surface sediment value for the same area of 7.3±2.1‰ (data in Voss et al., 2005) but still not significant different ($p<0.01$) (Table 7).

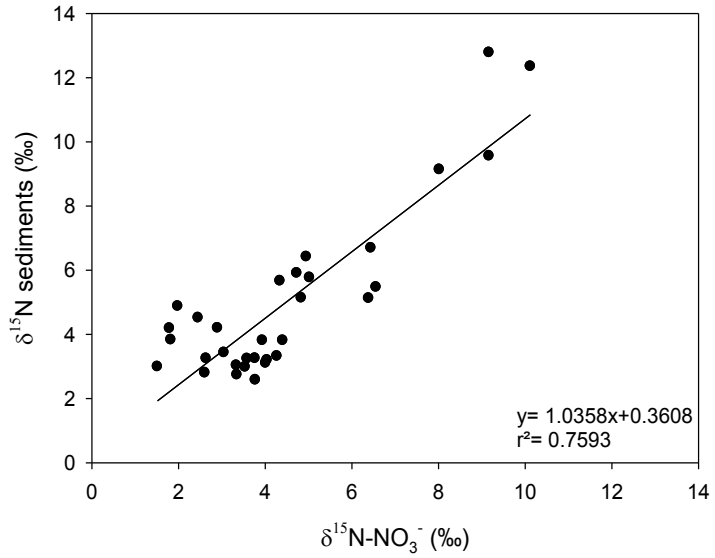

Figure 9: $\delta^{15}N$ from sediment samples vs. $\delta^{15}N$- NO_3^- from surface water samples. $\delta^{15}N$ values from sediments were taken from Voss et al. (2005). The positive slope suggests a tight coupling between $\delta^{15}N$- NO_3^- in surface waters and $\delta^{15}N$ in sediment samples.

Table 7: Comparison of $\delta^{15}N$-NO_3^- values from surface water samples and $\delta^{15}N$ values from sediments samples in sub-regions of the Baltic Sea.

	Baltic southern coastal areas/ Gulf of Finland	Central Baltic Proper	
$\delta^{15}N$ sediments (‰)	7.3 ± 2.1	3.5 ± 0.6	Voss et al. 2005
$\delta^{15}N$-NO_3^- surfacewater column (‰)	7.9±1.8	3.6 ± 1.0	This study

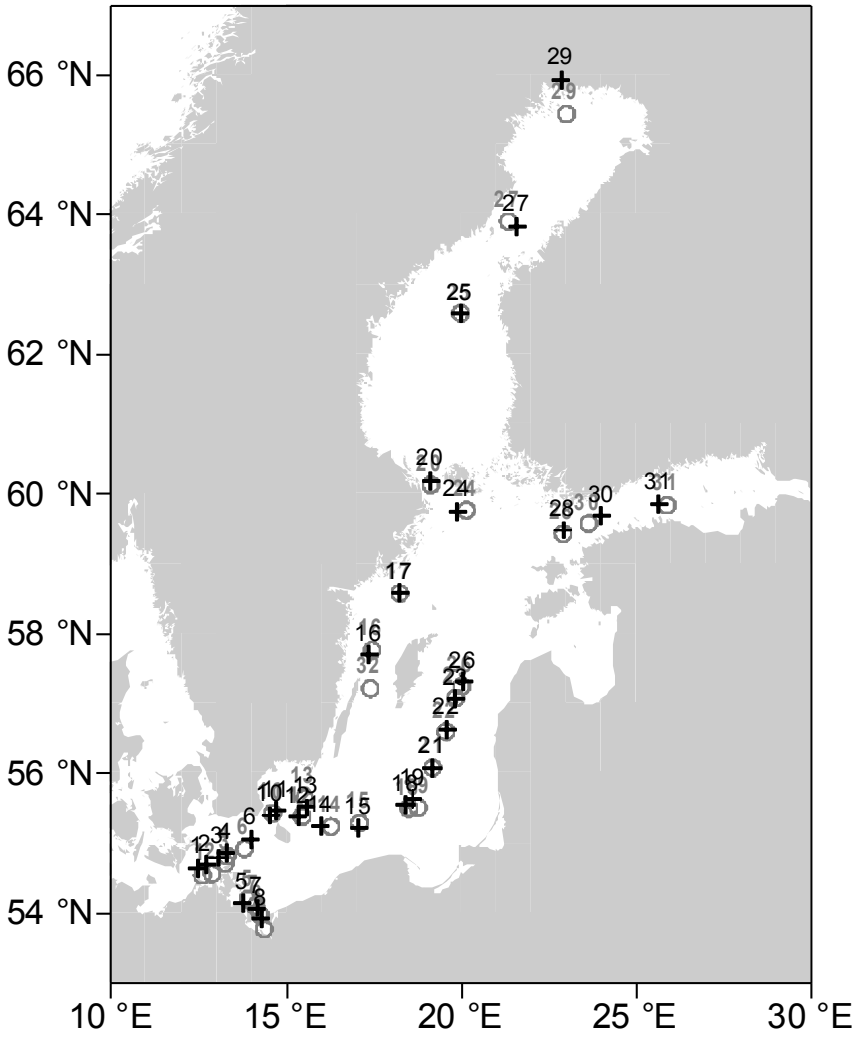

Figure 10: Station map for the comparison of isotope patterns in the water column and sediments. Gray circles are the stations referred to in Voss et al. (2005) and black crosses are those from this study. Isotope values were compared at stations with the same number.

1.4. Discussion

NO_3^- in the Baltic Sea

The measured winter surface water concentrations of up to 259 µmol l^{-1} are typical for eutrophied systems and similar values have been reported from the Chesapeake Bay and the coastal areas of the North Sea (Dähnke et al., 2010; Francis et al., 2013). The concentrations of nutrients in the sub-basins of the Baltic Sea reflect the densities of the human populations in the vicinity of the adjacent sub-catchments. Thus, in the near-coastal area of the southern Baltic Proper, NO_3^- concentrations were higher than in the northern parts, since the catchment areas of Germany, Poland, and the Baltic States are much more densely populated (>500 inhabitants km^{-2}) and the land is intensively used for agricultural purposes. The northern regions are dominated by boreal forests and less populated (<10

inhabitants km^{-2}) (Stepanauskas et al., 2002; Lääne et al., 2005; Voss et al., 2011). Consequently, for the southern Baltic Proper a relationship between fluvial NO_3^- loads and NO_3^- concentrations in coastal waters could be established that indicates a direct impact of riverine nutrients on coastal waters (Voss et al., 2011; HELCOM, 2009). However, there was no similar correlation between riverine N loads and nutrient concentrations either for the coastal areas of the Gulf of Bothnia or for the open waters of the Baltic Proper (Voss et al., 2011). The Gulf of Bothnia is the only sub-basin in which the effects of eutrophication are so far minor, although Lundberg et al. (2009) and Conley et al. (2011) reported a degradation in the water quality from north to south and from the outer to the inner coastal area of the Gulf, with seasonal hypoxia at many sites. Trends of increasing nutrient levels should be interpreted as a warning signal for the future and highlight the need for management approaches based on sound knowledge of the many potential sources of NO_3^-.

In the Gulf of Finland, which is regarded as the most heavily eutrophied sub-basin of the Baltic Sea, a consequence of high receiving nutrient loads from the Neva River and the city of St. Petersburg (Lundberg, 2005), NO_3^- concentrations were about two-fold higher (7.6±0.9 µmol l^{-1}) compared to the rest of the Baltic Sea sub-basins, where concentrations in winter were almost identical. This shows that NO_3^- concentrations alone cannot be used to identify NO_3^- sources for the sub-basins; rather, stable NO_3^- isotopes values allow for accurate source determination, as we will show in the following sections.

Sources of NO_3^-

The use of NO_3^-stable isotopes for source identification is complicated when the mixing of multiple N sources with overlapping isotopic ranges occurs together with microbial processes such as nitrification, assimilation, and denitrification (Kendall, 1998; Wankel et al., 2006). In this study, we assumed that the effects of fractionation by microbial processes were negligible because all our samples were collected in winter, at a mean temperature of 3.1±1.3 °C (data not shown), when microbial activity is low (Pfenning and McMahon, 1997), as confirmed in a study of nitrification in the Baltic Sea by Jäntti et al. (2011). They showed that in the Gulf of Finland although nitrification potentials may be high during cold months, in situ nitrification is undetectable whereas the rate increases progressively towards the summer.

We are aware that the variability of the source signals must be taken into account in source attributions. Both Xue et al. (2012, 2013) and Yang et al. (2013) showed that SIAR can be applied in NO_3^- source identification, although the resolution of this model is largely determined by the uncertainty of the isotopic composition of the sources. In the studies of both groups, the means and variances of the sources were calculated mostly from literature values, which were not obtained in the investigation areas, nevertheless they received consistent results. In contrast, in our study, the isotopic composition of the sources, except NO_3^- from N_2 fixation, was determined from samples obtained within the study area. In our calculations we considered the impact of the variability of the sources and report not only mean values and error estimates but also minimum and maximum contributions, as suggested by Fry (2013) (Table 6).

NO_3^- from agricultural runoff

The isotopic values of riverine NO_3^- were previously shown to be enriched when agricultural land is the source of inputs (Johannsen et al., 2008; Mayer et al., 2002; Voss et al., 2006). Catchments with high percentages of agricultural and/or urban land use export NO_3^- with $\delta^{15}N\text{-}NO_3^-$ values of around 7‰. In the same study,the oxygen isotope ratios of NO_3^- were almost uniformly 13±1‰ (Mayer et al., 2002). Johannsen et al. (2008) measured $\delta^{15}N\text{-}NO_3^-$ values of 11.3‰ in highly eutrophied rivers draining into the North Sea, whereas the highest $\delta^{18}O\text{-}NO_3^-$ value was 2.2‰. In the Oder River outflow, a main NO_3^- contributor to the Baltic Sea, $\delta^{15}N\text{-}NO_3^-$ of 7.6‰ and $\delta^{18}O\text{-}NO_3^-$ of 2.9‰ were determined (Korth et al., 2013). Our measurements for the Warnow and Nemunas Rivers fall in the expected range, with a mean $\delta^{15}N\text{-}NO_3^-$ of 9.2‰ and a mean $\delta^{18}O\text{-}NO_3^-$ of 3.1‰, and are consistent with the high percentages of agricultural land in the river catchment areas: 50% for the Warnow River (Pagenkopf, 2001) and 50% for the Nemunas River (Christoph Humborg, personal communication, 2011). For both, SIAR calculations indicated that 75.2–100% (mean 93.5±4.2%) of the NO_3^- pool is from agricultural runoff. NO_3^- with this signature seems to be transported to the central Baltic Sea, since SIAR-based estimates showed significant percentages of agriculturally derived NO_3^- in the Western Baltic Sea (41.0–66.5%; mean: 53.5±3.2%), the Baltic Proper (32.8–45.5%; mean: 39.0±1.6%), and the Gulf of Finland (40.9–63.4%; mean: 51.9±3.0%). However, high percentages were only expected for the Gulf of Finland and the Western Baltic Sea, where large N loads from agricultural land have been

documented (Hong et al., 2012). Indeed, for the Baltic Proper, the sizeable contribution of agricultural NO_3^- (39.0±1.6%) was surprising and contrasted with previous findings that nearly excluded riverine NO_3^- as a major nutrient source for the central Baltic Sea (Voss et al., 2005, 2011). However, Neuman (2000) estimated that 13% of the N input of the Oder River is transported to the central Baltic Sea, while Radtke et al. (2012) could show, using a source attribution technique in the three-dimensional ecosystem model ERGOM (Ecological ReGional Ocean Model), that at least a part of the dissolved inorganic nitrogen (DIN) load from the Vistula River, the main NO_3^- contributor to the Baltic Sea (Wulff et al., 2009), enters the Baltic Proper. This 3D model comprises a circulation model, a thermodynamic ice model, and a biogeochemical model and utilizes the Modular Ocean Model, MOM3.1 (Radtke et al., 2012).

Another explanation for the high estimated agricultural influence in our study could be the intrusion of water containing NO_3^- with similar NO_3^- isotope values as our agricultural NO_3^- source during mixing/advection from below the halocline. Deep-water NO_3^- in the Baltic Sea has a $\delta^{15}N$ of about 7‰ (Frey et al., 2014), which is higher than the average deep-water ocean NO_3^- signature of 5‰ (Sigman et al., 2000). This elevated $\delta^{15}N$ in NO_3^- mainly comes from water column denitrification in the oxic-anoxic interface in water at a depth of about 100 m (Dalsgaard et al., 2013). However, the year-to-year variations in DIN due to vertical mixing and advection from below the halocline are sensitive to hydrographic conditions. When the halocline is weak and well ventilated, oxygen conditions improve, resulting in higher DIN concentrations in deep waters and greater advection and/or mixing (Vahtera et al., 2007) such that the NO_3^- contribution from below the halocline is difficult to estimate.

Overall, the range of 32.8–45.5% (mean: 39.0±1.6%) determined for NO_3^- presumably originating from agricultural runoff has to be considered with caution, because the former imprint of deep water column denitrification and mixing/advection of this isotopically enriched $NO_3^-$from below the halocline with the residual winter surface NO_3^- pool could have resulted in an overestimation of the percentage of NO_3^- from agricultural runoff in the Baltic Proper.

NO_3^- from N_2 fixation

The average $\delta^{15}N$-NO_3^- value of 3.6‰ for the Baltic Proper is slightly lower than the ocean average of around 5%(Sigman et al., 2000) and presumably reflects the influence of N_2

fixation. This is because the $\delta^{15}N$ of newly fixed N is between -2 and 0‰ such that NO_3^- has slightly lower $\delta^{15}N$ values (Liu et al., 1996; Knapp et al., 2005). The $\delta^{18}O$-NO_3^-value of -0.5‰ in the Baltic Proper is also slightly lower than the ocean average of 1.5‰, and close to our theoretical considered value of -0.7±2.9‰ after the degradation and remineralization of N_2 fixers.

N_2 fixers are abundant in summer, reflecting the stimulation of their growth by the low N/P ratios.N in the cyanobacterial biomass is remineralized over the winter months and the resulting NO_3^- remains in the water masses down to the halocline. Our results show that the contribution of N_2 fixation by diazotrophs to the NO_3^- pool is 49.3–65.3% (mean 58.8±2.0%). This is slightly higher compared to the data reported by Wasmund et al. (2001), who estimated that 39% (370 ktons yr^{-1}) of a total input of 955 ktons N yr^{-1} (HELCOM, 2002) stems from N_2 fixations in the central Baltic Sea. Both Radtke et al. (2012) and Voss et al. (2005) concluded that N_2 fixation was the main NO_3^- source in the Baltic Proper. Using an independent approach, we were able to confirm the contribution of N_2 fixation in this area. In addition, we found that N_2 fixation is also a major source of NO_3^- in the Western Baltic Sea and the Gulf of Finland (respectively, 11.0–51.9% (mean 37.9±5.1%) and 32.7-59.0% (mean 45.5±3.2%)). This finding is consistent with our current understanding of N_2 fixation in the Gulf of Finland (Vahtera et al., 2005) whereas the western Baltic Sea is rather perceived as an area with no N_2 Fixation activity (Stal et al., 2003). In summary, our results provide important evidence that N_2 fixation by cyanobacteria is a significant N source not only in the Baltic Proper but also in the Western Baltic Sea and Gulf of Finland.

NO_3^- from atmospheric deposition

NO_3^- from atmospheric deposition is generally heavily enriched in ^{18}O (>60‰) because of reactions involving ozone (O_3), which is anomalously enriched in heavy oxygen isotopes(Durka et al., 1994; Kendall et al., 2007). This is consistent with the $\delta^{18}O$ measurements at the three stations around the Baltic Sea, where the averaged isotope value in winter was 77‰ (Table 4).

Our results show that direct inputs of atmospheric deposition contribute less NO_3^- than all other sources. Indeed, among all basins of the Baltic Sea, that has a total area of 415.266 km², the maximum mean contribution was in the Western Baltic Sea 0 to 3.5% (mean 1.1±0.5%). Moreover, using a dataset from Michaels et al. (1993), Duce et al. (2008)

estimated that even an extremely rare and large atmospheric deposition event distributed over a 25-m mixed-layer depth would increase the reactive N concentration only by around 0.045 µmol l^{-1}. A study in the Kattegat estimated an input of 52 kt N yr^{-1} from atmospheric deposition, which implied rather limited nutritional support for phytoplankton (Spokes et al., 2006). Taking into account that in the Baltic Proper, with an area of 211.069 km², in winter the mixed-layer depth is 80–100 m and that the residual NO_3^- pool, with a concentration of 3.6 µmol l^{-1},has a $\delta^{18}O\text{-}NO_3^-$ of -0.5‰, a similar rain event with a $\delta^{18}O$ of 76.7‰ (Table 7) would increase the $\delta^{18}O\text{-}NO_3^-$ of the residual NO_3^- pool only by 0.2–0.3‰, which is within our analytical error. Even though several rain events typically occur during winter, their influence seems to be too low to leave a detectable isotopic imprint. Additionally, the NO_3^- from atmospheric deposition is presumably intensively cycled through the organic N pool in spring and summer such that after several mineralization cycles its origin is difficult to recognize isotopically (Mayer et al., 2002).

In the Kalix River $\delta^{18}O\text{-}NO_3^-$ was clearly enriched (10.6‰) compared to the values determined for the Baltic Sea. We calculated that in this river up to 23.4% (mean 11.8±1.5%) of the NO_3^- originates from atmospheric deposition. Mayer et al. (2002) compared the isotopic NO_3^- signature of 16 watersheds in the USA and were able to show that riverine NO_3^- derived from atmospheric NO_3^- deposition and not from nitrification in soils is the dominant N input in predominantly forested watersheds, when riverine NO_3^-concentrations are generally low. Therefore only in the Kalix River, where up to 97% of the catchment with a size of 18.130 km² is covered by forests and NO_3^- concentrations are low during winter (Voss et al., 2011), was the imprint of NO_3^- from atmospheric deposition visible; by contrast, in the southern Baltic Sea and the rivers draining into it, the anthropogenic influence due to agriculture is very high and therefore masks atmospheric contributions. However, NO_3^- loads to the northern Baltic Sea from the Kalix River and other, similar boreal rivers are small, comprising only about 20% of the sea's total N load (Voss et al., 2011). Thus, overall, we assume that atmospheric deposition is a very minor source of NO_3^- in the Baltic Sea.

NO_3^- from pristine soils

In general, in rivers such as the Kalix River, whose catchments include pristine vegetation, $\delta^{15}N\text{-}NO_3^-$ values are low while those of $\delta^{18}O\text{-}NO_3^-$ are high (Voss et al., 2006). This finding was confirmed in the present study, in which$\delta^{15}N\text{-}NO_3^-$ and $\delta^{18}O\text{-}NO_3^-$ values of

1.6‰ and 10.6‰, respectively, were determined. In the Kalix River, the NO_3^- contribution from the runoff of pristine soils as determined by SIAR is 33.8–92.8% (mean 75.3±7.9%). In pristine soils the isotopic NO_3^- signal is mainly derived from nitrification, which is in agreement with previous studies of small catchments, where much of the NO_3^- was shown to be of microbial origin (Campbell et al., 2002; Mayer et al., 2002; Kendall et al., 2007). Similar $\delta^{15}N\text{-}NO_3^-$ values were reported for areas where pristine soils were also sampled. For example, $\delta^{15}N\text{-}NO_3^-$ and $\delta^{18}O\text{-}NO_3^-$ values of 1.9 and 2.8‰ were determined for Biscuit Bay (Burns et al., 2009) and 2.9 and 2.8‰ for the San River(Koszelnik and Gruca-Rokosz, 2013), respectively. The higher $\delta^{18}O\text{-}NO_3^-$ values of the Kalix River can, as discussed above, be attributed to atmospheric deposition.

For the Gulf of Bothnia, where the catchment is dominated by pristine areas like forests (50%) and shrubs (20%), NO_3^- from pristine soils contributes 91.7–100% (99.0±0.9%). However, for the Baltic Proper the NO_3^- contribution from pristine soils is negligible, because the NO_3^- derived from nitrification is very low in concentrations and remains in the Gulf because of the cyclonic circulation in the Bothnian Sea and Bothnian Bay (Humborg et al., 2003) and the high residence time of the water (7.4 years) which results in a rather slow exchange with the rest of the Baltic Sea (Myrberg and Andrejev, 2006).

Comparison of isotope patterns in the water column and sediments

Correlations between $\delta^{15}N$ values from the water column and surface sediment is a common feature in coastal basins, like Cariaco Basin (Thunell et al., 2004), Guaymas Basin, Monterey Bay, and San Pedro Basin (Altabet et al., 1999). This occurs when NO_3^- in the surface mixed layer is fully consumed, which is the case in the Baltic Proper during the spring bloom, when the only significant loss comes from the sinking of particulate nitrogen (Altabet et al., 1999). Moreover, high organic matter preservation seems to stimulate the similarity in the $\delta^{15}N$ in the surface water and sediments as seen in other depositional environments (Thunell et al., 2004).

Overall, the comparison with the sediment data set from Voss et al. (2005) shows that the isotopic signature of NO_3^- in the euphotic layer of the Baltic Sea is directly transferred to the particulate organic nitrogen pool and is subsequently found in the sediment surface as detritus, thus conserving information about the origin of this NO_3^-

source. Additionally, we could show how consistent the nitrogen input to the sediments is over the years. Even though, our surface water samples were sampled from 2008 to 2011, the surface sediment samples from 1993 to 2003 and deposited in the period of approximately 10 years before collection, the comparison of the $\delta^{15}N$ values showed that there is no significant difference. Coastal areas preserve the isotope signature of riverine sources while the open Baltic Sea sediments indeed mirror the nitrogen input dominated by N_2 fixation. Moreover the data demonstrate that no change over time in the input of NO_3^- sources has occurred.

1.5. Conclusions

By combining dual isotope data of winter NO_3^- ($\delta^{15}N$-NO_3^- and $\delta^{18}O$-NO_3^-) in surface waters with a Bayesian isotope mixing model (SIAR), we estimated the contribution of four major NO_3^- sources for the different basins of the Baltic Sea. A clear shift in the source of NO_3^- inputs, from agricultural sources in the south to runoff from pristine soils in the north, was identified. However, we could not fully determine how much of the agriculturally derived NO_3^- entering the Baltic Sea finally ends up in the open waters of its central region,where the addition of deep-water NO_3^- with similar isotope values might falsely, indicate a higher contribution. However, we were able to show that N_2 fixation is an important NO_3^- source in the central Baltic Sea while the contribution of NO_3^- from atmospheric deposition is only a minor one.

Because they are particularly sensitive to human pressure and global climate change, marginal seas, including the Baltic Sea, will no doubt be affected by the increases in temperature and precipitation predicted for the near future (BACC, 2008). Indeed, increasing atmospheric depositions of NO_3^- in the world's oceans have already been reported, by (Duce et al., 2008; Kim et al., 2011) and, may impact northern catchments of the Baltic Sea to a larger extent. Additionally, in coastal waters under increasing eutrophication pressure theefficiency of NO_3^- removal was shown to be reduced (Mulholland et al., 2008; Lunau et al., 2012), and this additional NO_3^-may alter the biogeochemical cycle. Therefore, the identification of NO_3^- sources, especially as anticipated in response to global climate change, is important for future environmental management strategies for the Baltic Sea and other marine environments. We suggest that with an adaption of the potential sources the

approach used in this study can easily be applied in other environments where NO_3^- is a major N contributor.

Chapter 2

Close coupling of N-cycling processes expressed in stable isotope data at the redoxcline of the Baltic Sea

Frey, C., Dippner J.W., Voss M.

Global Biogeochemical Cycles, **28**, 974-991

doi:10.1002/2013GB004642.

Abstract

Over the past decades,the hypoxic state of the central Baltic Sea has deteriorated because of eutrophication, but little is known about the extent to which related factors such as nitrogen removal have been altered. The Baltic Sea is a stratified semi-enclosed basin with a large, anoxic bottom-water mass in its central Gotland Basin and highly active microbial nitrogen transformation processes at the redoxcline, the interface between oxic and anoxic waters. In this study, we identified and quantified the dominant transformation processes of reactive nitrogen by exploiting fine-resolution profiles of $\delta^{15}N_{NO3}$,$\delta^{18}O_{NO3}$, and $\delta^{15}N_{NH4}$ through the pelagic redoxcline between 60 and 140 m. Our results showed increasing $\delta^{15}N_{NO3}$ and $\delta^{18}O_{NO3}$ values with decreasing nitrate concentrations, but the associated low apparent isotope effect (ε = ~5 ‰), as inferred from a closed system Rayleigh model, was not consistent with the high ε (~25 ‰) characteristic of denitrification in the water column. These findings could be explained by substrate limitation. The observed $\delta^{18}O_{NO3}$:$\delta^{15}N_{NO3}$ ratio of 1.38:1 rather than the usual 1:1 ratio typical for denitrification-dominated systems could be explained by the occurrence of both nitrification and denitrification We then developed a numeric reaction-diffusion model, according to which a realistic denitrification rate of 14 nmol N L^{-1} d^{-1} was estimated and a nitrification rate of 6.6 nmol N L^{-1} d^{-1} confirmed.Our study demonstrates the value of stable isotope data for investigating nitrogen transformation processes but also highlights that care is needed in interpreting systems with closely coupled processes such as those at ocean redoxclines.

2.1. Introduction

Oxygen-deficient zones (ODZs) have expanded globally since the 1960s (Diaz and Rosenberg, 2008; Stramma et al., 2008). They account for 30–50 % of oceanic nitrogen (N) loss and thus significantly counteract the accumulation of N in the oceans resulting from an excess N supply (Codispoti et al., 2001; Brandes and Devol, 2002; Gruber and Galloway, 2008). ODZs occur not only near upwelling areas but also in coastal and marginal seas with permanent or temporal stratification, such as the Black Sea, the CariacoBasin, and the Baltic Sea. They harbor unique microbial communities that rely on alternative electron acceptors for respiration when oxygen concentrations are low (Lam and Kuypers, 2011). Threshold

values for NO_3^--dependent respiration are below 2–4 µmol O_2 L^{-1}(Devol, 1978), although denitrifying activity has been reported at O_2 concentrations up to 20 µmol L^{-1}(Smethie and William, 1987; Lam and Kuypers, 2011). N_2 gas is produced by denitrification and by anammox, although the substrates required for these processes differ. In anammox reactions nitrite and ammonium are used to generate N_2 gas (Dalsgaard et al., 2003; Kuypers et al., 2003, 2005); in heterotrophic denitrification, nitrate is reduced during the degradation of organic material, while in chemolithoautotrophic denitrification sulfide serves as the electron donor(Lipschultz et al., 1990; Bange et al., 2000; Fuchsman et al., 2012).

Analyses of stable N isotopes in nitrate have greatly enhanced our understanding of the global balance of N sources and sinks (Brandes and Devol, 2002; Deutsch et al., 2004). They have allowed the use of isotope fractionation, in the form of an enrichment factor (ε), as a biochemical tracer and thus to gain insights into the controlling reactions. Difficulties in resolving the $\delta^{15}N_{NO3}$ budget with only one tracer prompted the addition of a second one, $\delta^{18}O_{NO3}$, to investigate the fixed N budget in marine systems (Casciotti et al., 2002; Sigman et al., 2005). This approach is possible because $\delta^{18}O_{NO3}$ and $\delta^{15}N_{NO3}$ are differentially sensitive to nitrate production and consumption, as outlined below.

Denitrification of dissolved nitrate in the water column is associated with a large isotope effect. Because ^{14}N and ^{16}O are preferentially consumed by microbes,the residual substrate pool is enriched, as reflected in the increased values of $\delta^{15}N_{NO3}$ and $\delta^{18}O_{NO3}$($^{15\text{ or }18}\varepsilon$ = 20–30 ‰) (Brandes et al., 1998; Kendall and McDonnell, 1998; Voss et al., 2001; Sigman et al., 2005). In contrast, sedimentary denitrification has little or no effect on nitrate isotope values in the overlying water column, because porewater nitrate consumption proceeds to completion under diffusion-limited conditions (ε = 0–5 ‰) (Brandes et al., 1998; Lehmann et al., 2007). Similarly, if denitrification is limited by the rate of nitrate supply, the observed ecosystem-level (apparent) isotope effect will be reduced in the water column of stratified, semi enclosed basins like the Cariaco Basin (Thunell et al., 2004) or in stratified lakes (Wenk et al., 2014). Also, in denitrifying cultures, a change in conditions, such as nutrient availability, small inputs of oxygen, or agitation, may reduce the apparent ε outside the cell compared to the enzyme-level isotope effect (Kritee et al., 2012). In marine systems, the kinetic isotope effects of denitrification are nearly identical for $\delta^{15}N_{NO3}$ and $\delta^{18}O_{NO3}$, and the $\delta^{15}N$ and $\delta^{18}O$ values of the residual nitrate increase in a 1:1 ratio(Sigman et al., 2005; Granger et al., 2008). Deviations above unity have been attributed to additional N-

transforming processes such as nitrification (Sigman et al., 2005; Wankel et al., 2009; Dähnke et al., 2010).

Nitrification is a two-step process in which ammonium is oxidized first to nitrite and then to nitrate by distinct groups of nitrifying microorganisms. Nitrification of ammonium or nitrite differentially affects the resulting $\delta^{15}N_{NO3}$ and $\delta^{18}O_{NO3}$ valuesand leads to the decoupling of these isotopesfrom the 1:1 ratio imparted by denitrification.The kinetic isotope effect for the first step of nitrification, the oxidation of ammonia to nitrite, is $^{15}\varepsilon_{NH4}$ = 14–38 ‰. Hence, this step contributes isotopically light N to the nitrite pool, if NH_4^+ is not completely consumed. However, the subsequent oxidation of nitrite to nitrate favours the heavier isotope, leading to inverse fractionation such that ε_{NO2} ~ −13 ‰ and ~ −7 ‰, for nitrogen and oxygen, respectively (Casciotti et al., 2003, 2010; Casciotti, 2009; Buchwald and Casciotti, 2010). The reason is that heavy isotope substitution stabilizes the transition state, making it more likely to react to nitrate (Casciotti, 2009). The net effect of complete nitrification is a relative depletion of residual $\delta^{15}N_{NO3^-}$, which opposes the relative enrichment of $\delta^{15}N_{NO3}$ associated with denitrification. Hence, in systems in which both nitrification and denitrification occur, the competing effects of the two processes may be difficult to distinguish based on ^{15}N isotopes of NO_3^- alone. By exploiting the dual isotope composition ($\delta^{15}N$ and $\delta^{18}O$) of nitrate the relative contributions of nitrification and denitrification in the transformation of nitrate isotopes under hypoxic conditions can be distinguished.

The permanently stratified basins of the central Baltic Sea reflect freshwater inputs at the surface and a strong halocline that prevents mixing of the upper oxygenated waters with the deeper anoxic and sulfidic waters. The bottom of the anoxic basin is periodically ventilated by saltwater inflowsfrom the North Sea but during periods of stagnation hydrogen sulfide (H_2S) accumulates below the halocline (Matthäus et al., 2008). This gives rise to an intermediate layer characterized by strong vertical redox gradients. Here, the hypoxic zone is defined as the horizon where O_2 concentrations are below 20 µmol L^{-1}(Paulmier and Ruiz-Pino, 2009). The redoxcline is located at the lower boundary of that layer and is therefore much smaller. It is defined as the depth at which measureable oxygen concentrations vanish and/or sulfide appears. In the Gotland Basin (central Baltic Sea), the depth of the redoxcline fluctuates on timescales of hours to days, in response to forcing by internal waves (Reissmann et al., 2009). This horizon shows a substantial loss of dissolved inorganic nitrogen

(DIN; nitrate, nitrite, and ammonium) (Brettar and Rheinheimer, 1991; Dalsgaard et al., 2013), driven by sulfide-dependent nitrate reduction, a feature unique to the Baltic Sea redoxcline (Rönner and Sörensson, 1985; Brettar and Rheinheimer, 1991; Hannig et al., 2006). Chemolithoautotrophic denitrification is an apparently dynamic process in which irregular bursts of N removal coincide with both the entrainment of oxygen and nitrate generation (Hietanen et al., 2012; Dalsgaard et al., 2013). The irregular pattern accounts for the difficulty in capturing denitrification activity in ^{15}N incubation experiments and in obtaining annual estimates of N removal (Hietanen et al., 2012). Anammox plays a negligible role in the redoxcline of the Baltic Sea, presumably because the responsible bacteria are sulfide-sensitive (Hannig et al., 2007; Hietanen et al., 2012). Above the redoxcline, there is intense nitrification activity (Hietanen et al., 2012) and the high-level expression of archaeal nitrification genes (AmoA) has been reported (Labrenz et al., 2010). Archeal nitrifiers have been found in environments with low oxygen, and even sulfidic conditions, unlike bacterial nitrifiers (Coolen et al., 2007; Erguder et al., 2009).

The presence of nitrification and sporadic denitrification at the same depth horizon complicates the evaluation of N losses in the Baltic Sea redoxcline. Therefore, the aim of this study was to clarify N dynamics in the redoxcline by making use of data on the natural abundance of the stable isotopes. This approach integrates all N transformation processes and thus offers an alternative to studying the fate of N using labeled substrates. Specifically, we used the distributions of $\delta^{15}N_{NO3}$, $\delta^{18}O_{NO3}$, and $\delta^{15}N_{NH4}$ throughoutthe redoxcline to evaluate the relative importance of nitrification and denitrification. Additionally, a closed-system (Rayleigh distillation) model was used to evaluate isotopic fractionation, and a numeric dynamic reaction-diffusion model was developed to better understand the stable isotope values and to quantitatively estimate the link between nitrification and denitrification within the pelagic redoxcline.

2.2. Material and Methods

Water sampling and nutrient analysis

Sampling was conducted in the central Baltic Sea from aboard the *R/VPenck* in July 2009, the *R/V Heincke* in June 2010, and the *R/V Pelagia* in May 2011 (Figure 11, Table 8). Samples were collected using a conductivity-temperature depth (CTD) rosette equipped with

5-L or 12-L Niskin bottles (Sea-Bird Electronics Inc). Water samples from finely resolved depths around the redoxcline were immediately analyzed for inorganic nutrients, O_2, and H_2S. NO_3^-, NO_2^-, NH_4^+, PO_4^{3-}, and O_2 were measured after the methods of Grasshoff(1983); the detection limits were 0.01, 0.01, 0.3, 0.01, and 1 µmol L^{-1}, respectively. H_2S was determined spectrophotometrically after the method of Fonselius (1983), with a detection limit of 0.02 µmol L^{-1}. Nutrients and H_2S were measured in 2011 with the QuAAtro continuous flow analyzer. Water samples of 1–2 L collected from each depth were filtered through precombusted GF/F filters (Whatman). Filters for the analysis of δ^{15}Nin particulate organic nitrogen (PON) and the filtrate for $\delta^{15}N_{NO3}$, $\delta^{18}O_{NO3}$, and $\delta^{15}N_{NH4}$ analyses were stored frozen at −20°C until further processing.

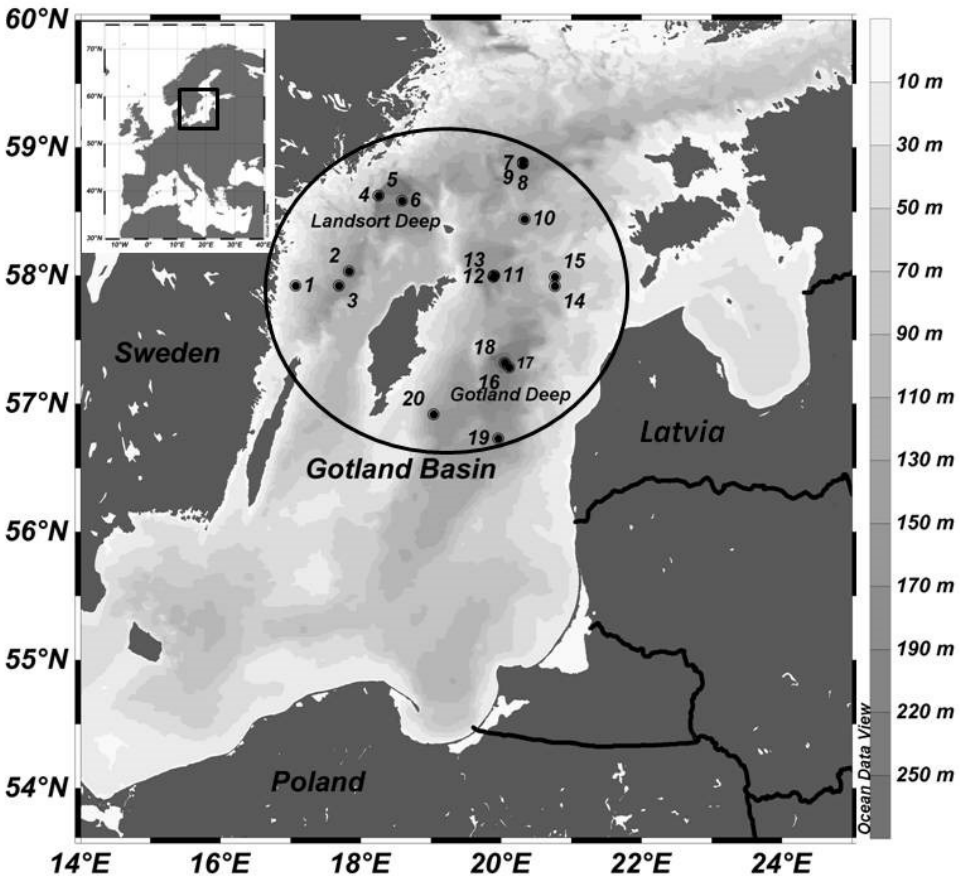

Figure 11: Study site in the central Baltic Sea showing all profiles sampled during the R/V Penck cruise of 2009 (stations 9,10,11,16,19,20), the R/V Heincke cruise of 2010 (stations 1,2,5,6,7,12,14,17), and the R/V Pelagia cruise of 2011 (stations 3,4,8,13,15,18).

Table 8: Sampling stations and their environmental parameters

Profile #	Year	Cruise	Station name	Station depth	Station distance to basin margin	Redoxcline depth	Hypoxic zone thickness	$[NO_3^-]$ (at max.)	NO_3^- max. thickness [1]	$\delta^{15}N$ - NO_3^- of NO_3^- max.	$\delta^{18}O$ - NO_3^- of NO_3^- max.	$[NO_2^-]$ at SNM	$[O_2]$ at SNM
				m	km	m	m	µmol L^{-1}	m	‰	‰	µmol L^{-1}	µmol L^{-1}
1	2010	Heincke	GB1	145	6.8	75	-	4.68	30	7.2	0.6	0.1	10.58
2	2010	Heincke	GB2	107	16.4	82.5	11	4.61	37	5.9	0.6	0.3	5.63
3	2011	Pelagia	GB2	200	20.9	78	13.5	5.04	25	6.2	-0.7	0.1	0.4
4	2010	Heincke	LD	439	7.1	73	6	4.21	-	7.2	1.1	-	-
5	2010	Heincke	LD	186	25.	72.5	4	4.38	37.5	8.0	3.2	0.32	18.76
6	2011	Pelagia	LD	400	6.3	80	15.5	5.4	35	6.6	-1.2	1.5	1.3
7	2009	Penck	LL19	180	29.8	85	14.5	5.83	40	7.6	-2.8	0.34	0
8	2010	Heincke	LL19	168	29.5	85	12	4.84	45	6.2	4.2	1.56	2.68
9	2011	Pelagia	LL19	169	25.2	97	22	6.19	35	5.6	-1.8	0.9	0
10	2009	Penck	TF285	128	10	90	17	5.77	-	9.9	-1.8	0.24	0
11	2009	Penck	F80	203	17.04	100	21	5.8	40	8.1	-1.8	-	-
12	2010	Heincke	F80	191	16.29	100	31	4.8	40	11.4	1.6	1.97	2.46
13	2011	Pelagia	F80	191	12.5	123	46	5.99	35	5.1	-0.2	0.5	0.9
14	2010	Heincke	LF3	100	8.39	-	-	6.7	-	7.1	1.5	-	-
15	2011	Pelagia	LF3	95	6.26	82	9	6.3	35	4.5	0.0	-	-
16	2009	Penck	BY15	243	24.44	100	35	7.51	50	7.4	-1.0	0.36	4.91
17	2010	Heincke	BY15	233	20.27	130	33	7.30	75	6.9	1.5	-	-
18	2011	Pelagia	BY15	232	20.1	128	52	6.6	65	6.5	-1.0	0.7	0
19	2009	Penck	272	150	13.93	130	35	8.18	70	6.9	-0.9	0.23	19.18
20	2009	Penck	In3	170	7.13	117	8	8.09	60	6.5	-1.2	-	-

SNM, secondary nitrite maximum; LD, Landsort Deep; BY15, Gotland Deep; F80, Fårö Deep; hypoxic zone, from <20 µmol O_2 L^{-1} until the first occurrence of H_2S; [1] NO_3^- maximum thickness measured from the first appearance to the disappearance of NO_3^-

Isotope analysis

For $\delta^{15}N_{PON}$ analysis, the filters were dried at 60°C, packed into tin cups, and measured online using a continuous flow-isotope ratio mass spectrometer (CF-IRMS, Finnigan Delta S, Thermo) connected to an elemental analyzer (CE1108) via an open split interface (Finnigan Conflow II). The ultrapure N_2 reference gas for stable isotope analysis was calibrated by means of IAEA standards and a Peptone (laboratory standard) is interspersed in each analytical run to control the isotopic composition. Delta values are given for nitrogen with respect to dinitrogen (N_2). The standard error for the $\delta^{15}N_{PON}$ data was < 0.2 ‰. Isotope values are expressed as per mil (‰) with respect to the standard (Eq. 1):

$$\delta^{15}N = \left(\frac{\left[\frac{^{15}N}{^{14}N} \right]_S}{\left[\frac{^{15}N}{^{14}N} \right]_R} - 1 \right) \times 1000 \quad (1)$$

where S is the sample and R is the reference gas calibrated against the IAEA standards.

$\delta^{15}N_{NO3}$ and $\delta^{18}O_{NO3}$ were analyzed according to the denitrifier method (Sigman et al., 2001; Casciotti et al., 2002) and N_2O was measured using a gas bench connected to a CF-IRMS system (Delta Plus, Thermo). The method makes use of the N_2O-reductase-deficient bacterial strain *Pseudomonas aureofaciens* (ATTC 13985), which quantitatively converts NO_3^- and NO_2^- to N_2O. The sample volume was always adjusted to obtain a final N_2O concentration of 10 nmol. The analytical precision was ± 0.2 and ± 0.8 for the $\delta^{15}N_{NO3}$ and $\delta^{18}O_{NO3}$ values, respectively. The standards were USGS 34 ($\delta^{15}N$ = −1.8 ‰ vs. atmospheric N_2; $\delta^{18}O$ = −27.9 ‰ vs. VSMOW (Vienna standard mean ocean water)) and IAEA N3 ($\delta^{15}N$ = 4.7 ‰ vs. atmospheric N_2; $\delta^{18}O$ = 22 ‰ vs. VSMOW) for correction with the blank and for oxygen isotopic exchange with water [*Böhlke et al.*, 2003, *McIlvin and Casciotti,* 2011]. Only samples with NO_3^- > 1 µmol L^{-1} were analyzed. The denitrifier method implicitly measures the isotope composition of combined NO_3^- and NO_2^-. If NO_2^- is abundant, the reported isotopic composition may be biased by the NO_2^- in the sample. When the percentage of NO_2^- is > 2 % of the NO_3^- concentration, the oxygen isotope correction leads to an analytical artifact due to calibration with nitrate reference material (Casciotti et al., 2007), reflecting the method's differential isotopic discrimination of oxygen atoms that results in different offsets between NO_2^- or NO_3^- and the N_2O generated from either molecule during the analysis (Casciotti and McIlvin, 2007). Corrections were not applied to the data sets from the cruises in 2009 and

2010 because sample storage (frozen at −20°C) was not appropriate for the conservation of NO_2^- and the determination of its isotope composition (Casciotti et al., 2007). Therefore, $\delta^{18}O$ values were not used if the relative amount of NO_2^- in the NO_3^- pool exceeded 2 %, which occurred when a secondary nitrite maximum was present. For $\delta^{15}N$ values in NO_3^-, this exclusion was not necessary. In 2011, sample collection was modified to remove NO_2^- with sulfamic acid immediately after sampling, which enabled the consideration of all $\delta^{18}O_{NO3}$ data (Granger and Sigman, 2009). To annotate the difference clearly in the following text, all samples from which NO_2^- was not removed are designated NO_x (NO_3^- + NO_2^-) and $\delta^{15}N_{NOx}$; samples from which NO_2^- was removed are designated NO_3^- and $\delta^{15}N_{NO3}$.

For the analysis of $\delta^{15}N_{NH4}$,NH_4^+ was extracted from samples containing >1 µmol ammonium L^{-1} according to a modified procedure of Velinsky et al.(1989). NH_4^+ was extracted by distilling > 50% of a basic sample (pH > 10) into an acid trap, with subsequent capture on a zeolite molecular sieve. The zeolite was filtered onto a precombusted GF/F filter, which was dried at 60°C overnight and then subjected to IRMS. Two blanks and three standards were prepared for each set of 10–15 samples. Sample concentrations of NH_4^+ were between 1 and 10 µmol L^{-1}. The isotope composition in the solid NH_4Cl standards was determined by their direct combustion. Solid and liquid standards compared well, with values of −1.07 ‰ and −1.08 ‰, respectively, verifying that fractionation did not occur during sample processing. The $\delta^{15}N$ value of the NH_4^+ standard has an error of 0.4 ‰ (n = 36). The blank contained 0.6 ± 0.1 µmol N L^{-1} (n = 26); a blank correction, after Fry et al.(1992), was applied. Only samples with a recovery rate of 75–125 % were used.

Isotopic fractionation using the Rayleigh model

To define the isotopic fractionation factor ε, a simple Rayleigh model for closed systems was applied (Mariotti et al., 1981). This model follows the relationship shown in Eq. (2) and assumes that the isotope effect associated with denitrification (ε) is constant:

$$\delta^{15}N_{substrate(t=n)} = \delta^{15}N_{substrate(t=0)} + \varepsilon \ln(f) \quad (2)$$

It makes use of the $\delta^{15}N$ of the substrate at a given time point (t=n) and at the beginning of the reaction (t=0). The variable f is the fraction of the substrate pool that is left unreacted. It is defined as the substrate concentration (t = n) c_t divided by the initial substrate concentrationc_0 (c_t/c_0). Thus, the slope of the regression line of $\delta^{15}N_{substrate}$ or $\delta^{18}O_{substrate}$ as a

function of ln[f] yields the isotopic enrichment factor ε(Mariotti et al., 1981, 1988). $\delta^{15}N_{NO3,t=0}$ from the nitrate maximum area was used as the starting value for our model exercise because it lies at the upper boundary of the denitrification zone and is the source of nitrate for further transformation in the hypoxic zone. The average values were 7.0 ± 1.5 ‰ for $\delta^{15}N_{NO3,t=0}$ and 0.1 ± 1.8 ‰ for $\delta^{18}O_{NO3,t=0}$.

A common tool to estimate c_0 is N*, which quantifies the deviation of the NO_3^-:PO_4^{3-} ratio from the Redfield stoichiometry of 16:1. N* has been used as an indicator of denitrification in the global open ocean (Gruber et al., 1997; Deutsch et al., 2001). Potentially, it also can be used to estimate the N-deficit in the Baltic Sea. However, because the anoxic waters of the Baltic Sea receive large quantities of additional PO_4^{3-} from the anoxic sediments and from the degradation of sinking particles (Conley et al., 2002; Jilbert et al., 2011), N* is typically severely overestimated. Therefore, rather than using N* to calculate f in Eq. (2), we estimated the fraction of unreacted nitrate as the deviation from of the maximum nitrate value in the profile from zero nitrate. This was done separately for each station. The uncertainty introduced by using t_0 values from the nitrate maximum will be evaluated.

Dynamic reaction-diffusion model

A non-linear numerical horizontal reaction–diffusion model was developed to evaluate isotope fractionation when coupled reactions such as nitrification and denitrification occurred. It was also used to estimate denitrification and nitrification rates as well as the respective fractionation factors. This extended version of the denitrification model of Voss et al. (2001) consists of four coupled non-linear reaction-diffusion equations, for $^{14}NO_3$, $^{15}NO_3$, $^{14}NH_4$, and $^{15}NH_4$ (Eqs. 7–10).

$$\frac{\partial}{\partial t}\left[{}^{14}NO_3\right] = A\frac{\partial^2}{\partial x^2}\left[{}^{14}NO_3\right] - J_D + J_N \tag{7}$$

$$\frac{\partial}{\partial t}\left[{}^{15}NO_3\right] = A\frac{\partial^2}{\partial x^2}\left[{}^{15}NO_3\right] - J_D\alpha_1 Q_1 + J_N\alpha_2 Q_2 \tag{8}$$

$$\frac{\partial}{\partial t}\left[{}^{14}NH_4\right] = A\frac{\partial^2}{\partial x^2}\left[{}^{14}NH_4\right] - J_N \tag{9}$$

$$\frac{\partial}{\partial t}\left[{}^{15}NH_4\right] = A\frac{\partial^2}{\partial x^2}\left[{}^{15}NH_4\right] - J_N\alpha_2 Q_2 \tag{10}$$

where J_D is the denitrification rate, J_N the nitrification rate, A the coefficient of horizontal eddy diffusivity, and ∂/∂t and $\partial^2/\partial x^2$ are partial derivatives in time and space. According to Mariotti et al.(1981), α_i is the fractionation factors for ^{15}N, which is related to the enrichment factors ε_i by:

$$\alpha_i = \exp(\varepsilon_i / 1000) \tag{11}$$

Q_i are the ratios:

$$Q_1 = \frac{\left[{}^{15}NO_3\right]}{\left[{}^{14}NO_3\right]} \qquad Q_2 = \frac{\left[{}^{15}NH_4\right]}{\left[{}^{14}NH_4\right]} \tag{12}$$

which make the system non-linear. The grid size of the model was Δx = 1 km. The model covered the area of the GotlandBasin horizontally from x = 0 to x =x_e. The boundary condition was the Dirichlet condition at x = 0, with the values obtained from observations (see section boundary conditions). At x = x_e, the von Neumann condition of $\partial/\partial x^{14}NO_3$ = $\partial/\partial x^{15}NO_3$ = $\partial/\partial x^{14}NH_4$ =$\partial/\partial x^{15}NH_4$ = 0 was applied. The initial values for the ratios Q_1 and Q_2 were also taken from measurements. The steady-state system was solved using a tridiagonal matrix solver (Roache, 1976).

2.3. Results

Hydrographic conditions in the central Baltic Sea

During the sampling cruises, a typical stratification prevailed in the central Baltic Sea but its extent differed between the eastern and western Gotland Basin (Figure 12; Table 8). The depth of the halocline varied between 55 m and 75 m (Figure 12).A steep vertical oxygen gradient characterized the western portion of the basin, with oxygen disappearing at 72–80 m (LD, profiles 4-6), whereas in the eastern portion the decrease was more gradual, with oxygen disappearing between 100 and 130 m (BY15, profiles 16–18; Table 8, Figure 12d). Hydrogen sulfide was first detected at 73 m and 137 m in the western and eastern Gotland Basin, respectively (Figure 12e).Based on a definition of the hypoxic zone of O_2<20 µmol L^{-1} until the first detection of H_2S (Paulmier and Ruiz-Pino, 2009), its thickness varied

from 52 m (profiles 7–20) to < 15.5 m (Table 8). Consequently, a specific depth (70–135 m) or density layer (6–9 kg m³) could be used to identify the hypoxic zone for individual profiles, but no single range of values defined the hypoxic zone over the entire basin (Figure 12). The distance of the stations from the margins of the basin ranged from 6.3 to 29.8 km (Table 8).

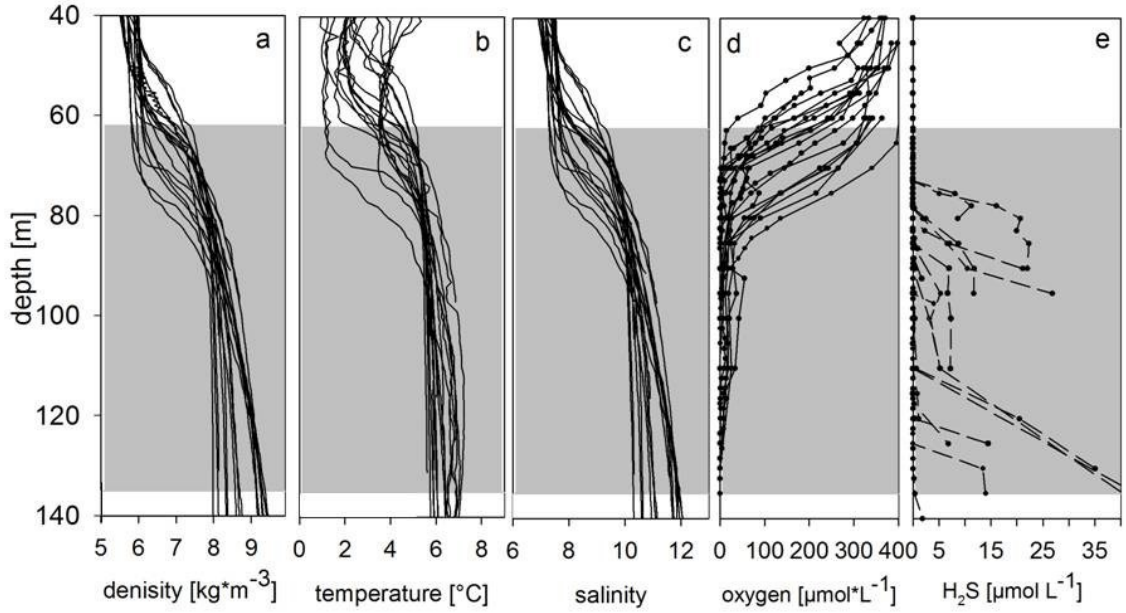

Figure 12: (a) Density, (b) temperature, (c) salinity, (d) oxygen (Winkler method), and (e) sulfide profiles of the stratified water body of the Gotland Basin.The gray shaded area indicates the range where the oxygen concentration is < 20 µM L^{-1} until the first detection of H_2S in a sample from at least one station.

Vertical and spatial distribution of nutrients/N species

Nitrogen compounds and the stable isotope data for one typical station in the eastern and in the western Gotland Basin are shown at different sampling times (6 profiles) to illustrate the general variability (Figures 13 and 14). An overview of all variables and all 20 profiles is given in Table 1. The maximum NO_3^- concentrations above the redoxcline (4.2–8.2 µmol L^{-1}; Table 1) were higher than the average winter concentration (2.8–3.9 µmol L^{-1}) in surface waters (Nausch et al., 2008). The different thicknesses of the hypoxic zones were best reflected in the vertical extent of the nitrate maximums, which varied from 37.5 m up to 75 m (Table 8). Below the NO_3^- maximum, NO_3^- concentrations decreased to below the detection limit at around 72 m (Figure 13a) and 135 m (Figure 14c), while an overlap of hydrogen sulfide and nitrate was only present in 13 out of 20 stations (data not shown). Ammonium was not present at the depth of the nitrate maximum and only began to

increase in the hypoxic zone, where it accumulated to concentrations above 5 µmol L^{-1} (Figure 13 and 14).

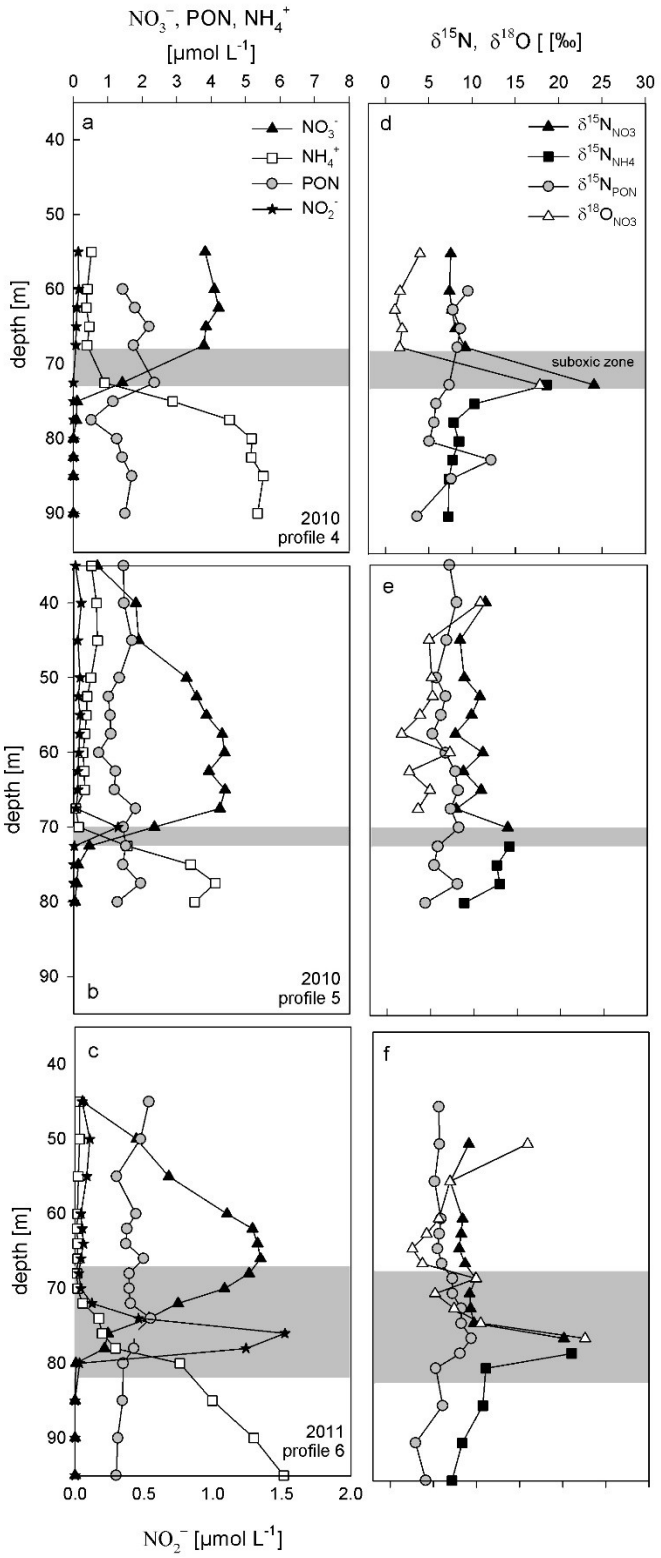

Figure 13: (a–c) Depth profiles from the western Gotland Basin of [NO_3^-], [NH_4^+], [PON], and [NO_2^-] and (d–f) the corresponding depth profiles at the Landsort Deep for $\delta^{15}N_{NO3}$, $\delta^{15}N_{NH4}$, $\delta^{15}N_{PON}$, and $\delta^{18}O_{NO3}$ during three different sampling periods (profiles 4–6). Shaded areas indicate the hypoxic zone, from an O_2 concentration of 20 µmol L^{-1} until the first appearance of H_2S, shown for each profile.

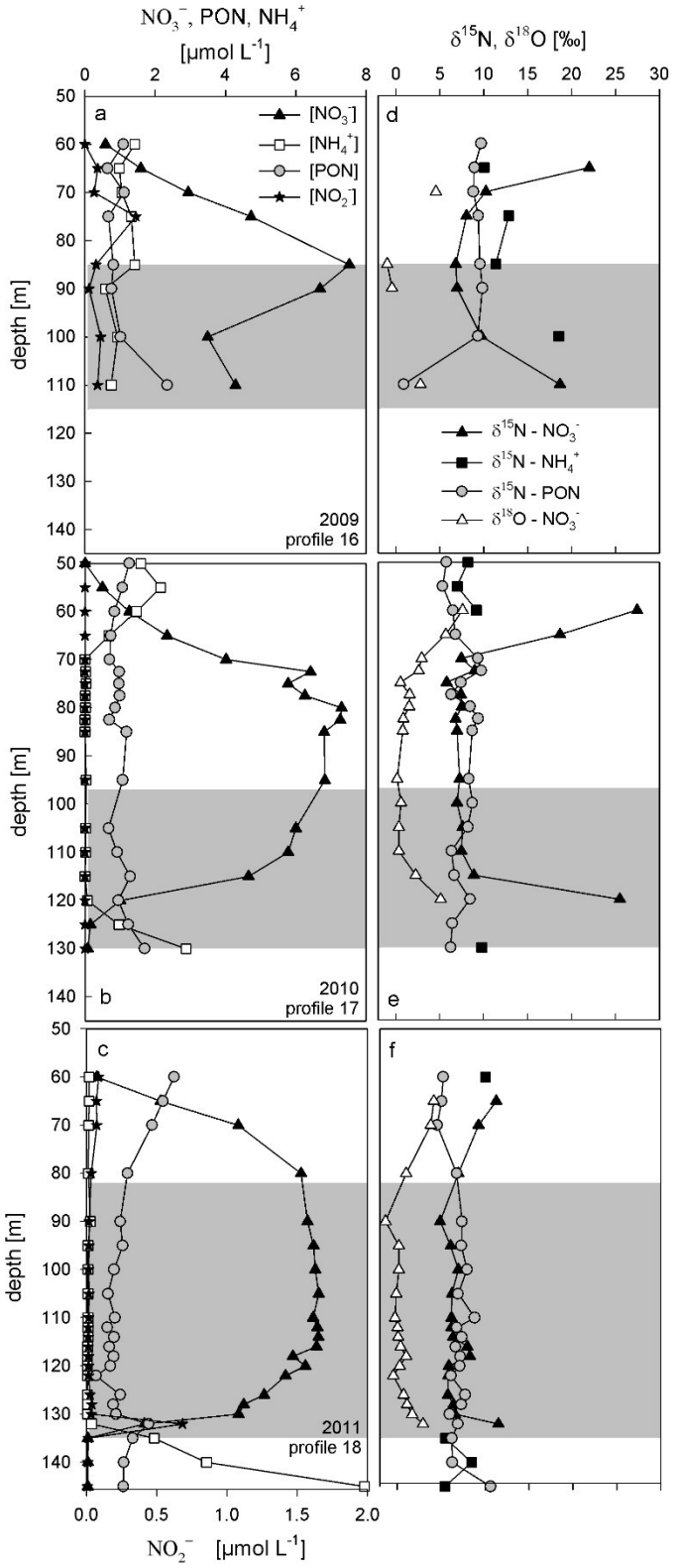

Figure 14: (a–c) Depth profiles from the eastern Gotland Basin of [NO_3^-], [NH_4^+], [PON], and [NO_2^-] and (d–f) the corresponding depth profiles at the Gotland Deep for $\delta^{15}N_{NO3}$, $\delta^{15}N_{NH4}$, $\delta^{15}N_{PON}$, and $\delta^{18}O_{NO3}$ during the three different sampling periods (profiles 16–18). Gray shaded areas indicate the hypoxic zone, from an O_2 concentration of 20 µmol L^{-1} until the first appearance of H_2S, shown for each profile.

NO_2^- is an intermediate product in nitrification and denitrification. A secondary nitrite maximum in hypoxic waters occurs when NO_2^- oxidation becomes the rate limiting step in nitrification or when denitrification is incomplete. In 2010, the highest secondary nitrite maximum (1.97 µmol L^{-1}) was measured at F80 (profile 12, Table 8). A maximum in NO_2^- was not detected at all of the stations, perhaps due to the spatial resolution of the sampling depths (2-m intervals). O_2 concentrations at the NO_2^- maximum were as high as 19.8 µmol L^{-1} (profiles 6, 8, 12 in Table 8) while in other published studies of ODZs a secondary nitrite maximum was detectable at O_2 concentrations below 1 µmol L^{-1}(Naqvi et al., 2008and references therein). High $\delta^{15}N_{NO3}$ values were takento indicate denitrification, even at oxygen concentrations >1 µmol L^{-1} and the boundary for the active denitrification zone is set to an oxygen concentration of 20 µmol L^{-1}.

Stable isotope data in nutrients and PON

$\delta^{15}N_{PON}$ data throughout the sampled depth horizons fluctuated around 7.4 ± 1.8 ‰ (Figures 13, and 14). The depth-related patterns of the $\delta^{15}N_{NO3}$ and $\delta^{18}O_{NO3}$ profiles were quite similar in the eastern and western Gotland Basin during all three years of sampling (Figures 13d–f, and 14d–f). Their average values at the maximum NO_3^- concentration were 7.0 ± 1.5 ‰ and 0.1 ± 1.8 ‰ for $\delta^{15}N_{NO3}$ and $\delta^{18}O_{NO3}$, respectively (Table 8). Both $\delta^{15}N$ and $\delta^{18}O$ varied over a wide range, from 5 to 35 ‰ and from −2 to 22 ‰, respectively (Figure 15). Above and below the nitrate maximum, the decrease in NO_3^- concentrations was associated with an increase in $\delta^{15}N_{NO3}$ and $\delta^{18}O_{NO3}$, although this relationship varied between profiles (Figures 13d–f, 14d–f). $\delta^{15}N_{NH4}$ values averaged 7.9 ± 1.9 ‰ in the upper anoxic zone (Figures 13 and 14) and increased up to 22 ‰ at the redoxcline (Figures 13 and 14).

At O_2 concentrations above 20 µmol L^{-1} there were no significant differences between $\delta^{15}N_{NO3}$ and $\delta^{15}N_{NOx}$ or between $\delta^{18}O_{NO3}$ and $\delta^{18}O_{NOx}$ (Figure 15b,d). At O_2 concentrations below 20 µmol L^{-1}, $\delta^{18}O_{NO3}$ was higher than $\delta^{18}O_{NOx}$ (Figure 15c), with maxima of 22 ‰ and 19 ‰, respectively (Figure 15c). The bias towards lower values when high amounts of NO_2^- were included in the analysis is particularly visible in the slope of only 0.47:1 for the linear regression of $\delta^{18}O_{NOx}$ vs. $\delta^{15}N_{NOx}$(Figure 16).The relative enrichments in $\delta^{18}O_{NO3}$ vs. $\delta^{15}N_{NO3}$ did not follow the 1:1 line typical for marine denitrification but showed a strong correlation, with a slope of 1.38 (Figure 16). Furthermore, based on the Rayleigh

model (Eq. 2) the isotope enrichments of $\delta^{15}N_{NO3}$ and $\delta^{18}O_{NO3}$ were ε_{15N} = - 4.7 ‰ and ε_{18O} = - 7.0 ‰ (Table 9).

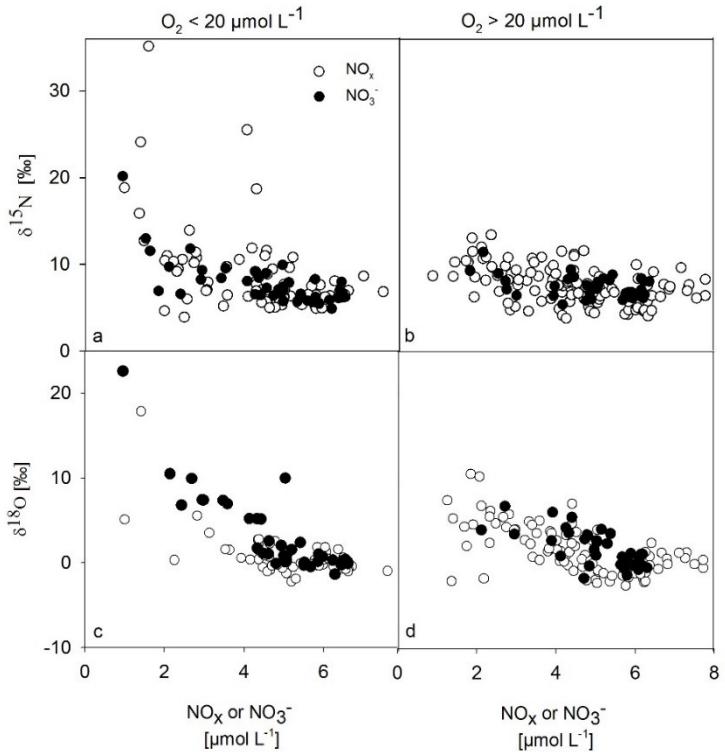

Figure 15: NO_3^- (black dots) and NOx (white dots) concentrations plotted against (a, b) $\delta^{15}N$ and (c, d) $\delta^{18}O$ for O_2 concentrations below (a, c) and above (b, d) 20 µmol L^{-1}.

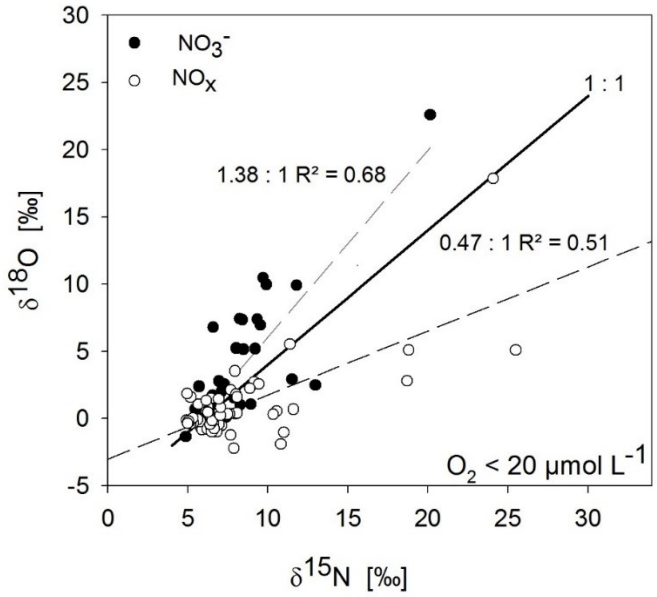

Figure 16: $\delta^{15}N$ vs. $\delta^{18}O$ for samples from the hypoxic zone. $\delta^{15}N_{NOx}$ and $\delta^{18}O_{NOx}$ are shown for all three sampling periods (white dots) and $\delta^{15}N_{NO3}$ and $\delta^{18}O_{NO3}$ for 2011 (black dots). Solid black line indicates the 1:1 increase known for marine denitrification. Regression lines are significant for NO_3^- ($p < 0.001$) and bulk NO_x ($p < 0.001$).

Table 9: Fractionation factors for denitrification in the hypoxic zone calculated from the slope of the regression line in a plot of ln[f] vs. the isotope values. Fractionation factors for nitrification were estimated from the slope of the regression line usinga plot of ln [NH_4^+] vs. the isotope values. For $\delta^{15}N_{NO3}$, $\delta^{18}O_{NO3}$, and $\delta^{15}N_{NH4}$,only the values from the 2011 study were used.

Zone	Process	Substrate	ε	R^2	n
< 20 µmol O_2 L^{-1}					
	Denitrification	$\delta^{15}N_{NO3}$	4.7	0.58*	43
		$\delta^{18}O_{NO3}$	7.0	0.45*	43
	Nitrification	$\delta^{15}N_{NH4}$	3.8	0.41	28

* Significant regression line for ln [substrate] vs. the isotope values ($p < 0.0001$)

Model details

The model set-up considers a stable hydrographic situation with no internal waves under steady state conditions. Under these conditions reliable rates are delivered. Nitrite accumulation and turnover are not specifically addressed.

Boundary conditions

The values for the Dirichlet boundary conditions at x = 0 were obtained from observations in which the NO_3 concentration was 5.5 µmol L^{-1} and $\delta^{15}N_{NO3}$ = 6.8 ‰. These boundary conditions are averages from the nitrate maximum of the modeled stations and were also used in the Rayleigh model. The sensitivity of the modeled parameters towards changes in the boundary conditions is described in supplemental Text S2. The boundary conditions of the NH_4^+ concentration and $\delta^{15}NH_4$ values were regressed from values in the oxic portion of the redoxcline (red line in Fig. 17a). As a boundary condition, the NH_4^+ concentration was determined to be 5 µmol L^{-1}, with $\delta^{15}N_{NH4}$ = 2.5 ‰. The main source of ammonium is diffusion from below; its generation during the remineralization of organic matter is not considered in the model.

Estimation of model parameters

The model has six parameters: the denitrification rate J_D, the nitrification rate J_N, the horizontal eddy diffusivity A, the horizontal extent of the Gotland Basin x_e, and the

fractionation factor α_i for NO_3^- and NH_4^+. Since the maximum distance between sampling stations was 242 km, x_e was set at 250 km.

In a first step, we modeled the ammonium isotope values provided by Equations 9 and 10. The parameters for the model were the nitrification rate, the coefficient of eddy diffusivity, and the NH_4^+ enrichment factor. A nitrification rate of J_N = 6.6 nmol N L^{-1} d^{-1}, which is slightly below the rate reported by Hietanen et al.(2012), was used as a fixed value. Thus, these equations, with two free parameters (eddy diffusivity and the NH_4^+ enrichment factor), are the only ones that could be unequivocally solved.

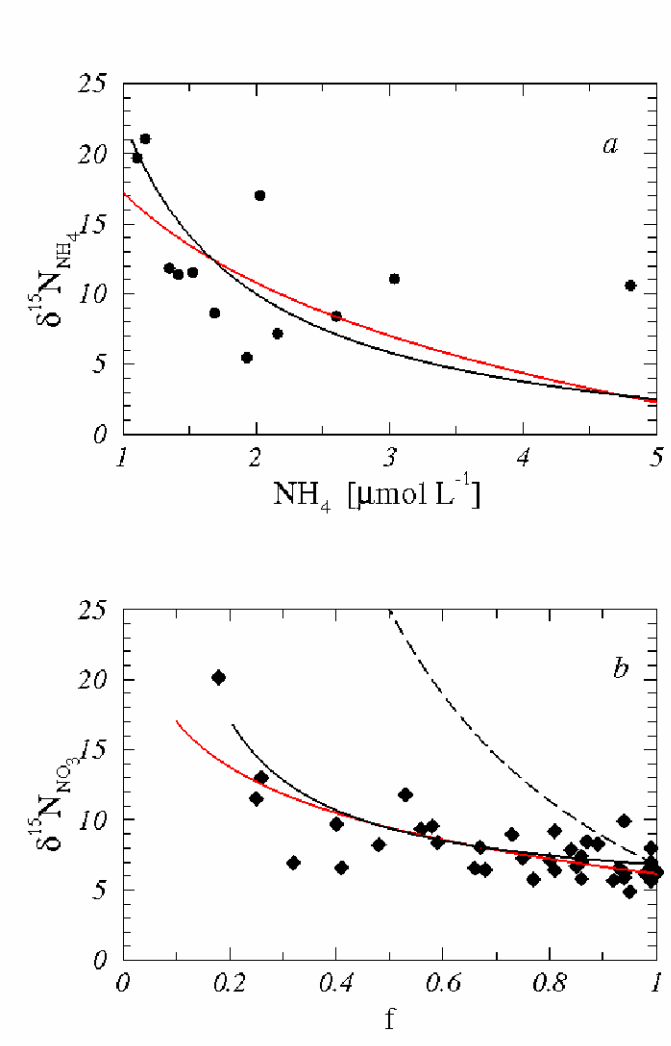

Figure 17: Model results for (a) $\delta^{15}N_{NH4}$ and (b) $\delta^{15}N_{NO3}$ (black lines) and independent samples from 2011 (symbols) with the corresponding data regression lines after Rayleigh (red lines). In (a), $\delta^{15}N_{NH4}$ was used to estimate the nitrification rate and the isotopic enrichment of nitrification in the model considering the 4.8 µmol L^{-1} NH_4^+ value as outlier. The equation for the data regression line is y = -9.288ln(x) + 17.236 with a R^2 = 0.35 (red line). In (b), the dashed line represents the model result with $\varepsilon_{denitrification}$ = −20 ‰ without nitrification, and the solid black line the model result with $\varepsilon_{denitrification}$ = −1.9 ‰ and $\varepsilon_{nitrification}$ = 8.5 ‰. The data regression line (red line) follows the equation y = -4.729ln(x) + 6.1692 with a R^2 = 0.58.

The best model simulation (black line in Fig. 17a) in relation to the Rayleigh plot (red line) was obtained using an isotopic enrichment factor of ε_2 = -8.5 ‰, which is in the range of −5 to −38 ‰ reported in the literature(Delwiche and Steyn, 1970; Miyake and Wada, 1971; Mariotti et al., 1981; Yoshida, 1988; Casciotti et al., 2003). The model is able to reproduce the observations using these parameters and an eddy diffusivity of A = 600 m^2s^{-1}, which depends on time and space scales as described in the literature. In the Gotland Sea, at a water depth of 200 m, estimates from tracer spreading rates over a period of days are on the order of 10 m^2s^{-1} on a 10-km scale (Holtermann and Umlauf, 2012). This value can be considered as the lower threshold value of horizontal eddy diffusivity. Investigations at the halocline in the Gotland Sea demonstrated the existence of large eddies at a water depth of 70–120 m, which indicates a much larger eddy diffusivity (Reißmann, 2005). Based on the ocean diffusion diagram of Okubo(1971) on a horizontal scale of 250 km and a time scale of weeks to months, the estimated coefficient of eddy diffusivity is 400–900 m^2s^{-1}. Thus, our selected eddy diffusivity is in that range.

In a second step, the above values were adopted and Equations 7–10 were used to estimate the denitrification rate and the NO_3^- enrichment factor. The best model simulation (Fig. 17b, black line) compared to an independent Rayleigh regression of $\delta^{15}N_{NO3}$ over f (red line) was obtained with a denitrification rate of J_D = 14 nmol N L^{-1} d^{-1} and an isotopic enrichment factor of NO_3^- of ε_1 = - 1.9 ‰. The sensitivity of these parameters is described in supplemental text S3.

Furthermore, we tested whether the model simulates the data under the assumption that denitrification is the only fractionation process acting in the redoxcline, with a typical denitrification factor of ε = −20 ‰. In the absence of nitrification, it was impossible to reproduce the observations (Fig. 17b dashed line).

2.4. Discussion

This study focuses on nitrogen turnover processes in the zone below the halocline with decreasing oxygen concentrations. To separate oxygen-dependent processes from those independent of oxygen, the zone was divided into an upper portion, with high O_2 concentrations, and a lower portion, with hypoxicconditions. In the oxic portion (>20 µmol

O_2 L^{-1}), NO_3^- is produced through nitrification while in the hypoxic portion (<20 µmol O_2 L^{-1}) NO_3^- reduction is the major N conversion process.

Processes in the oxic zone

The stable oxygen isotope data ($\delta^{18}O_{NOx}$) at the nitrate maximum in the oxic zone revealed that nitrate is mainly produced by nitrification and is not impacted by allochthonous nitrate sources such as atmospheric deposition. The deposited nitrate is characterized by $\delta^{18}O$ values as high as 80 ‰ and would be easily detectable in $\delta^{18}O_{NOx}$ data. The contribution of this nitrate source to the surface-water in the central Baltic Sea is negligible in winter (Korth et al., 2014) and very minor in summer (Rolff et al., 2008). Our sampling was always performed in summer, when a stable thermoclineprevents nitrate input from above. Furthermore, the discharge by major rivers into the Baltic Proper of up to 190 kt nitrate annually also does not directly reach the central Baltic Sea(Voss et al., 2005; Radtke et al., 2012). Hence, only internal recycling processes account for nitrate production at the studied depth interval.

$\delta^{18}O_{NOx}$ values in the Baltic Sea are lower than the average $\delta^{18}O_{NO3}$ values in the deep water of the open ocean (~ 0.1 ± 1.8 ‰ vs. 1.5–2.5 ‰) (Casciotti et al., 2002; Lehmann et al., 2005), because $\delta^{18}O_{H2O}$ in the central Baltic Sea is lower than that in the open ocean (−6 ± 0.4 ‰ vs. ~ 0‰; see sf5). A theoretical $\delta^{18}O_{NO3}$ for nitrate produced by nitrification in Baltic Sea seawater can be calculated according to previous studies where 5/6 moles of oxygen in seawater nitrate derive from water molecules ($\delta^{18}O_{H2O}$ of -6 ‰) and only 1/6 are from dissolved oxygen ($\delta^{18}O_{O2}$ of 23.5 ‰ (atmospheric value) (Bender, 1990)) (Sigman et al., 2005; Casciotti and McIlvin, 2007; Casciotti, 2009). Applying the ratio to our data resulted in a theoretical $\delta^{18}O_{NO3}$ valueof −1 ‰, which is in the range of our observations (Table 8). Our conclusion is consistent with the high nitrification rates reported by Bauer(2003) for this same depth horizon, despite slight uncertainties in the exact source of oxygen.

$\delta^{15}N_{NOx}$ values in the nitrate maximum were, on average, 7.0 ± 1.5 ‰ and isotopically similar to those in suspended particles at this depth (Figure 14), but higher than the average deep-water $\delta^{15}N_{NO3}$ content in the ocean (~5 ‰) (Wu et al., 1997; Sigman et al., 2000; Lehmann et al., 2005). In an open oceanic environment, the $\delta^{15}N$ in subsurface nitrate usually reflects the $\delta^{15}N$ of the sinking particles (Altabet and McCarthy, 1986; Altabet, 1988)

whereas the suspended PON pool becomes isotopically enriched due to processes such as macrozooplankton feeding below the mixed layer (Altabet and McCarthy, 1986; Altabet, 1988). In the Baltic Sea, sinking PON has an average $\delta^{15}N$ of 4.3 ± 0.7 ‰ (Wasmund et al., 2011) and is therefore isotopically lighter than the suspended pool. This is consistent with open ocean findings (Altabet, 1988), but the isotopic difference between the nitrate pool and the sinking particles cannot be easily explained. We can only speculate that the difference is related to the much shallower Baltic Sea compared to the open ocean and to the effects of zooplankton feeding and microbial processes on particulate matter of different sinking speeds. The isotopically enriched nitrate in the Baltic Sea may also reflect nitrogen removal during denitrification and the isotopic enrichment of nitrate, which is then mixed with the nitrate originating from the degradation of sinking particles.

Processes in the hypoxic zone

Chemolithoautotrophic denitrification is the major N loss process in the hypoxic zone (Brettar and Rheinheimer, 1991) whereas heterotrophic denitrification is of minor importance (Dalsgaard et al., 2013). The anammox process, by which ammonium and nitrite react to yield N_2, hardly occurs in the Gotland Basin, due to the high H_2S concentrations (Hietanen et al., 2012; Dalsgaard et al., 2013). Dissimilatory nitrate reduction to ammonium (DNRA) is also likely to play only a minor role since it is mostly coupled to anammox, which provides the necessary NH_4^+(Lam et al., 2009; Ward et al., 2009).

We found an apparent underexpression of the N isotope effect in the stable isotope values of nitrate (Table 9) and a higher ratio of $\delta^{18}O$ to $\delta^{15}N$ enrichment associated with nitrate reduction (Figure 16). The following potential reasons for the low community fractionation factor are considered in detail below: 1) nitrate/substrate-limiting conditions, and potential overestimation of the fraction of NO_3^- removed and the role of its initial $\delta^{15}N$, 2) a low organism-level isotope effect for chemolithoautotrophic denitrification, 3) the impact of sedimentary denitrification on the overall nitrate pool, and 4) the co-occurrence of nitrate generation (nitrification) with nitrate removal.

Low apparent isotope enrichment for nitrate reduction

The stability of interfaces in the water column exerts considerable influence on nutrient dynamics because these interfaces separate the water body from rapid vertical exchange processes and from the oxygen supply (Lam and Kuypers, 2011; Dalsgaard et al., 2013). In the world's largest ODZs, the eastern tropical North Pacific, the eastern tropical South Pacific,and the Arabian Sea, apparent enrichment factors for denitrification are as high as ε = 30 ‰ (Brandes et al., 1998; Voss et al., 2001; Ryabenko et al., 2012) (Table 10), similar to the intrinsic/organismal isotope effect reported for heterotrophic denitrifying cultures (Barford et al., 1999; Fuchsman et al., 2008; Granger et al., 2008 and references therein). In the hypoxic zone of the Baltic Sea, the apparent enrichment factor of ε_{15N}, estimated using the Rayleigh closed-system approach, was 4.7 ‰, whereas the observed $\delta^{15}N_{NO3}$ was 35.1 ‰ (similar to values in other anoxic basins, Table 10). The difference between the ODZs and the Baltic Sea can be explained by the dynamics of open ocean systems, where the apparent isotope effect of denitrification is not significantly influenced by the denitrification rate but by the nitrate pool, which is constantly resupplied by advection (Brandes et al., 1998; Voss et al., 2001; Sigman et al. 2005). In small stratified anoxic basins, however, nitrate fractionation is apparently much lower since the pool of PON or NH_4^+ is small and turns over rapidly, resulting in a constant resupply of only small amounts of nitrate (Lehman et al., 2003; Thunell et al., 2004). In the Santa Barbara Basin (ε_{15N} = 5 ‰) and the Cariaco Basin (ε_{15N} = 1.5 ‰), the apparent isotope effect of denitrification based on the Rayleigh model was also lower than in the open ocean, and more similar to that at the redoxcline of the Baltic Sea (Sigman et al., 2005; Thunell et al., 2004). This feature of a small, rapidly consumed pool of nitrate was already reported in sediments, where it resulted in similarly low fractionation values (Brandes and Devol, 1997; 2002; Lehman et al., 2004).

Table 10: Summary of NO_3^- isotope values in the hypoxic zones as reported in the literature and in this study.

Region	*Hypoxic zone*	*Max. $\delta^{15}N$ [‰]*	*Max. $\delta^{18}O$ [‰]*	*$\varepsilon^{15}N$ (Rayleigh)*	*$\varepsilon^{18}O$ (Rayleigh)*	*References*
ETNP	ODZ	16	-	25	-	Brandes et al.,(1998); Sigman et al.,(2003)
ETNP	ODZ	18.7	-	30 ± 7.5	-	Voss et al.,(2001)
ETNP	ODZ	15	12	18.9	18.9	Sigman et al.,(2005)
ETSP	ODZ	22	-	11.5	-	Ryabenco et al.,(2012)
ETSP	ODZ	31	27	18-22	14-22	Casciotti et al.,(2013)
Arabian Sea	ODZ	11	-	22	-	Brandes et al.,(1998)
Arabian Sea	ODZ	26	23	34.5	28.8	Gaye et al.,(2013)
Black Sea	Permanently anoxic basin	18	-	-	-	Fuchsman et al.,(2008)
Cariaco Basin	Permanently anoxic basin	9	-	1.5	-	Thunell et al.,(2004)
Lake Lugano - south basin	Seasonally anoxic	27.2	15.7	11.2	6.6	Lehmann et al. 2003
LakeLugano - north basin	Permanently anoxic basin	~ 25	~ 17	9.1 ± 0.6	8.0 ± 0.8	Wenk et al. 2014
Santa Barbara Basin	Hypoxic basin	12	6	5	-	Sigman et al. 2003
Baltic Sea	Anoxic basin	35.1	22.3	4.7	7.0	this study

ETNP, eastern tropical North Pacific; ETSP, eastern tropical South Pacific

The fractionation factor δ is robust against changes in the width of the hypoxic zone. A smaller hypoxic zone results in lower initial concentrations of nitrate and a smaller fraction of nitrate that is removed.When the zone of denitrification is smaller (e.g., 0–5µmol L^{-1} oxygen instead of 0–20µmol L^{-1}oxygen) the fractionation factor increases slightly, i.e. to ε=5.2‰ rather than 4.7‰. If the initial $\delta^{15}N_{NO3}$ is only 5‰, as in the case of deep-ocean nitrate, ε_{15N} increases up to 6.1 ‰. Hence, the bias in ε_{15N} introduced by the initial nitrate values is low, ±1.5 ‰, and ε_{15N} is still far below the fractionation factors of open ocean ODZs.

Modeling of the isotope fractionation of well-constrained water layers requires an open system approach. In the Cariaco Basin, Thunell et al., (2004) were able to reproduce measured $\delta^{15}N_{NO3}$ values by applying a reaction-diffusion model, using an εfor denitrificationof 25 ‰. The denitrification model of Voss et al., (2001), which is similar to that of Thunell et al.,(2004), provides similar denitrification results for the open eastern tropical North Pacific. However, the fractionation factor used in the denitrification model of Voss et al., (2001) is not applicable to the complicated conditions of the Baltic Sea (Figure 17b, dashed line). In contrast to the open ocean, the Baltic Sea has a small nitrate pool and advection is minor, such that an additional nitrate source has to be considered. Accordingly, we extended the model by the inclusion of two ammonium equations (Eqs. 9, 10) and by that, taking into account the process of nitrification (see sect.Close coupling of nitrification and denitrification).

For a provision of nitrate and sulfide simultaneously, vertical mixing must occur on very small but recurrent time scales, which indeed seem to be characteristic of the oxic-anoxic interface of the Baltic Sea (Lass, 2003). When hypoxic water containing NO_3^- mixes with the sulfidic waters below the redoxcline, all of the NO_3^- is rapidly denitrified (Brettar and Rheinheimer, 1991; Dalsgaard et al., 2012), in which case intrinsic N isotope fractionation will be small. Hence, substrate limitation may partially account for the underexpression of the N isotope effect.

The lower apparent enrichment factor in the Baltic Sea compared to other open ocean ODZs may reflect the true level of fractionation by chemolithoautotrophic bacteria. So far, the contribution by chemolithoautotrophic denitrifiers to the fractionation of nitrate has not been addressed, but recent results suggest that a lower value is also reasonable for heterotrophic denitrification under environmental conditions (Kritee et al., 2012).

In the Santa Barbara Basin, the relatively low ε for $\delta^{15}N_{NO3}$ values in the water column were explained by the input of nitrate from N-limited sedimentary denitrification (Sigman et al., 2003). This basin is not entirely anoxic year-round but instead undergoes regular flushing with oxygenic waters in spring. Consequently, denitrification may occur in sediments below the hypoxic layer such that nitrate is released into the overlying water column. By contrast, the GotlandBasin is entirely anoxic year round, with increasing concentrations of ammonium (and H_2S) from the hypoxic zone towards the bottom. Thus, denitrification in these waters and in the sediments remains substrate-limited throughout the year. Sedimentary denitrification may occur at the basin edges at a depth where the oxic-anoxic interface meets the sediments, a layer of a few meters thickness (Dalsgaard et al., 2013). In our model, sedimentary denitrification is not included; however, we cannot entirely exclude the effects of sedimentary processes on the isotope signal of the water column. The impact of sedimentary denitrification together with nitrate-limiting diffusion processes, and denitrification by chemolithotrophs likely contribute to the underexpression of the $\delta^{15}N$ signature in nitrate.

Close coupling of nitrification and denitrification

The assumption of co-occurring nitrification and denitrification is supported by the $\delta^{18}O_{NO3}$.In the hypoxic zone, the ratio $\delta^{18}O_{NO3}$:$\delta^{15}N_{NO3}$ is 1.38:1 (Figure 16), which implies a greater enrichment in $\delta^{18}O_{NO3}$ than in $\delta^{15}N_{NO3}$, while the ratio of $\delta^{18}O_{NOx}$ to$\delta^{15}N_{NOx}$ of ~ 0.5 suggests a large influence of $\delta^{18}O$-depleted nitrite. Denitrification leads to a coupled increase in $\delta^{18}O_{NO3}$ and $\delta^{15}N_{NO3}$,with a slope of ~ 0.5 in freshwater systems (Böttcher et al., 1990; Mengis et al., 1999; Lehmann et al., 2003) and a slope of 1 in marine systems (Granger et al., 2008). Methodological uncertainties and varying salinities were unable to explain the difference between the freshwater and marine slopes (Granger et al., 2008), but variations in nitrate-reducing enzymes in different strains of denitrifiers have been considered (Granger et al., 2008, Dähnke and Thamdrup, 2013).

In our study, the slope of the ratio $\delta^{18}O_{NO3}$:$\delta^{15}N_{NO3}$ was higher than either of the two slopes (0.5 or 1) obtained for denitrification. The ratio 1.38:1 may reflect the impact of simultaneous nitrification and denitrification of NO_3^- and NO_2^- that results in the decoupling of N and O isotopes, with light oxygen atoms preferentially lost to the H_2O pool (“branching fractionation”) and thus the greater enrichment of $\delta^{18}O_{NO3}$ than of $\delta^{15}N_{NO3}$(Casciotti, 2009;

Sigman et al., 2005). Depending on the amount of nitrite that accumulates, the $\delta^{18}O_{NO3}$ can be increased or decreased with respect to $\delta^{15}N_{NO3}$ by NO_2^- reoxidation (Casciotti and Buchwald, 2012). The larger the amount of nitrite that accumulates, the greater the abiotic exchange of oxygen atoms between water and nitrite, resulting in larger $\delta^{18}O_{NO3}$ values(Buchwald et al., 2012). This may be the case at stations with a pronounced secondary nitrite maximum. The high scatter in our $\delta^{18}O_{NO3}$ vs. $\delta^{15}N_{NO3}$ plot could reflect the varying NO_2^- concentrations between stations (Table 8).While there are several plausible explanations for the $\delta^{15}N_{NO3}$ data, when combined with the slope of the $\delta^{18}O_{NO3}$: $\delta^{15}N_{NO3}$ relationship they support the close and immediate coupling of denitrification and nitrification in the redoxcline of the Gotland Basin.

The reaction-diffusion model provided useful insights into the coupling of processes. Only when nitrification was included was there a good match with the observed $\delta^{15}N_{NO3}$ in the hypoxic zone (Figure 17b). A potential chronological separation of nitrification and denitrification, as hypothesized by Dalsgaard et al., (2013), may occur in nature only when turbulent mixing creates hypoxic layers that are thicker than those that are usually present (Table 8). In such cases, nitrification continues until oxygen is depleted, after which denitrification takes over and nitrate is accordingly consumed. Modeling of this specific condition requires a more complex approach than the one used in this study. Moreover, our model only considers full nitrification from NH_4^+ to NO_3^- but not the generation of nitrite (since we lack stable isotope data for nitrite). However, it produced a meaningful $\delta^{15}N_{NH4}/[NH_4^+]$ relationship with a $\varepsilon_{nitrification}$ value of 8.5 ‰, resulting from fractionation during nitrification (Figure 17a). It also was able to reproduce the observed $\delta^{15}N_{NO3}$ vs. f relationship, with an apparent $\varepsilon_{denitrification}$ of 1.9 ‰, as first described in sedimentary environments with limited water and substrate supplies (Brandes and Devol, 1997; Lehman et al., 2004). This $\varepsilon_{denitrification}$ value is even lower than the one based on the Rayleigh model (4.7‰, Table 9; Figure 17b, red line). Consequently, even our low apparent N isotope effect for nitrate reduction may be too high when nitrification occurs, which has been found by Casciotti et al., (2013). They showed that nitrite oxidation can increase the apparent N isotope effect in nitrate by inverse fractionation relative to the organism-level isotope effect of denitrification. The occurrence of nitrite oxidation in parallel with denitrification seems to be relatively common, since it was also demonstrated in studies of the ODZs in the Arabian Sea (Gaye et al., 2013) and off the coast of Peru(Casciotti et al., 2013). In the Baltic Sea and

other systems in which the concentrations of nitrite are too low to compute its stable isotopes, our model presents a reliable method to determine coupled nitrification-denitrification. To further refine the possible N processes (i.e. the ratio of nitrite oxidation to nitrite reduction) in the redoxcline, the N and O isotope systematics of nitrite are needed. Our findings suggest that denitrification in the water column is substrate limited and that both denitrification and nitrification are necessary to explain the data.

The estimated denitrification rate obtained with our model was 14 nmol N L^{-1} d^{-1}, (Figure 7a, solid line), which is slightly lower than the rate measured in situ (Hietanen et al., 2012 and references therein). Assuming that nitrification accounts for 6.6 nmol N L^{-1} d^{-1}, the remaining portion (7.4 nmol N L^{-1} d^{-1}) must derive from diffusion into the hypoxic zone.

2.5. Summary and Conclusions

This study used stable N and O isotope values of NO_3^- and NH_4^+ to understand the coupling of denitrification and nitrification within the redoxcline of the Baltic Sea. We found a low apparent nitrate enrichment factor associated with denitrification. The chemolithoautothrophic nature of denitrification may contribute to the low N isotope fractionation in nitrate but other processes are likely to be involved as well, such as nitrate-limiting diffusion and/or consumption of the entire nitrate pool. The increased ^{18}O:^{15}N ratio associated with nitrate reduction clearly indicated the presence of nitrification.

Our data show that redoxclines are hotspots of microbial turnover and potentially important sites of coupled nitrogen turnover processes, as mirrored in the stable isotope signatures of nitrate and the reduced fractionation. To model these systems, we made use of coupled equations for the rate processes and stable isotopes that reliably reproduced the isotope values of the N species. According to our estimates, roughly half of the nitrate from nitrification readily undergoes denitrification and thus may escape rate measurements in these dynamic zones.

Chapter 3

N and O isotope fractionation in nitrate during chemolithoautotrophic denitrification by *Sulfurimonas gotlandica*

Frey, C., Hietanen S., Juergens K., Labrenz M., Voss M.

Environmental Science and Technology **48**: 13229-13237

DOI: 10.1021/es503456g

Abstract

Chemolithoautotrophic denitrification is an important mechanism of nitrogen loss in the water column of euxinic basins but its isotope fractionation factor is not known. *Sulfurimonas gotlandica* GD1^T, a recently isolated bacterial key player in Baltic Sea pelagic redoxcline processes, was used to determine the isotope fractionation of nitrogen and oxygen in nitrate during denitrification. Under anoxic conditions, nitrate reduction was accompanied by nitrogen and oxygen isotope fractionation of 23.8 ± 2.5 ‰ and 11.7 ± 1.1 ‰, respectively. The isotope effect for nitrogen was in the range determined for heterotrophic denitrification, with only the absence of stirring resulting in a significant decrease of the fractionation factor. The relative increase in $\delta^{18}O_{NO3}$ to $\delta^{15}N_{NO3}$ did not follow the 1: 1 relationship characteristic of heterotrophic, marine denitrification. Instead, $\delta^{18}O_{NO3}$ increased slower than $\delta^{15}N_{NO3,}$ with a conserved ratio of 0.5: 1. This result suggests that the periplasmic nitrate reductase (Nap) of *S. gotlandica* strain GD1^T fractionates the N and O in nitrate differently than the membrane-bound nitrate reductase (Nar), which is generally prevalent among heterotrophic denitrifiers and is considered as the dominant driver for the observed isotope fractionation. Hence in the Baltic Sea redoxcline, other, as yet-unidentified factors likely explain the low apparent fractionation.

3.1. Introduction

During denitrification in the ocean, fixed nitrogen (N) is lost to the atmosphere. The process involves the reduction of nitrate and nitrite to gaseous nitrogen, N_2O and N_2, coupled to the oxidation of organic (heterotrophic) or inorganic (chemolithoautotrophic) substances. In the water column, denitrification takes place at depths where the oxygen concentration is low, and it leaves a characteristic imprint on ambient nitrate isotope values(Brandes et al., 1998; Lehmann et al., 2003). So far, there are no data regarding the N isotope effect for marine chemolithoautotrophic denitrifiers, although most N_2 loss in euxinic water columns has been attributed to this pathway(Hannig et al., 2007; Jensen et al., 2009; Hietanen et al., 2012; Dalsgaard et al., 2013; Wenk et al., 2014).

The dissimilatory reduction of nitrate to nitrite strongly discriminates against heavy isotopes of nitrogen (^{15}N) such that the remaining substrate pool is enriched with ^{15}N, while

the product becomes comparatively lighter. The kinetic fractionation factor, ε, is defined as ($[k_{light}/k_{heavy}]$ -1)×1000 (given in ‰), where k_{light} and k_{heavy} refer to the relative rates of reaction of the light and heavy isotopes. The N isotope effect for denitrification has a broad range: 1–30 ‰ in freshwater and terrestrial environments(Delwiche and Steyn, 1970; Mariotti et al., 1981; Böttcher et al., 1990; Lehmann et al., 2003), 10- 30 ‰ in culture studies of heterotrophic denitrifying bacteria(Wellman et al., 1968; Barford et al., 1999; Granger et al., 2008), and 20- 30 ‰ in open ocean systems(Brandes et al., 1998; Voss et al., 2001). Culture studies also show an effect on N isotope fractionation of the type of organic electron-donor(Wunderlich et al., 2012); however, whether this applies to inorganic electron donors is not yet known.

Variations in ε have been explained using an efflux or conceptual model(Shearer et al., 1991; Granger et al., 2004, 2008; Karsh et al., 2012), which describes the net organism-level isotope effect (ε_{org}) associated with each step in nitrate reduction: uptake (ε_{in}), efflux (ε_{out}), and reduction (ε_{NR}). Reduction is the first irreversible step (Wunderlich et al., 2012)that causes the isotope fractionation associated with nitrate reduction(Mariotti et al., 1981; Shearer et al., 1991; Needoba et al., 2004), and the extent of the enzymatic nitrate reduction isotope effect (ε_{NR}) outside the cell is modulated by the ratio of efflux to uptake. The model was first applied to assimilative membrane-bound nitrate reductases (Nas) and later to dissimilative Nar, whose isotope effects on N in nitrate have been studied extensively(Granger et al., 2004, 2008; Karsh et al., 2012; Kritee et al., 2012). By contrast, comparatively, little is known about the isotope effect of the periplasmic nitrate reductase (Nap). Whereas Nar and Naslead to a 1 : 1 increase in oxygen and nitrogen isotope ratios in nitrate during assimilation and heterotrophic denitrification(Casciotti et al., 2002; Granger et al., 2004, 2008; Sigman et al., 2005; Karsh et al., 2012; Kritee et al., 2012), Nap-catalyzed denitrification in *Rhodobacter sphaeroides* has a low $\delta^{18}O$ to $\delta^{15}N$ ratio of 0.6.

Here we present results from experiments using cultures of a chemolithoautotroph, *Sulfurimonas gotlandica* strain $GD1^T$, belonging to a group of *Epsilonproteobacteria* which can be considered the major denitrifiers in the Baltic Sea redoxcline(Grote et al., 2012; Bruckner et al., 2013). There, hydrogen-sulfide-driven denitrification is the dominant N-loss pathway(Brettar and Rheinheimer, 1991; Hannig et al., 2007; Hietanen et al., 2012; Dalsgaard et al., 2013). Besides high N losses, we identified a low fractionation of nitrate in the Baltic Sea redoxcline, which may be explained in part by the chemolithoautrotrophic

nature of the process(Frey et al., 2014). In this bacterium, the first chemolithoautotrophic strain from a pelagic redox zone to be investigated for $^{15}\varepsilon$ and $^{18}\varepsilon$ during denitrification, Nap is the only nitrate reductase and is thus the major enzyme catalyzing nitrate reduction(Grote et al., 2012). The effect of oxygen on Nap-mediated denitrification by *S. gotlandica* is unknown but it might account for the low apparent fractionation of nitrate in the Baltic Sea. To identify and quantify microbial nitrate reduction in the environment by means of stable isotopes, robust knowledge of the determinants of isotope enrichment factors is necessary. The goal of this study was to investigate Nap-catalyzed, chemolithoautotrophic denitrification in *S. gotlandica* for (1) its oxygen sensitivity, (2) its fractionation factors of nitrate under variable growth conditions, and (3) its effect on the $\delta^{18}O$: $\delta^{15}N$ ratio in nitrate.

3.2. Materials & Methods

Strain

S. gotlandica is a slightly curved rod- or spiral-shaped, metabolically very versatile bacterium capable of using a wide variety of electron-donors (e.g., reduced sulfur compounds), and electron-acceptors (e.g., nitrate and nitrite) for growth(Labrenz et al., 2013). It is responsible for the major portion of chemoautotrophic production at the oxic-anoxic interface of the Baltic Sea, where it reaches a maximum abundance of 20–30 % of total prokaryotes (Grote et al., 2008). 16S rRNA gene sequence phylogeny analysis placed the Baltic Sea isolate within the genus *Sulfurimonas*, subgroup *Sulfurimonas* GD17 and the class *Epsilonproteobacteria* and with 93.7–94.2% similarity to the other species of the genus *Sulfurimonas*: *S. autotrophica, S. paralvinellae*, and *S. denitrificans* (Labrenz et al., 2013). *S. gotlandica* contains the gene cluster *napAGHBFLD*, encoding the periplasmatic nitrate reductase (Nap). It does not carry the genes *narGHI*, encoding the membrane-bound nitrate reductase (Nar)(Grote et al., 2012), which is common among *Epsilonproteobacteria*(Kern and Simon, 2009).

Growth conditions in batch cultures

Artificial brackish water medium (ABW) used for anoxic cultivation(Bruns et al., 2002) was buffered with 10 mmol L^{-1} HEPES or, to exclude the use of organic carbon or nitrogen during the pulsed oxygen experiment, with 2 mmol L^{-1} $NaHCO_3$, yielding a pH of 7.3. The

media and solutions were prepared with boiled ultra-pure water, flushed with dinitrogen for at least 30 min, and autoclaved. The medium was then supplemented with 1 mL per L of a sterile, anoxic trace element solution SL10 (Widdel and Bak, 1992), 0.2 mL of a selenite-tungstate solution (Widdel and Bak, 1992), and 1 mL of a 10-vitamin solution (Balch et al., 1979). The electron acceptor was 1 ,2, or 5 mmol L^{-1} of KNO_3 and the electron donor 1, 2, or 5 mmol L^{-1} NaS_2O_3, as described in previous studies(Grote et al., 2012; Mammitzsch et al., 2014). Cultures were initiated from frozen stocks and acclimated for 10 generations to a temperature of 10°C or 15°C in the experimental medium. Samples for bacterial cell counts were preserved in 100 μL of formaldehyde (final concentration 3–4 %) and quantified by counting DAPI (4',6-diamidino-2-phenylindole)-stained cells using epifluorescence microscopy (Axioskop 1, Zeiss).

Experimental design and sampling

Cells were grown in 1-L glass bottles (rinsed with 10% HCL and ultra-pure water, combusted at 200°C) sealed with rubber stoppers (Glasgerätebau Ochs, Germany) and incubated in the dark.

Two different experimental set-ups were used. In the first, the oxygen sensitivity of denitrification was evaluated using ^{15}N labeled nitrate. Two mL of bacteria in the early stationary phase of growth were inoculated into 1 L of medium; growth was monitored until the bacteria reached the exponential growth phase. Incubations were done without headspace and the cultures were continuously stirred with a magnetic bar, which prior to its use was kept in an oxygen-free container for 5 days to avoid oxygen contamination. The physical set-up was tested for its efficacy in excluding the external environment by adding a known amount of oxygen to the incubation bottle without bacteria. No change in its concentration occurred over the time course of the experiment. Oxygen was sequentially added in duplicate treatments at concentrations of 10, 15, and 20 μmol L^{-1} within 12 h by injecting different volumes of sterile 100 % oxygen-saturated medium. The oxygen concentration was followed continuously with an oxygen electrode OX-10 (Unisense, Denmark) with a detection limit of 0.3 μmol oxygen L^{-1}. The sensor was applied through the rubber stopper (Figure 18). After the first addition of the oxic medium, the bottles were amended with $^{15}NO_3^-$ ($K^{15}NO_3$, 99 atom %, Cambridge Isotope Laboratories; final concentration 0.7 mmol L^{-1}), yielding 50–80 % labeling of the nitrate pool. An anoxic

reservoir was connected to the incubation bottles by Viton tubing. At each sampling point the reservoir was purged with N_2, creating an overpressure that pushed the oxygen-free medium into the incubation bottle, from which a 3-mL sample was collected in a glass vial (Labco, 3 mL Exetainer) for gas analysis and a 1-mL sample in a microcentrifuge tube for cell counts. A helium headspace was introduced in the glass vials immediately through the septum; at the same time, 1 mL of sample was withdrawn from each vial for NO_x^- concentration measurements. Bacterial activity in the glass vial samples was terminated by adding 100 μL of 7.3 mol $ZnCl_2$ (Merck) L^{-1}. The vials were stored upside down at room temperature until the $^{28}N_2$, $^{29}N_2$, and $^{30}N_2$ isotope ratios were analyzed. Samples for NO_x^- concentration measurements were taken from the glass vials, immediately filtered through a pre-washed syringe tip (0.2-μm polyethersulfone, VWR International LLC) to terminate the reactions, and frozen until the analyses.

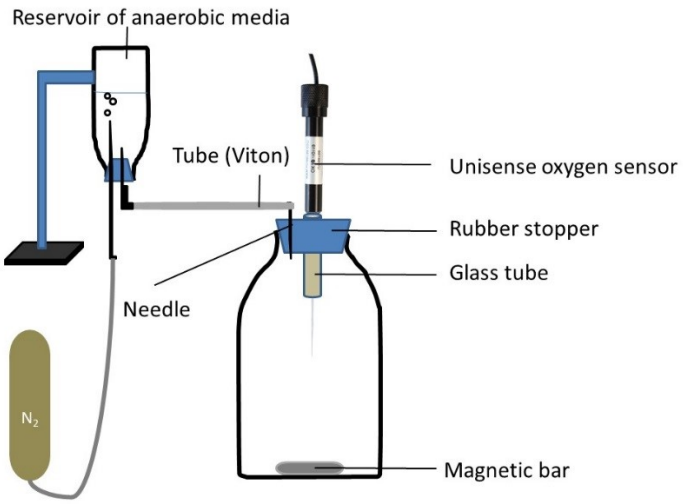

Figure 18: The set-up used for oxygen manipulations.

The second set-up was designed to quantify the intrinsic N and O fractionation factors of nitrate under different conditions: stirred vs. unstirred, hypoxic vs. anoxic, and marine vs. brackish medium. Oxygen contamination during sampling was avoided by a 200-mL N_2 headspace in the bottles and an excess pressure of 1.5 bar. Each bottle contained 1000 mL of medium, which was inoculated with bacteria in the early stationary phase of growth. To test the effect of stirring, five replicates were continuously stirred while five others remained unstirred. To test the effect of oxygen addition on fractionation, two stirred bottles were pulsed with oxygen (3×) using the same set-up described for the oxygen sensitivity experiment but with the inclusion of headspace. To test the effect of full marine conditions on the fractionation, six replicates were adapted for 10 generations in artificial

seawater medium AQUIL(Price et al., 1989). From each of the 18 glass bottles, subsamples for cell counts, nitrate and nitrite concentration, and nitrate isotopes were taken, either daily or twice a day, throughout the lag, exponential, and stationary phases of growth. For nutrients and nitrate isotope analysis, 5-mL samples were filtered (see above) and immediately frozen at -20°C until further analysis.

At the end of all experiments, samples were taken for CARD-FISH (catalyzed reporter deposition fluorescence in situ hybridization) analysis, to verify that the cultures were not contaminated. Bacteria were enumerated with a specific *Sulfurimonas* subgroup GD17 probe, SUL90 (CGTGCGCCACTAATCATA)(Grote et al., 2007).

Chemical and isotope analysis

The nitrate concentration was determined based on the reduction of nitrate to nitrite by vanadium (III) chloride(Doane and Horwáth, 2003) followed by spectrophotometric detection(Grasshoff et al., 1983). Since nitrite accumulation was not found in previous studies(Grote et al., 2012) nor was it detected in this study, nitrite removal for isotope analysis was deemed unnecessary.

The isotope ratios of $^{28}N_2$, $^{29}N_2$, and $^{30}N_2$ of the labeled samples from the oxygen sensitivity experiment were analyzed by gas chromatographic isotope ratio mass spectrometry (GC-IRMS; Thermo Finnigan Delta V plus with ConFlo III, Thermo Fisher Scientific) by directly injecting a 100-μL headspace sample from the glass vial. The concentrations of labeled products were calculated as the excess relative to the N_2 concentration in air. ^{15}N-labeled N_2O was also quantified by first separating it from N_2 in a GC column followed by its quantitative reduction to N_2 on a hot copper column.

Nitrate isotope analysis for the fractionation experiment was done on a Thermo Finnigan Gasbench II/ Delta V Plus IRMS (Thermo Fisher Scientific) using the denitrifier method for dual-isotope measurements of $\delta^{15}N$ and $\delta^{18}O$ (Sigman et al., 2001; Casciotti et al., 2002). The bacterial strain *Pseudomonas aureofaciens* (ATTC 13985), which lacks N_2O reductase, was used to convert nitrate and nitrite quantitatively to N_2O, which was then extracted, purified, and analyzed. The individual sample size was adjusted to contain 20 nmol N_2O and standardized by comparison with international reference substances IAEA-N3: $\delta^{15}N$ 4.7‰ vs. atmospheric N_2; $\delta^{18}O$ 25.6‰ vs. VSMOW (Vienna standard mean ocean water); and USGS 34: $\delta^{15}N$ -1.8‰ vs. atmospheric N_2; $\delta^{18}O$ -27.9‰ vs. VSMOW(Böhlke et al.,

2003). The standard deviations of the standards were ± 0.2 for $\delta^{15}N$ and ± 0.4 for $\delta^{18}O$. The blank was determined by analyzing a *P. aureofaciens* culture without sample injection. O isotopes ratios were corrected for their exchange with water during the reduction of nitrate to N_2O (Casciotti et al., 2002; Böhlke et al., 2003). Replicate measurements were done with 10 % of the samples in a separate batch. Isotopic ratios in nitrate are reported using delta (δ) notation in units per mil (‰),

$$\delta^{15}\mathrm{N}_{\mathrm{sample}} = \left([\tfrac{^{15}N}{^{14}N}]_{sample} \Big/ [\tfrac{^{15}N}{^{14}N}]_{reference} - 1\right) \times 1000 \quad (1)$$

Calculations

N_2 production (denitrification) rates per cell were calculated as:

$$N_2[\mu\mathrm{mol} \times \mathrm{cell}^{-1} \times \mathrm{h}^{-1}] = \left({}^{29}N_2 + 2 \times {}^{30}N_2\right) \times \left(\frac{{}^{15}[NO_3^-] + {}^{14}[NO_3^-]}{{}^{15}[NO_3^-]}\right) \times \frac{1}{2} \times cells^{-1} \times {t_n}^{-1} \quad (13)$$

where $^{29}N_2$ and $^{30}N_2$ represent the $^{29}N_2$ or $^{30}N_2$ produced at each time point, $^{15}[NO_3^-]$ is the concentration of ^{15}N- nitrate (μmol L^{-1}), and $^{14}[NO_3^-]$ is the ^{14}N- nitrate concentration (μmol L^{-1}) at the beginning of the incubation; t_n is the incubation time (hours); and "cells" refers to the number of cells × mL^{-1} at t_n. The kinetic fractionation factor imparted on N and O in nitrate during growth was derived from the following linear equation(Mariotti et al., 1981) :

$$\varepsilon = 10^3 ln \frac{10^{-3}\delta(NO_3^-) + 1}{10^{-3}\delta(NO_3^-)_{\ initial} + 1} \times \ln\left[\frac{c(NO_3^-)_{\ measured}}{c(NO_3^-)_{\ initial}}\right]^{-1} \quad (14)$$

where ε is the isotopic enrichment factors for nitrogen and oxygen, δ is the $\delta^{15}N$ or $\delta^{18}O$ value, and c is the nitrate concentration. A linear derivation was used to plot $\delta^{15}N$ and $\delta^{18}O$ against ln(*f*)(Mariotti et al., 1981).

$$\delta^{15}\mathrm{N} = \delta^{15}\mathrm{N}_{\mathrm{initial}} + {}^{15}\varepsilon(\ln(f)) \quad (2)$$

where *f* is the residual nitrate fraction. .

Cell-specific nitrate reduction (CSNR) rates were calculated by dividing nitrate consumption by the average cell numbers during exponential phase. The latter was chosen because during stationary phase only a small portion of total cells are typically active, leading to an underestimation of the CSNR rate.

Differences between $^{15}\varepsilon$ values were tested for statistical significance with an ANOVA combined with Dunnett's post-hoc test.

3.3. Results

Oxygen sensitivity of chemolithoautotrophic denitrification

Labeled $^{29+30}N_{excess}$ increased linearly over the incubation time (Figure 19a, c), with N_2 production rates, normalized per cell (Eq. 13), reaching a maximum after 30 min in standard culture conditions (control treatment, Figure 19b). N_2 production rates per cell were zero in the presence of oxygen but increased after the disappearance of oxygen (Fig. 19d). In the control, N_2 production rates were twice as high (0.5 fmol cell^{-1} h^{-1}) as in the pulsed oxygen treatments (Figure 19b, d). When oxygen was first introduced into the bottles (10 μmol L^{-1}), denitrification immediately ceased and the bacteria began to consume oxygen. N_2 production recovered only after the added oxygen was completely consumed (Figure 19c, d). Neither NO_2^- nor N_2O accumulation was ever detected. The addition of 20 μmol oxygen L^{-1} had the same effect. After the third addition of oxygen (15 μmol×L^{-1}), denitrification was initiated already at an oxygen concentration of 3 μmol L^{-1} (Figure 19c, d); however, by that time the cells had started to form aggregates indicating anoxic microniches.

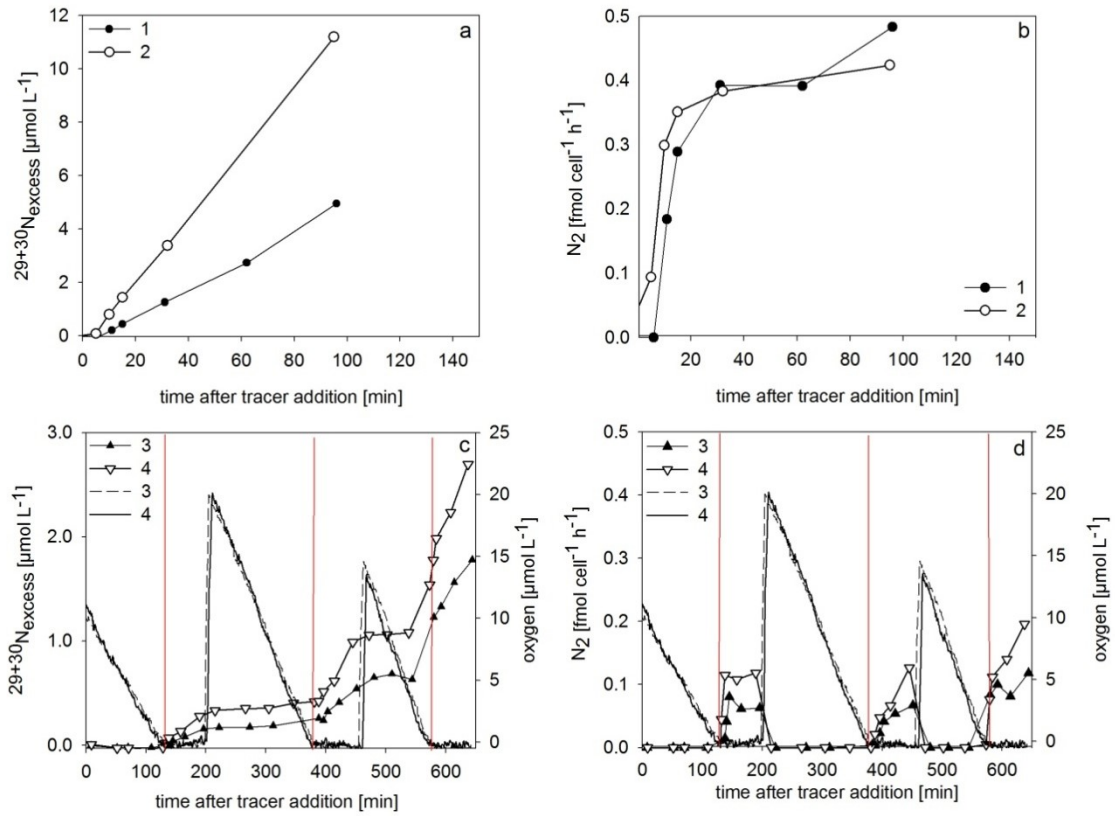

Figure 19: Effects of pulsed oxygen supplied to anoxically grown Sulfurimonas cultures on labeled $^{29+30}N_{excess}$ production (a, c) and the N_2 production rate per cell (b, d). Note the different scales used to plot $^{29+30}N_{excess}$ production. (a, b) Control treatment with standard culture conditions and without oxygen addition (duplicates 1, 2). (c, d) The effect of multiple

oxygen pulses (lines) in duplicate treatments (3, 4). Oxygen was measured continuously with an electrode. Red lines indicate the time point at which the oxygen concentration was zero.

Nitrate N and O isotope fractionation by a chemolithoautotrophic denitrifier

Nitrate decreased over time in all batches, consistent with its reduction to N_2,while cell numbers increased from 3.0×10^5 cells mL^{-1} to maximum cell numbers of around 3×10^7 cells mL^{-1} (Figure 20). NO_2^- accumulation was not detected. With decreasing nitrate concentrations, $\delta^{15}N$ and $\delta^{18}O$ in the residual nitrate pool increased (Figure 20).

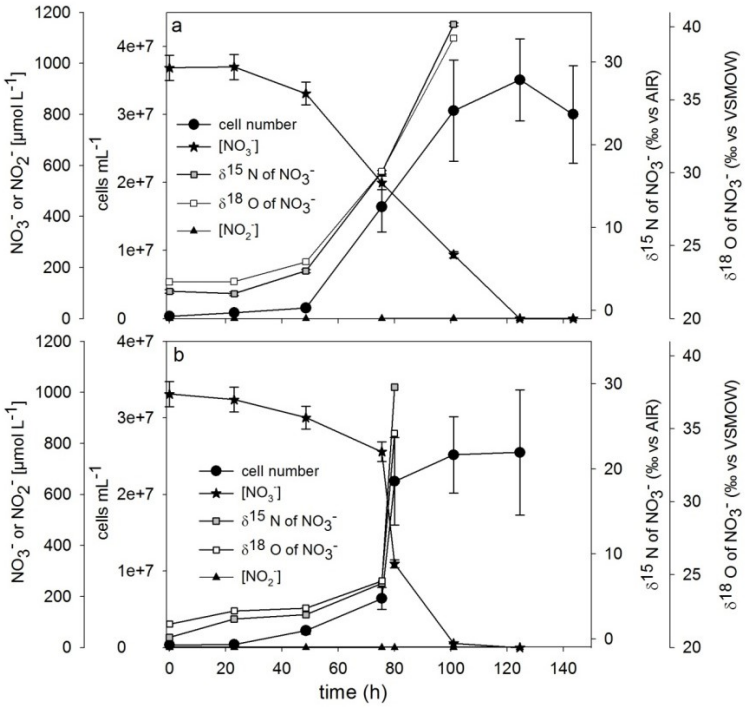

Figure 20: Cell growth of *Sulfurimonas gotlandica*strain GD1^{T}from the time of inoculation (black circles). Changes in nitrate and nitrite concentrations and the stable isotope values of N and O in nitrate in the growing culture (a) for the control treatment (brackish, anoxic, stirred) and (b) for the marine treatment (marine, anoxic, stirred) are shown. Error bars indicate the standard deviations.

As predicted by the Rayleigh model (Eq. 2), there was a significant linear relationship between $\delta^{15}N$ and $\delta^{18}O$ vs. the natural logarithm of the fraction of remaining nitrate (Figure 21, $p < 0.0001$). The slopes of the lines in a plot of the δ-values vs. the natural logarithm of the nitrate fraction approximated the N and O isotope effect ($^{15}\varepsilon$ and $^{18}\varepsilon$), calculated based on Equation 4 in Table1. The range of the slopes, and thus the N and O isotope effects they represented, significantly differed only between the unstirred and the other treatments ($p<0.01$). The unstirred treatment yielded the lowest ε: 15.5 ± 2.5 ‰ and 9.1 ± 2.3 ‰, for N and O, respectively (Figure 21, Table 11). Mean N and O isotope effects were highest in the treatment based on marine conditions, 25.1 ± 2.2 ‰ and 12.0 ± 1.0 ‰ (Table 11), but these results did not differ significantly from those of the control ($^{15}\varepsilon$ = 21.9 ± 1.9 and , $^{18}\varepsilon$ = 11.2 ±

1.3 ‰, p> 0.01) or the pulsed oxygen treatments ($^{15}\varepsilon$ = 24.6 ± 3.2 and, $^{18}\varepsilon$ = 12.0 ± 0.9 ‰; p>0.01). The fractionation factor was constant throughout the time course of the incubations (Table 11). From the dual isotope plot of $\delta^{18}O$ vs. $\delta^{15}N$, the difference between the slopes of the different treatments was not significant, with a mean $\delta^{18}O$: $\delta^{15}N$ ratio of 0.51 ± 0.06 ‰ (Figure 22a, Table 11).

Table 11: Conditions and parameters varied for Sulfurimonas gotlandica culture in this study. Nitrate nitrogen (N) and oxygen (O) isotope effects ($^{15}\varepsilon$ and $^{18}\varepsilon$) were computed for individual experiments and for the corresponding $\varepsilon^{18}O : \varepsilon^{15}N$ relationships.

Treatment	Batch no.	Condition	Temp (°C)	Initial $[NO_3^-]$ (mmol L^{-1})	Isotope samples (n)	$^{15}\varepsilon$	±SD	$^{18}\varepsilon$	±SD	$^{18}\varepsilon : {}^{15}\varepsilon$	CSNR *	[(μmol cell $^{-1}$ min^{-1})×10^{-12}]
Control brackish, anoxic, stirred	-											
	1	organic buffer	15	5	5	24.29	0.37	13.04	0.18	0.54	29.58	
	2	organic buffer	15	5	4	21.17	0.37	10.64	0.25	0.50	21.67	
	3	inorganic buffer	10	1	5	23.05	0.27	12.13	0.34	0.53	24.01	
	4	inorganic buffer	10	1	5	19.45	0.39	10.17	0.50	0.52	20.73	
	5	inorganic buffer	10	1	5	21.36	0.65	9.97	0.25	0.47	27.93	
Brackish, anoxic, unstirred	6	organic buffer	15	1	5	15.16	1.61	9.35	1.03	0.62	16.87	
	7	organic buffer	15	1	5	17.69	0.85	12.02	0.67	0.68	17.86	
	8	organic buffer	10	1	5	13.08	0.66	7.88	0.67	0.60	21.69	
	9	organic buffer	10	1	5	18.46	0.33	10.13	0.78	0.55	34.32	
	10	organic buffer	15	5	4	13.20	0.45	6.04	0.16	0.46	21.32	
Brackish, oxygen-pulsed, stirred	11	inorganic buffer	10	2	10	26.81	3.23	12.63	0.98	0.48	34.66	
	12	inorganic buffer	10	2	11	22.35	2.25	11.34	2.09	0.51	30.86	
Marine, anoxic, stirred	13	organic buffer	10	1	5	25.96	1.36	11.23	0.23	0.43	35.24	
	14	organic buffer	10	1	5	25.49	1.30	12.34	1.16	0.48	27.63	
	15	inorganic buffer	10	2	7	23.76	1.74	11.32	1.49	0.48	22.35	
	16	inorganic buffer	10	2	7	27.72	2.12	13.84	0.64	0.50	51.66	
	17	inorganic buffer	10	2	7	26.07	1.25	12.08	0.69	0.46	41.09	
	18	inorganic buffer	10	2	7	21.47	2.55	11.34	0.99	0.53	23.66	

*Calculated only from the time point at which the changes in cells and nitrate concentrations were exponential; CSNR, cell-specific nitrate reduction rate

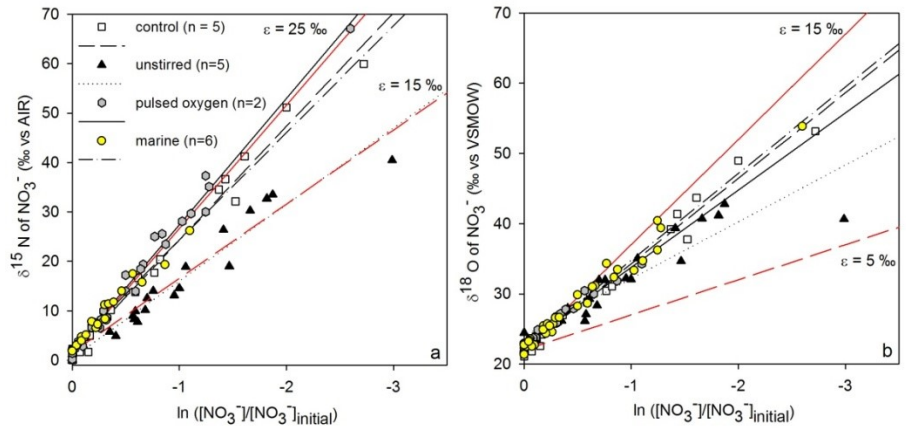

Figure 21: Rayleigh plots of the change in the N and O isotopic composition of nitrate as a function of the natural logarithm of fractional nitrate consumption (reverse scale) by *Sulfurimonas gotlandica*under four different growth conditions. (a) $\delta^{15}N$ and (b) $\delta^{18}O$.

In all stirred treatments, the CNSR correlated positively with $^{15}\varepsilon$ (Figure 22b). The unstirred treatment showed a large scatter in $^{15}\varepsilon$, with no apparent trend (Figure 22b).

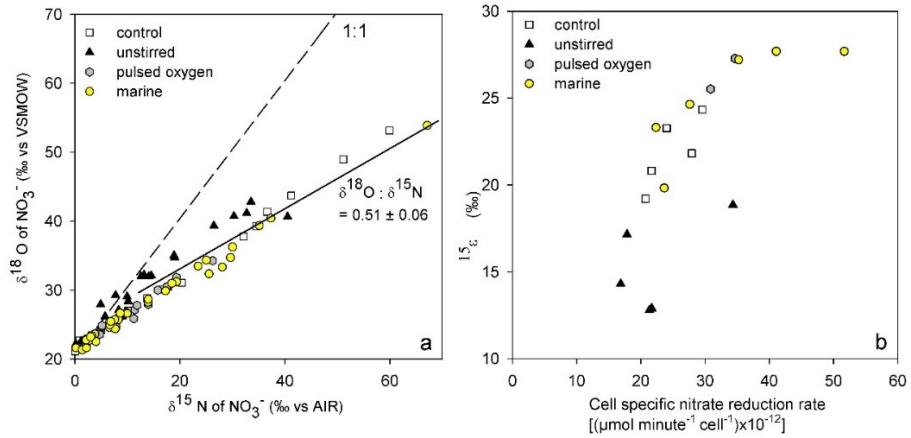

Figure 22: (a) The $\delta^{18}O$ of nitrate plotted against the corresponding $\delta^{15}N$ in nitrate for *S. gotlandica* grown under four different conditions. (b) N isotope effect versus the cell-specific nitrate reduction (CSNR) rate of *Sulfurimonas gotlandica* as a function of treatment. $^{15}\varepsilon$ and CSNR values were calculated from an exponentially growing culture.

3.4. Discussion

Oxygen sensitivity of chemolithoautotrophic denitrification

Oxygen inhibited the first step of denitrification given that in the presence of oxygen neither its end (N_2) nor its intermediate (NO_2^-, N_2O) products accumulated (Figure 19). Nitrate reduction is highly regulated in response to varying O_2 concentrations, both at the gene expression and the enzyme levels(Ferguson, 1994; Zumft, 1997). In *P. denitrificans*, nitrate reduction by Nar is inhibited by oxygen; thus, instead, Nap catalyzes aerobic

denitrification(Bell et al., 1990; Bedzyk et al., 1999). However, our results clearly demonstrate that this is not the case in *S. gotlandica* Nap, which is incapable of aerobic denitrification.

In this study, strain GD1 was able to reduce oxygen, but with our experimental design we were unable to determine whether energy from oxygen reduction was used for growth(Ferguson, 1994) or whether oxygen was reduced to generate conditions favorable for denitrification, similar to the antioxidative defense system of sulfate-reducing bacteria(Brioukhanov et al., 2010). In fact, most denitrifying organisms are able to switch between oxic- and NO_3^--dependent modes of respiration and *S. gotlandica* likely respires oxygen, given that its genome includes a gene encoding a putative cbb3-type cytochrome c oxidase with the potential to mediate microaerobic respiration(Grote et al., 2012).

The recovery of denitrification in the presence of oxygen after the last addition of oxygen (Figure 1c) suggested the formation of anoxic microniches within the cell aggregates during the last phase of the experiment. Cells in the anoxic core of the aggregate may have been able to carry out denitrification, while those on the surface may have continued to reduce oxygen, a phenomenon well-known from studies of sinking aggregates in the ocean(Ploug et al., 1997). Nonetheless, while *Sulfurimonas* spp.aggregates are a common feature in batch cultures, in the redoxcline this species occurs mainly as freely dispersed single cells(Grote et al., 2007, 2008). Therefore, a scenario invoking aggregates is unlikely to occur in the Baltic Sea and was more likely a culture artifact.

Cell-specific N_2 production rates increased more slowly in the oxygen-treated set-up, indicating that repeated pulses of oxygen lowered the denitrification performance of the cells, albeit temporarily (Figure 1d). This was also the case in the different *P. aeruginosa* cultures, in which oxygen exposure lowered N_2 production rates(Thomas et al., 1994).

N isotope fractionation in nitrate by chemolithoautotrophic denitrification under varying conditions

The fractionation factor for N associated with thiosulfate-driven nitrate reduction was between 13 and 28‰, which is in the reported range of that associated with heterotrophic denitrification(Granger et al., 2008). A similar variability of $^{15}\varepsilon$ was found in different batches of the same heterotrophic denitrifier rather than between different

strains(Granger et al., 2008), indicating cellular rather than strain-related differences(Kritee et al., 2012).

Although in this study thiosulfate was the only electron-donor tested; *S. gotlandica*oxidizes sulfur of different oxidation states as well as organic compounds, such as acetate or pyruvate. In the latter case, maximal cell numbers achieved are more than a magnitude lower, which is indicative of a chemolithoautotrophic lifestyle(Labrenz et al., 2013). For a heterotrophic, Nap-catalyzing denitrifier, *Rhodobacter spheroides*, the magnitude of $^{15}\varepsilon$ was within the range reported for other heterotrophic, Nar-catalyzed denitrifiers(Granger et al., 2008). Since our $^{15}\varepsilon$, obtained with an inorganic electron donor, was in the same range as in studies with organic electron donors, we hypothesize that $^{15}\varepsilon$ will be similar with an organic source, but this remains to be confirmed.

There was no significant difference in the average ε of N between the oxygenated, marine or control treatments (Figure 21; Table 11): 23.8 ± 2.5 ‰. An ε that is robust to changes in salinity or oxygen concentration might reflect the fact that nitrate uptake is not an active, energy-dependent process, because of the location of the periplasmic nitrate reductase (Figure 23). Nap is a soluble enzyme in the periplasm and nitrate can freely diffuse along its concentration gradient through the outer membrane (r1), where uptake cannot be regulated actively such that energy from nitrate reduction is not needed. By contrast, membrane-bound Nar has its catalytic site in the cytoplasm, for which active nitrate transporters are needed at the inner membrane (r4). This can limit the rate of Nar-catalyzed nitrate reduction (Figure 23); hence impacting εexpression.

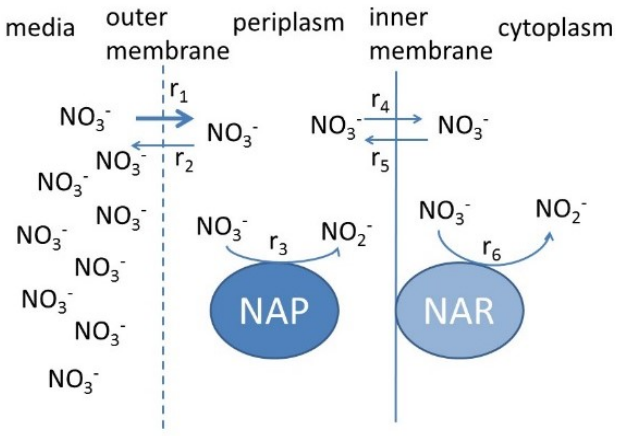

Figure 23:Nitrate uptake and reduction. During Nap-catalyzed nitrate reduction, nitrate diffuses in (r1) and out (r2) of the cell via the outer membrane and the periplasm, without the need for active transport. This nitrate is reduced (r3) by periplasmic nitrate reductase.During Nar-catalyzed nitrate reduction, in addition to diffusion through the outer membrane, active transport through the inner membrane is necessary (r4 and r5). In the cytoplasm, nitrate is then reduced (r6) by membrane-bound Nar. (modified after(Granger et al., 2008))

Considering the high concentrations of nitrate used for the batch culture (1 mmol L^{-1} at least), a more than sufficient amount of nitrate can be assumed to have passively diffused along the osmotic gradient into the cell. Diffusion is not rate-limiting as long as enough nitrate is present in the extracellular environment (nitrate always >120 μmol L^{-1}); accordingly, in our study the nitrate concentration did not have a limiting effect on fractionation in all stirred treatments.

Nitrate reduction did not take place in the presence of oxygen, ruling out a direct effect of oxygen on isotope fractionation during denitrification. Previous studies showed that the effect of oxygen on $^{15}\varepsilon$ during denitrification is culture-dependent (Barford et al., 1999; Kritee et al., 2012).A reduced ε in the presence of oxygen due to a reduced CSNR rate was previously reported(Kritee et al., 2012), but oxygen does not seem to be the reason for the low $\varepsilon_{apparent}$ of 4.7‰ found in the Baltic Sea redoxcline(Frey et al., 2014) .

The only significant impact on $^{15}\varepsilon$ occurred under unstirred conditions, as previously described for a *Marinobacter* culture(Kritee et al., 2012). In that study; diffusion limitation due to a diffusive boundary layer around each cell was excluded as an explanation because the bacterial cells were too small and the substrate concentrations too high to result in a concentration gradient, which may also have been the case in our study. Moreover, *S. gotlandica* is very motile(Labrenz et al., 2013) and has a positive chemotactic response to nitrate,(Grote et al., 2012) making diffusion limitation for single cells highly unlikely. Instead, the lower $^{15}\varepsilon$ in the unstirred treatment can be explained by the development of nitrate gradients inside the bottle as a result of aggregate formation (as discussed above). In the absence of stirring, the highest cell density was at the bottom of the bottles (where a visible cell layer formed), where nitrate consumption would have been correspondingly higher and the nitrate concentration correspondingly lower. The cell aggregates would also have caused a diffusion limitation at the bottom, leading to a lower $^{15}\varepsilon$ for the whole culture in the respective bottle. As the intracellular and external nitrate concentrations become increasingly similar, the supply of intracellular nitrate (r1, Fig 23) is too low to maintain saturated enzyme activity. This has also been described for Nar, as the nitrate transporters (r4) are saturated. The result is a decrease in nitrate efflux (r5=0; r2=0) as the fraction of gross nitrate influx and hence the expression of ε_{NR} (r3, r6) outside the cell are reduced, leading to a lower $^{15}\varepsilon$ (Granger et al., 2008; Karsh et al., 2012).

The $^{15}\varepsilon$ range within treatments varied by 5‰, with an increase in $^{15}\varepsilon$ in the presence of high cell-specific nitrate reduction rates. This was also the case in a previous study, suggesting that at high nitrate efflux/uptake ratios (r5/r4), ε_{NR} is fully expressed outside the cell, and vice versa(Kritee et al., 2012). Only in the unstirred treatment was there no dependence of ε_{NR} on the CSNR rate, as the effect was masked by substrate limitation (as discussed above). According to a previous study, this relationship is dependent on the energetic need for nitrate uptake(Kritee et al., 2012), which for *S. gotlandica* is not applicable. In this bacterium, the change in $^{15}\varepsilon$ may be a more direct response to changes in enzyme-specific activity, while the direct mechanism regulating this relationship has yet to be determined.

Impact of Nap-catalyzed denitrification on the $\delta^{18}O$: $\delta^{15}N$ ratio in nitrate

The constant ratio of $\delta^{18}O$: $\delta^{15}N$ of ~ 0.5 across the different treatments differs from the constant ratio of ~1 determined for the respiratory and assimilatory nitrate reductase(Granger et al., 2004, 2008;Karsh et al., 2012; Kritee et al., 2012). In both cases, internal enzymatic reduction is responsible for the fractionation of N and O isotopes in nitrate. Fractionation during nitrate uptake and efflux is minimal as there is no N-O bond breakage(Kritee et al., 2012). The different behaviors of Nap and Nar are surprising, since the two enzymes are evolutionarily closely related and because eukaryotic and prokaryotic Nar are less closely related but their $\delta^{18}O$: $\delta^{15}N$ ratios in nitrate are similar (Granger et al., 2008; Karsh et al., 2012).

Nap is present only in proteobacteria, which can also harbor Nar or both enzymes(Zumft, 1997; Philippot, 2002). The physiological role of Nap depends on the bacterial species, but the enzyme has been associated with secondary functions such as aerobic denitrification, the transition to anaerobic respiration, and the dissipation of excess reducing equivalents(Bell et al., 1990; Zumft, 1997; Bru et al., 2007). In *Pseudomonas* sp. strain G-179, periplasmic nitrate reductase is required for the first step in denitrification, although the mechanism used to gain energy is unclear because the Nap system is not directly coupled to the generation of ATP(Bell et al., 1990; Bedzyk et al., 1999). In *S. gotlandica*, the gene within the Nap cluster that is responsible for electron transfer to generate energy has yet to be identified (see supplemental text S4.). It cannot be fully

excluded that functional differences in the Nap enzymes of different strains account for the different $\delta^{18}O$: $\delta^{15}N$ ratios in nitrate determined in those strains.

We suggest that the lower ratio of O vs. N fractionation during nitrate reduction in this study than in previous studies (Granger et al., 2004, 2008, 2010; Karsh et al., 2012; Wunderlich et al., 2012) can be explained by differences in the catalytic steps between Nar and Nap. Studies on the catalytic mechanism of Nap revealed that nitrate binds directly to a reduced molybdenum (Mo) center of the catalytic site with a rapid binding and dissociation compared to catalysis(Fourmond et al., 2008; Xie and Cao, 2010; Jacques et al., 2014) . Thus, all nitrate that binds to the catalytic site reacts, independent of the rate of internal electron transfer. In Nar, nitrate can also bind to an oxidized Mo center, such that the catalytic step depends on internal electron transfer, which may then be the rate-limiting stepc (Karsh et al., 2012). One possible implication is that this difference results in a different intramolecular isotope effect, which involves competition between an isotopically light and an isotopically heavy atom within the substrate for the active site(Northrop, 1981). For example, enzyme-substrate binding with the nitrate molecules $^{18}O^{14}N^{16}O_2$ and $^{14}N^{16}O_3$, can lead to a partitioning of the intermediates into Mo-^{18}O-$^{14}N^{16}O_2$ or Mo-^{16}O-$^{14}N^{16}O_2$, followed by N-O bond breakage, which is faster for lighter isotopes ($^{16}O > ^{18}O$). Thus, the nitrate pool is similarly enriched with ^{15}N but differently in ^{18}O. Presumably, in Nar-mediated reactions, light oxygen (^{16}O) is more likely split from light N-nitrate (^{14}N), whereas Nap also splits heavy oxygen (^{18}O) from light N-nitrate (^{14}N), leading to a slower enrichment of ^{18}O than of ^{15}N in nitrate when Nap is active.

Implications for the Baltic Sea and other seas

In the Baltic Sea redoxcline, the overlap of nitrate and hydrogen sulfide is often coupled to the entrainment of hypoxic waters into sulfidic layers, and denitrification activity is restricted to zones where both substances occur(Hannig et al., 2007; Hietanen et al., 2012; Dalsgaard et al., 2013). *S. gotlandica* is consistently present in hypoxic and sulfidic water layers(Grote et al., 2012). Our findings suggest that the bacterium does not initiate denitrification until anoxic conditions are fully established, even when hypoxic, nitrate-rich waters mix with sulfidic waters and appropriate electron-donors (thiosulfate, sulfur, or hydrogen sulfide) and electron-acceptors (nitrate) are present.

Furthermore, the fractionation factors for nitrate reduction in chemolithoautotrophic denitrification are in the same range as those for heterotrophic denitrification and the presence of oxygen does not lower ε. Hence, the low fractionation factor determined from field data of the Baltic Sea must stem from other factors, such as the close coupling of nitrification with denitrification or substrate limitation(Frey et al., 2014). Our study shows that Nap-catalyzed denitrification yields a $\delta^{18}O$:$\delta^{15}N$ratio of 0.5 in nitrate, which seems to be the isotopic baseline for denitrification in the Baltic Sea redoxcline, with chemolithoautotrophic denitrification as the major N loss process and *S. gotlandica* primarily responsible for it. While for nitrate assimilation a ratio of 1: 1 for $\delta^{18}O$:$\delta^{15}N$ could be validated for all marine and terrestrial aquatic systems regardless of the responsible enzyme (Granger et al., 2010), for dissimilative nitrate reduction the ratio differs between Nar and Nap–mediated processes. In Lake Lugano, the $^{18}\varepsilon$:$^{15}\varepsilon$ ratio is 0.89 (Wenk et al., 2014), predominantly attributed to chemolithoautotrophic denitrification (Wenk et al., 2013)(Wenk et al., 2014). The higher value than the one determined in our study may reflect the co-occurrence of nitrification, the presence of anammox, or differences in the contributions of Nap- vs. Nar-mediated denitrification. Whether Nap-catalyzed denitrification is a feature more common in chemolithoautotrophic than in heterotrophic denitrifiers cannot be concluded from this study, and it remains to be examined whether in other chemoautotrophic denitrifying bacteria, particularly those that do not possess the Nap gene, fractionation factors are in a similar range. Most freshwater and groundwater studies have shown an isotopic ratio of 0.5:1 in nitrate for denitrification(Böttcher et al., 1990; Lehmann et al., 2003); hence, Nap-catalyzed denitrification can account for the isotopic baseline in these systems.

Conclusions and outlook

Three studies were carried out as part of this thesis, in which the N cycle of the Baltic Sea was investigated by means of stable isotopes (Figure 24). In the first study, the importance of fourmajor N sources in different regions of the Baltic Sea was evaluated. The second study addressed N loss at the oxic-anoxic interface within the water-column of the central Baltic Sea, focusing, as discussed in Chapter 3, on the key-denitrifier *Sulfurimonas gotlandica*strain GD1^{T}. The dual isotopes of nitrate were exploited to unravel dominating sources or processes. The results highlight the potential and broad application of the use of stable isotopes in nutrient cycling and pin-point interesting new avenues for future research.

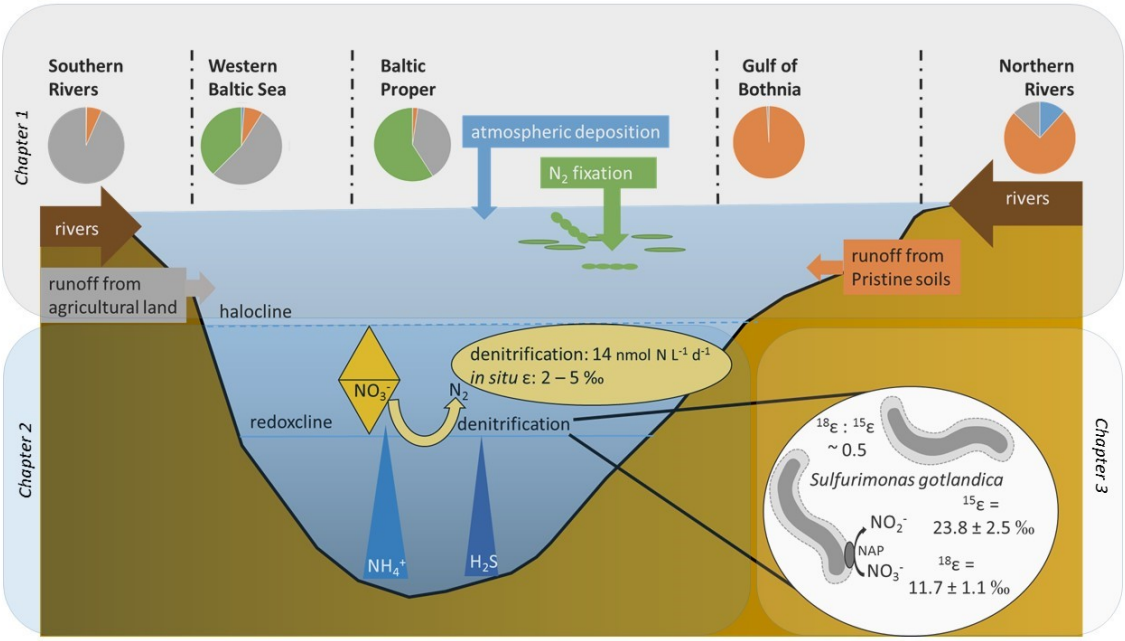

Figure 24: The pie charts show the contributions of the four sources of nitrate (N_2 fixation, atmospheric deposition, runoff from agricultural land, runoff from pristine soils) to total nitrate inputs for the particular regions of the Baltic Sea (Chapter 1). Nitrate turnover at the redoxcline is shown, with the major results from the field study (Chapter 2). The circular inset on the right shows the results from the laboratory studies (Chapter 3).

Identification of major nitrate sources and their implications for the Baltic Sea

Nitrate sources differ between northern and southern rivers, reflecting regional differences in land use and population density of the Baltic Sea's drainage area (Voss et al., 2011; HELCOM, 2013). While in northern rivers 75% of the nitrate derives from nitrification activity in pristine soilsunaffected by human activity, in southern rivers 95% of the nitrate is from agricultural runoff (Figure 24).In the central Baltic Sea, which is separated from coastal areas by an anti-clockwise circulation with closed streamlines that restrict the mass transport of dissolved substances (Voss et al. 2011), ~60% of its nitrate comes from N_2fixation (Figure 24). Studies using the $\delta^{15}N$ imprint in surface sediments (Voss et al., 2005) and model studies (Neumann et al., 2002)concluded that N_2 fixation is the main nitrogen source and that nitrogen derived from the major riversis sequestered along the coastal rim. According to the results of chapter 1, 39% of the nitrate in the central Baltic Seaderives from agricultural runoff (Figure 24), thus contradicting the results of those previous studies (Neumann et al., 2002; Voss et al., 2005). However, caution is requiredin interpreting the results of Bayesian mixing models, due to the underlying assumptions regarding the sources. In the model devised for this study, the only source with a high $\delta^{15}N$ was agricultural runoff, despite the fact that nitrate from below the halocline (nitrate maximum in the water column)has a similar $\delta^{15}N$ value of 7- 8‰. The upward mixing of nitrate was not consideredas a source in the model, although the mixture of this nitrate into the upper water layers during storm events in winter and fall could not be ruled out. The magnitude of the impact of this potential nitrate source to the surface water in the central Baltic Sea remains to be investigated.

If sources overlap in isotope values, then the model's output must be scutinized and a Bayesian mixing model becomes of limited use. Other limitations are the number of sources that can be identified, which is always dependet on the number of tracers and on thetemporal variation of the NO_3^- sources(Fry, 2013).This can introduce further uncertaintiesas it will reveal a great variability in nitrate contributions. However, if source patterns change due to climate change, human land use, or changes in fossil fuel

combustion, then the signature transfer will change and a different isotope landscape (isoscape) for nitrate isotope distribution will emerge. Hence, Bayesian mixing models are very useful in the early detection of such changes and therefore provide a reliable approach to assess the temporal and spatial variations of major NO_3^- sources in the Baltic Sea.

The ecological relevance of pelagic redoxclines for N-cycling in the Baltic Sea

A numerical model was successfully applied to a nitrate isotope dataset from the Baltic Sea redoxcline andallowed the estimation of an integrated denitrification rate of 14 nmol N L^{-1} $h^{-1}$for this zone (Figure 25). This low rate is an average rate over several days to weeks, combining very active periods as well as those of low activity. From ^{15}N incubation experiments it is known that activity patterns are very patchy and depend on the supply rates of nitrate and hydrogen sulfide (Hietanen et al., 2012; Dalsgaard et al., 2013). While in the open ocean the supply and composition of organic matter control the processes by which fixed nitrogen is lost, in systems with sulfidic bottom waters N loss is decoupled from organic matter and driven by sulfur compounds (Figure 25).

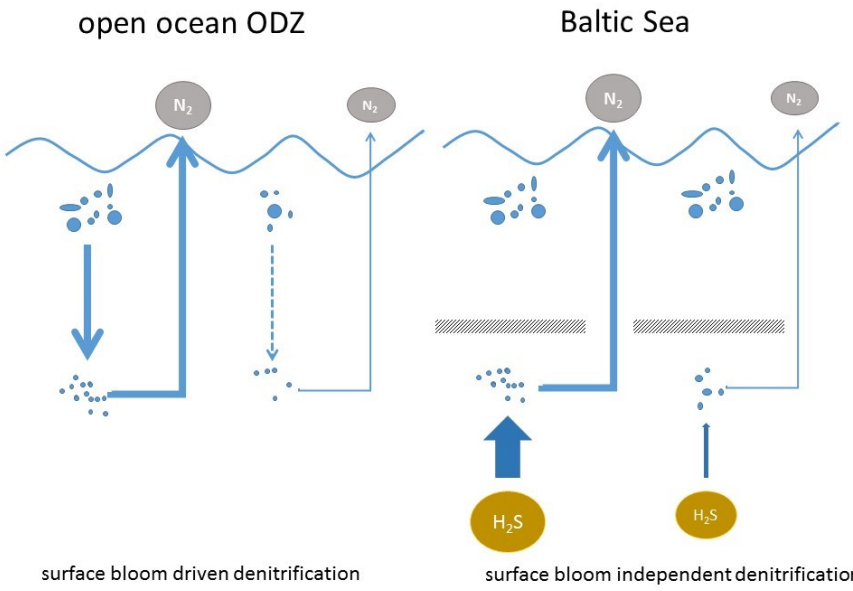

Figure 25: The dynamics of N loss in (a) open oceans, where sinking organic matter is the major driver for denitrification, and (b) the Baltic Sea (and other basins with sulfidic bottom waters), where denitrification is driven by the supply rate of hydrogen sulfide.

Chemolithotrophs account for high light-independent CO_2 fixation rates throughout sulfidic layers of the Baltic Sea (Grote et al., 2008; Jost et al., 2008; Glaubitz et al., 2009) and may fuel further sulfate reduction, which potentially stabilizes the sea's sulfidic conditions and hence supports further N loss (Schunck et al., 2013). In sulfidic systems, like the Baltic Sea, chemoautotrophic production is of major importance (Grote et al., 2008; Glaubitz et al., 2009; Labrenz et al., 2010) and seems to be the driving force for N loss.

Specific isotope fractionation in nitrate by a key-microbial player indenitrification in the Baltic Sea redoxcline

The fractionation factor of N in nitrate via chemolithoautotrophic denitrification was similar to that resulting from heterotrophic denitrification (Figure 26). This study provided evidence that the discrepancy between the $\delta^{18}O$:$\delta^{15}N$ ratio of around 0.5:1 in freshwater and the 1:1 ratio obtained in laboratory/marine studies could be related to differences in the major enzymes responsible for respiratory nitrate reduction. While the membrane-bound nitrate reductase (Nar) leads to a 1:1 increase in $\delta^{18}O$:$\delta^{15}N$, the periplasmic nitrate reductase (Nap) increases O and N isotope values by a ratio of 0.5, which can lead to ecosystem- wide differences.

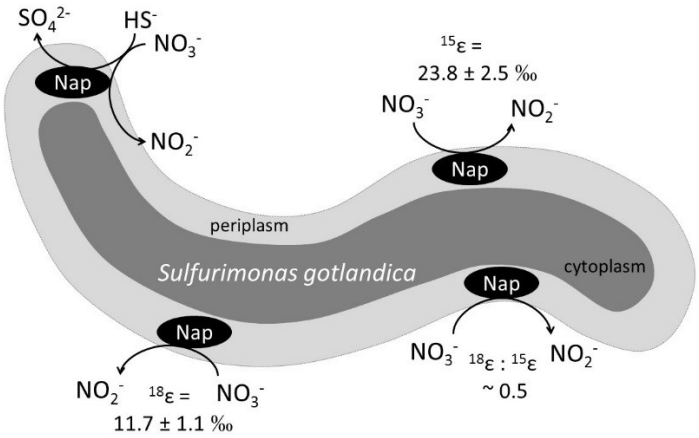

Figure 26: Summary of the findings for the denitrifying *EpsilonproteobacteriaSulfurimonas gotlandica*.

The culture study showed higher fractionation factors (13-20‰; Figure 26) than measured *in situ* (2-5‰; Figure 24). This implies that denitrifying *S. gotlandica* has a

limited supply of electron donor and/or electron acceptor *in situ*, due to strict, barely overlapping substrate gradients. Nitrate limitation could be simulated in culture indirectly by not stirring the cultures, which created a gradient similar to thatin nature. The simulated nutrient limitation resulted in a lower fractionation factor, which at least in part explained the low ε in the Baltic Sea redoxcline. However, in the cultures, nitrate concentrations were never below 120µmol L^{-1}whereas in other studies nitrate concentrations of 2-35µmol L^{-1}wereneeded to achieve a lower ε (Kritee et al. 2012). Accordingly, fractionation factors in culture never reached values similar to those*in situ*.

The observation that $\delta^{18}O$:$\delta^{15}N$ infreshwater and terrestrial systems is< 1could reflect the difference in the relative importance of Nap vs. Nar in respiratory nitrate reduction, but further investigations are needed. Clearly, Nar is used for assimilative and dissimilative nitrate reduction and hence is more abundant than Nap among different ecosystems. In a study of the contents of NarG and NapA gen numbersin 18 different environments, higher NapA than NarG gen copy numbers were determined in surface river water and groundwater, suggesting the importance of Nap in these environments(Bru et al., 2007). However, that study did not investigate a marine site, hence whether Nap is more important in freshwater than in marine systemsis unknown. However, differences in the contribution of the two enzymes might still account for the difference in isotope expression in the two different ecosystems, and knowledge of the presence or absence of Nap or Nar could be used to predict the $\delta^{18}O$: $\delta^{15}N$ of nitrate in a particular ecosystem. Based on the predicted baseline (0.5 or 1 :1) the deviation from that slope can be used for further interpretations of determineddual isotopes of nitrate.

With a ratio of 0.5 for $\delta^{18}O$:$\delta^{15}N$ in nitrateas a baseline for denitrification in the Baltic Sea,the *in situ* ratio of 1.5:1 probably reflects nitrification activity in that zone. Nitrification rates ofammonia-oxidizing archaea of the phylum *Thaumarcheota*were shown to be highest in the hypoxic zone and remainactive under sulfidic conditions,but at a lower rate(Berg et al., 2014). While the exact mechanism of nitrification in sulfidic layers is thus far unknown (Berg et al. 2014), those results supportour findings of a close coupling of nitrification and denitrificationin the Baltic Sea redoxcline. The finding that *S. gotlandica* does not initiate denitrification until full anoxia is established, even if both substrates are available, has important implications. Nitrification and denitrification may even co-occur in sulfidic layers, a possibility that has been overlooked because the

nitrate produced by nitrification is immediately reduced to N_2.Sufficient nitrate for isotope analysis mainlyoccurs under hypoxic conditions, butalthoughthe entire zone of denitrification was not examined in this thesis; it was possible to track processes taking place in the sulfidic zone as well, because they are imprinted in the nitrate lying above this zone.

Re-evaluating the N isotope budget of the Baltic Sea

Marine nitrogen budgets have been applied to resolve the quantity and balance of the marine nitrogen cycle and to constrain and understand the controlling factors(Brandes and Devol, 2002; Deutsch et al., 2004; Brandes et al., 2007). For the Baltic Sea, the first nitrogen budget based on stable isotope data of three major sources and sinks was calculatedalmost 10 years ago (Voss et al., 2005). With the new findings generated as part of this thesis input data can be updated and the nitrogen isotope mass balance model from Voss et al., (2005) accordingly recalculated (Table 12).

Table 12: Fluxes, means, and standard deviation of $\delta^{15}N$- NO_3^- for different sources and sinks in the Baltic. The balance of the budget is centered around N_2 fixation and sedimentary denitrification. Values changed based on the findings in this thesis are shown in bold.

Process	Flux (kt N y^{-1})	mean $\delta^{15}N$ (‰)	STD $\delta^{15}N$ (‰)	Reference
sources				
rivers	316[a]	**9.9**	**1.5**	**Chapter 1**
atmosphere	185[b]	**0.3**	**1.4**	**Chapter 1**
N_2 fixation	370[d](set to variable in the model)	0.2	1.0	Meyer-Harms et al.,(1999)
sinks				
burial	113[c]	5.3	2.3	Voss et al., (2005)
water column denitrification	100 -550	**-5**[*]	**3**	**Chapter 2**
sediment denitrification	426 - 652[e](set to variable in the model)	**-18.9**[*]	**0.9**	Dähnke et al., (2013)

[a]HELCOM (1998); [b]HELCOM (1997); [c]Emeis et al. (2000); [d]Wasmund et al. (2001); [e]Deutsch et al. 2010;
[*]numbers represent ε rather than a mean $\delta^{15}N$

Originally, the model was developed to constrain the global marine-fixed nitrogen isotopic budget proposed by Brandes and Devol (2002) and subsequnetly adapted to Baltic Sea settings by Voss et al. (2005). It solves two equations with six source and sink terms anddefines sediment denitrification and N_2 fixation rates as a function of variable source and sink estimates. In Chapter 1 of this thesis, new mean $\delta^{15}N$ values of the two sources, rivers and atmospheric deposition, were obtained and the model was accordingly updated (Table 12). The fractionation factor of 20 ‰ for water column denitrification in the Baltic Seareported in Voss et al. (2005) was reduced to 2- 5 ‰ based on findings in Chapter 2.For sedimentary denitrification, the isotope effect was found to be higher in the Baltic Sea than previously assumed (Dähnke and Thamdrup, 2013)and the new value was adopted in the model (Table 12). Using the water column denitrification rate of 14nmol N L^{-1} d^{-1} from Chapter 2, a minimal and maximal area of the hypoxic zone from Conley et al. (2009) (11050 km² and 67700 km², respectively), and an extension of the hypoxic zone measured in Chapter 2 from 4- 52 m (Table 12), a N removal rateof 31- 411 kt N $yr^{-1}$was calculated. The estimated N removal flux showed a high variation but is in the range of values calculated by Dalsgaard et al.,(2013). In recent studies, the role of water-column denitrification in N removal was found to be just as important as that of sediment denitrification (Hietanen et al., 2012; Dalsgaard et al., 2013). Hence, in the model presented herein, fluxes for water column denitrification increased from 47 kt N yr^{-1} in Voss et al. (2005) to a maximum of 550 kt N yr^{-1}. Two isotope budgets, with water column denitrification rates of 100 and 550 kt N yr^{-1},were calculated to account for the high variability of N loss (Figure 27). For both, the sedimentary denitrification required to balance the budget was not as high as the 855 kt N yr^{-1} reported by Voss et al. (2005)(Figure 27).In the first budget,a water column N loss of100kt N yr^{-1} equaled the sedimentary N loss (100 kt N yr^{-1}) (Figure 27a). In the second budget, with a water column denitrification rate of550 kt N yr^{-1}, the obtained N_2 fixation rateof 350 kt N yr^{-1} was close to the estimate of annual N_2 fixation of 370 kt N yr^{-1}(Wasmund et al., 2001). However, N loss in the sediments becomes less important with 350 kt N yr^{-1}compared 550 kt N yr^{-1} in the water column (Figure 27b).One practical implication of these newly calculated budgets is that with increasing hypoxia the function of sediments as a nitrogen filter is reduced, as previously found for the Gulf of Finland (Jäntti and Hietanen, 2012).

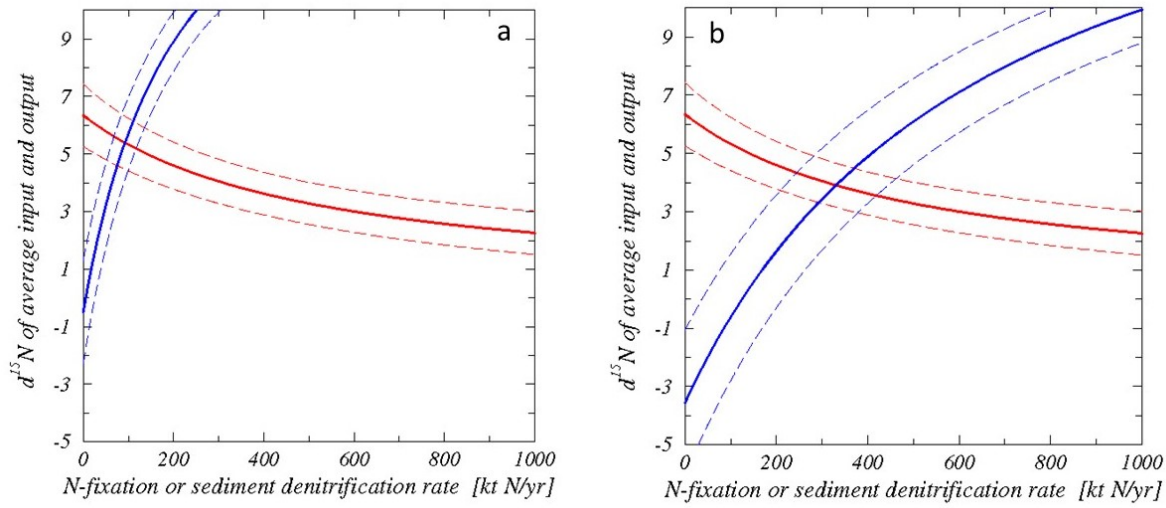

Figure 27: Model results with updated input data taken from Table 12. In (a) a water column denitrification flux of 100 kt N yr^{-1} was applied and in (b) a rate of 550 kt N yr^{-1} was used. Blue lines denote the sinks term (sedimentary denitrification) and red lines the sources term (N_2 fixation); where the lines cross, the budget is balanced.

A recent N budget estimated higher N removal by sediment denitrification (426- 652 kt N yr^{-1}) than determined using above described approach, but it allocated equal removal by denitrification in the water column and by sediments(Deutsch et al., 2010). Considering the increasing hypoxiaof the water column in the Baltic Sea(Conley et al., 2009), N removal is apparently shifting from sediments to the water column. Uncertainties remain whether more N is transported to the open sea when coastal sediments turn anoxic, or whether denitrification in the water column can replace the capacity of sediments with respect to N loss.

Outlook

In this thesis, the isotope values in nitrate and different modeling approaches were applied to investigate the dominat N turnover processes in the redoxcline and the different nitrate sources entering the Baltic Sea. This allowed a determination of the impact of N not only on an ecosystem level, but also on a species-specific level.The contribution of different dissimilative nitrate reductases on fractionation factors and their variable influences with respect to certain environmental changes, such as N starvation and redox conditions, should be analyzed in further studies. Enzyme essays conducted for this purpose will help to differentiate the effects of uptake and efflux

compared to the reduction by the enzyme. A mechanistic understanding will provide an important basis for future isotope research in the marine environment. For example, nano-scale resolution secondary ion mass spectrometry (Nano-Sims) and single-cell genomics can be applied to determine how N is converted on a species level and how that conversion influences the stable isotope signature in substrates, products, and the organism itself, and where in the cell N is metabolized. Finally, the findings of this thesis provide the first steps towards developing a nitrate isotope landscape for the Baltic Sea, includingtemporal and spatial relationships. This approach may also be used for other nitrogen compounds in the Baltic Sea and will help to better evaluate and predict changes in nitrogen sources.

To preserve the ecosystem function of the Baltic Sea, a further reduction in N inputs is necessary. Models have predicted that global warming will result in reduced oxygen solubility at higher temperatures and increasedstratification of the water column due to stronger temperature gradients in the upper waters (Bopp et al., 2002; Matear and Hirst, 2003). Furthermore, reactive N inputs are predicted to rise as a product ofincreased freshwater runoff and theincreasing deposition of atmospheric anthropogenic fixed nitrogen into the ocean, and particularly coastal waters (Duce et al., 2008). This, in turn, is expected to contribute to the expansion and intensification of ODZs(Conley et al., 2011)and thereby alter marine ecosystems. Hence combating these expansions in the face of unabated global warming remains one of the major challenges confronting the world's oceans, as well as the Baltic Sea.

Bibliography

Altabet, M.A. (1988) Variations in nitrogen isotopic composition between sinking and suspended particles: implications for nitrogen cycling and particle transformation in the open ocean. *Deep. Res.***35**: 535–554.

Altabet, M.A. and McCarthy, J.J. (1986) Vertical patterns in ^{15}N natural abundance in PON from the surface waters of warm-core rings. *J. Mar. Res.***44**: 185–201.

Altabet, M.A., Pilskaln, C., Thunell, R., Pride, C., Sigman, D., Chavez, F., and Francois, R. (1999) The nitrogen isotope biogeochemistry of sinking particles from the margin of the Eastern North Pacific. *Deep Sea Res. Part I Oceanogr. Res. Pap.***46**: 655–679.

Andersen, J.H., Axe, P., Backer, H., Carstensen, J., Claussen, U., Fleming-Lehtinen, V., et al. (2010) Getting the measure of eutrophication in the Baltic Sea: towards improved assessment principles and methods. *Biogeochemistry***106**: 137–156.

Babbin, A.R., Keil, R.G., Devol, A.H., and Ward, B.B. (2014) Organic matter stoichiometry, flux, and oxygen control nitrogen loss in the ocean. *Science***344**: 406–8.

BACC (2008) Assessment of climate change for the Baltic Sea Basin Bolle,H.-J., Menenti,M., and Rasool,I. (eds) Springer, Berlin Heidelberg.

Balch, W.E., Fox, G.E., Magrum, L.J., Woese, C.R., and Wolfe, R.S. (1979) Methanogens: reevaluation of a unique biological group. *Microbiol. Rev.***43**: 260–296.

Bange, H.W., Rixen, T., Johansen, A.M., Siefert, R.L., Ramesh, R., Ittekkot, V., et al. (2000) A revised nitrogen budget from the Arabian Sea. *Global Biogeochem. Cycles***14**: 1238–1297.

Barford, C.C., Montoya, J.P., Altabet, M.A., and Mitchell, R. (1999) Steady-State Nitrogen Isotope Effects of N_2 and N_2O Production in *Paracoccus denitrificans*. *Appl. Environ. Microbiol.***65**: 989–994.

Bartnicki, J. and Fagerli, H. (2008) Airborne load of nitrogen to European seas. *Ecol. Chem. Eng. S-Chemia I Inz. Ekol. S***15**: 297–313.

Bauer, S. (2003) Structure and function of nitrifying bacterial communities in the eastern Gotland Basin (central Baltic Sea). *Inst. Balt. Sea Res. Warn.* 120pp.

Bedzyk, L., Wang, T., Ye, R.W., and Wang, T.A.O. (1999) The periplasmic nitrate reductase in *Pseudomonas sp* . strain G-179 catalyzes the first step of denitrification. *J. Bacteriol.***181**: 2802–2806.

Bell, L.C., Richardson, D.J., and Ferguson, S.J. (1990) Periplasmic and membrane-bound respiratory nitrate reductases in *Thiosphaera pantotropha*. The periplasmic enzyme catalyzes the first step in aerobic denitrification. *FEBS Lett.***265**: 85–7.

Bender, M.L. (1990) The ^{18}O of dissolved O_2 in seawater: a unique tracer of circulation and respiration in the deep sea. *J. Geophys. Res.***95**: 22243–22252.

Berg, C., Vandieken, V., Thamdrup, B., and Jürgens, K. (2014) Significance of archaeal nitrification in hypoxic waters of the Baltic Sea. *ISME J* in press.

Böhlke, J.K., Mroczkowski, S.J., and Coplen, T.B. (2003) Oxygen isotopes in nitrate: new reference materials for ^{18}O:^{17}O:^{16}O measurements and observations on nitrate-water equilibration. *rapid Commun. mass Spectrom.***17**: 1835–1846.

Bopp, L., Le Quéré, C., Heimann, M., Manning, A.C., and Monfray, P. (2002) Climate-induced oceanic oxygen fluxes: Implications for the contemporary carbon budget. *Global Biogeochem. Cycles***16**: 1–13.

Böttcher, J., Strebel, O., Voerkelius, S., and Schmidt, H.L. (1990) Using isotope fractionation of nitrate-nitrogen and nitrate-oxygen for evaluation of microbial denitrification in a sandy aquifer. *J. Hydrol.***114**: 413–424.

Bourbonnais, A., Lehmann, M.F., Butterfield, D. a., and Juniper, S.K. (2012) Subseafloor nitrogen transformations in diffuse hydrothermal vent fluids of the Juan de Fuca Ridge evidenced by the isotopic composition of nitrate and ammonium. *Geochemistry, Geophys. Geosystems***13**: 1-23.

Bourbonnais, A., Lehmann, M.F., Waniek, J.J., and Schulz-Bull, D.E. (2009) Nitrate isotope anomalies reflect N2 fixation in the Azores Front region (subtropical NE Atlantic). *J. Geophys. Res.***114**: 1-16.

Brandes, J.A. and Devol, A.H. (2002) A global marine-fixed nitrogen isotopic budget: Implications for Holocene nitrogen cycling. *Global Biogeochem. Cycles***16**: 1–14.

Brandes, J.A., Devol, A.H., Yoshinari, T., Jayakumar, D.A., and Naqvi, S.W.A. (1998) Isotopic composition of nitrate in the central Arabian Sea and eastern tropical North Pacific: A tracer for mixing and nitrogen cycles. *Limnol. Oceanogr.***43**: 1680–1689.

Brettar, I., Labrenz, M., Flavier, S., Boetel, J., Kuosa, H., Christen, R., and Hoefle, M.G. (2006) Identification of a *Thiomicrospira denitrificans*-like *Epsilonproteobacterium* as a catalyst for autotrophic denitrification in the Central Baltic Sea. *Appl. Environ. Microbiol.***72**: 1364–1372.

Brettar, I. and Rheinheimer, G. (1991) Denitrification in the central Baltic: evidence for H_2S-oxidation as motor of denitrification at the oxic-anoxic interface. *Mar. Ecol. Prog. Ser.***77**: 157–169.

Brioukhanov, A., Pieulle, L., and Dolla, A. (2010) Antioxidative defense systems of anaerobic sulfate-reducing microorganisms. In, Méndez-Vilas,A. (ed), *Current Research,*

Technology and Education Topics in Applied Microbiology and Microbial Biotechnology. Formatex Research Center, pp. 148–159.

Bru, D., Sarr, A., and Philippot, L. (2007) Relative abundances of proteobacterial membrane-bound and periplasmic nitrate reductases in selected environments. *Appl. Environ. Microbiol.***73**: 5971–4.

Bruckner, C.G., Mammitzsch, K., Jost, G., Wendt, J., Labrenz, M., and Jürgens, K. (2013) Chemolithoautotrophic denitrification of epsilonproteobacteria in marine pelagic redox gradients. *Environ. Microbiol.***15**: 1505–1513.

Brunner, B., Contreras, S., Lehmann, M.F., Matantseva, O., Rollog, M., Kalvelage, T., et al. (2013) Nitrogen isotope effects induced by anammox bacteria. *Proc. Natl. Acad. Sci. U. S. A.***110**: 18994–9.

Bruns, A., Cypionka, H., and Overmann, J. (2002) Cyclic AMP and Acyl Homoserine Lactones increase the cultivation efficiency of heterotrophic bacteria from the central Baltic Sea. *Appl. Environ. Microbiol.***68**: 3978–3987.

Buchwald, C. and Casciotti, K.L. (2010) Oxygen isotopic fractionation and exchange during bacterial nitrite oxidation. *Limnol. Oceonography***55**: 1064–1074.

Buchwald, C., Santoro, A.E., McIlvin, M.R., and Casciotti, K.L. (2012) Oxygen isotopic composition of nitrate and nitrite produced by nitrifying cocultures and natural marine assemblages. *Limnol. Oceanogr.***57**: 1361–1375.

Burns, D., Boyer, E., Elliott, E., and Kendall, C. (2009) Sources and transformations of nitrate from streams draining varying land uses: evidence from dual isotope analysis. *J. Environ. Qual.***38**: 1149–1159.

Campbell, D., Kendall, C., Chang, C.C.Y., Silva, S.R., and Tonnessen, K.A. (2002) Pathways for nitrate release from an alpine watershed: Determination using $\delta^{15}N$ and $\delta^{18}O$. *Water Resour. Res.***38**: 1–9.

Canfield, D.E., Stewart, F.J., Thamdrup, B., De Brabandere, L., Dalsgaard, T., Delong, E.F., et al. (2010) A cryptic sulfur cycle in oxygen-minimum-zone waters off the Chilean coast. *Science.***330**: 1375–1378.

Carpenter, E., Montoya, J., Burns, J., Mulholland, M.R., Subramaniam, A., and Capone, D.G. (1999) Extensive bloom of a N_2-fixing diatom/cyanobacterial association in the tropical Atlantic Ocean. *Mar. Ecol. Prog. Ser.***185**: 273–283.

Carpenter, E.J., Harvey, H.R., Fry, B., and Capone, G.G. (1997) Biogeochemical tracers of the marine cyanobacterium *Trichodesmium*. *Deep. Res. I***44**: 27–38.

Carpenter, E.J. and Romans, K. (1991) Major role of the cyanobacterium *Trichodesmium* in nutrient cycling in the north atlantic ocean. *Science***254**: 1356–8.

Carstensen, J., Conley, D.J., Bonsdorff, E., Gustafsson, B.G., Hietanen, S., Janas, U., et al. (2014) Hypoxia in the Baltic Sea: biogeochemical cycles, benthic fauna, and management. *Ambio***43**: 26–36.

Casciotti, K.L. (2009) Inverse kinetic isotope fractionation during bacterial nitrite oxidation. *Geochim. Cosmochim. Acta***73**: 2061–2076.

Casciotti, K.L., Böhlke, J.K., McIlvin, M.R., Mroczkowski, S.J., and Hannon, J.E. (2007) Oxygen isotopes in nitrite: analysis, calibration, and equilibration. *Anal. Chem.***79**: 2427–36.

Casciotti, K.L. and Buchwald, C. (2012) Insights on the marine microbial nitrogen cycle from isotopic approaches to nitrification. *Front. Microbiol.***3**: 1–14.

Casciotti, K.L., Buchwald, C., and McIlvin, M. (2013) Implications of nitrate and nitrite isotopic measurements for the mechanisms of nitrogen cycling in the Peru oxygen deficient zone. *Deep Sea Res. Part I Oceanogr. Res. Pap.***80**: 78–93.

Casciotti, K.L., McIlvin, M., and Buchwald, C. (2010) Oxygen isotopic exchange and fractionation during bacterial ammonia oxidation. *Limnol. Oceonography***55**: 753–762.

Casciotti, K.L. and McIlvin, M.R. (2007) Isotopic analyses of nitrate and nitrite from reference mixtures and application to Eastern Tropical North Pacific waters. *Mar. Chem.***107**: 184–201.

Casciotti, K.L., Sigman, D.M., Hastings, M.G., Böhlke, J.K., and Hilkert, A. (2002) Measurement of the oxygen isotopic composition of nitrate in seawater and freshwater using the denitrifier method. *Anal. Chem.***74**: 4905–4912.

Casciotti, K.L., Sigman, D.M., and Ward, B.B. (2003) Linking diversity and stable isotope fractionation in Ammonia-Oxidizing bacteria. *Geomicrobiol. J.***20**: 335–353.

Codispoti, L.A. (2007) An oceanic fixed nitrogen sink exceeding 400 Tg N a^{-1} vs the concept of homeostasis in the fixed-nitrogen inventory. *Biogeosciences***4**: 233–253.

Codispoti, L.A. (2010) Interesting times for marine N_2O. *Science* **332**: 1339–1340.

Codispoti, L.A., Brandes, J.A., Christensen, J.P., Devol, A.H., Naqvi, S.W.A., Paerl, H.W., and Yoshinari, T. (2001) The oceanic fixed nitrogen and nitrous oxide budgets: Moving targets as we enter the anthropocene? *Sci. Mar.***65**: 85–105.

Conley, D.J., Björk, S., Bonsdorff, E., Carstensen, J., Destouni, G., Gustafsson, B.G., et al. (2009) Hypoxia-related processes in the Baltic Sea. *Environ. Sci. Technol.***43**: 3412–3420.

Conley, D.J., Bonsdorff, E., Carstensen, J., Destouni, G., Gustafsson, B.G., Hansson, L.-A., et al. (2009) Tackling hypoxia in the Baltic Sea: is engineering a solution? *Environ. Sci. Technol.***43**: 3407–11.

Conley, D.J., Carstensen, J., Aigars, J., Axe, P., Bonsdorff, E., Eremina, T., et al. (2011) Hypoxia is Increasing in the Coastal Zone of the Baltic Sea. *Environ. Sci. Technol.***45**: 6777–6783.

Conley, D.J., Carstensen, J., Vaquer-Sunyer, R., and Duarte, C.M. (2009) Ecosystem thresholds with hypoxia. *Hydrobiologia***629**: 21–29.

Conley, D.J., Humborg, C., Rahm, L., Savchuk, O.P., and Wulff, F. (2002) Hypoxia in the Baltic Sea and Basin-Scale Changes in Phosphorus Biogeochemistry. *Environ. Sci. Technol.***36**: 5315–5320.

Coolen, M.J.L., Abbas, B., Van Bleijswijk, J., Hopmans, E.C., Kuypers, M.M.M., Wakeham, S.G., and Sinninghe Damsté, J.S. (2007) Putative ammonia-oxidizing Crenarchaeota in suboxic waters of the Black Sea: a basin-wide ecological study using 16S ribosomal and functional genes and membrane lipids. *Environ. Microbiol.***9**: 1001–1016.

Dähnke, K., Emeis, K., Johannsen, A., and Nagel, B. (2010) Stable isotope composition and turnover of nitrate in the German Bight. *Mar. Ecol. Prog. Ser.***408**: 7–18.

Dähnke, K. and Thamdrup, B. (2013) Nitrogen isotope dynamics and fractionation during sedimentary denitrification in Boknis Eck, Baltic Sea. *Biogeosciences Discuss.***10**: 681–709.

Dalsgaard, T., De Brabandere, L., and Hall, P.O.J. (2013) Denitrification in the water column of the central Baltic Sea. *Geochim. Cosmochim. Acta***106**: 247–260.

Dalsgaard, T., Canfield, D.E., Petersen, J., Thamdrup, B., and Acuna-González, J. (2003) N_2 production by the anammox reaction in the anoxic water column of Golfo Dulce, Costa Rica. *Nature***422**: 606–608.

Dalsgaard, T., Thamdrup, B., Farías, L., and Peter Revsbech, N. (2012) Anammox and denitrification in the oxygen minimum zone of the eastern South Pacific. *Limnol. Oceanogr.***57**: 1331–1346.

Delwiche, C.C. and Steyn, P.L. (1970) Nitrogen isotope fractionation in soils and microbial reactions. *Environ. Sci. Technol.***4**: 929–935.

Deutsch, B., Forster, S., Wilhelm, M., Dippner, J.W., and Voss, M. (2010) Denitrification in sediments as a major nitrogen sink in the Baltic Sea: An extrapolation using sediment characteristics. *Biogeosciences Discuss.***7**: 2487–2521.

Deutsch, B., Mewes, M., Liskow, I., and Voss, M. (2006) Quantification of diffuse nitrate inputs into a small river system using stable isotopes of oxygen and nitrogen in nitrate. *Org. Geochem.***37**: 1333–1342.

Deutsch, C., Gruber, N., Key, R.M., and Sarmiento, J.L. (2001) Denitrification and N_2 fixation in the Pazific Ocean. *Global Biogeochem. Cycles***15**: 483–506.

Deutsch, C., Sigman, D.M., Thunell, R.C., Meckler, A.N., and Haug, G.H. (2004) Isotopic constraints on glacial/interglacial changes in the oceanic nitrogen budget. *Global Biogeochem. Cycles***18**: 1–22.

Devol, A.H. (1978) Bacterial oxygen uptake kinetics as related to biological processes in oxygen deficient zones of the oceans. *Deep Sea Res.***25**: 137–146.

Diaz, R.J. and Rosenberg, R. (2008) Spreading dead zones and consequences for marine ecosystems. *Science.***321**: 926–929.

Doane, T. a. and Horwáth, W.R. (2003) Spectrophotometric determination of nitrate with a single reagent. *Anal. Lett.***36**: 2713–2722.

Duce, R.A., LaRoche, J., Altieri, K., Arrigo, K.R., Baker, A.R., Capone, D.G., et al. (2008) Impacts of atmospheric anthropogenic nitrogen on the open ocean. *Science.***320**: 893–897.

Durka, W., Schulze, E., Gebauer, G., and Voerkeliust, S. (1994) Effects of forest decline on uptake and leaching of deposited nitrate determined from ^{15}N and ^{18}O measurements. *Nature***372**: 765–767.

Eichner, C. (2000) Mikrobielle Modifikation des Isotopensignals des Stickstoffs im marinen partikulären Material. *Inst. Balt. Sea Res. Warn.*1– 101.

Elmgren, R. (2001) Understanding Human Impact on the Baltic Ecosystem: Changing Views in Recent Decades. *Ambio***30**: 222–231.

Emeis, K.C., Struck, U., Leipe, T., Pollehne, F., Kunzendorf, H., and Christiansen, C. (2000) Changes in the C, N, P burial rates in some Baltic Sea sediments over the last 150 years - Relevance to P regeneration rates and the phosphorus cycle. *Mar. Geol.***167**: 43–59.

Erguder, T.H., Boon, N., Wittebolle, L., Marzorati, M., and Verstraete, W. (2009) Environmental factors shaping the ecological niches of ammonia-oxidizing archaea. *FEMS Microbiol. Rev.***33**: 855–869.

Eugster, O. and Gruber, N. (2012) A probabilistic estimate of global marine N-fixation and denitrification. *Global Biogeochem. Cycles***26**: 1–15.

Ferguson, S. (1994) Denitrification and its control. *Antonie Van Leeuwenhoek* 89–110.

Finni, T., Kononen, K., Olsonen, R., and Wallström, K. (2001) The histroy of cyanobacterial blooms. *Ambio***30**: 172–178.

Fonselius, S. (1983) Determination of hydrogen sulphide. In, Grasshoff (ed), *Methods of Seawater Analysis*. Wiley, Weinheim.

Francis, C. a, O'Mullan, G.D., Cornwell, J.C., and Ward, B.B. (2013) Transitions in nirS-type denitrifier diversity, community composition, and biogeochemical activity along the Chesapeake Bay estuary. *Front. Microbiol.***4**: 237.

Frey, C., Dippner, J.W., and Voss, M. (2014) Close coupling of N-cycling processes expressed in stable isotope data at the redoxcline of the Baltic Sea. *Global Biogeochem. Cycles***28**: 974–991.

Fry, B. (2013) Alternative approaches for solving underdetermined isotope mixing problems. *Mar. Ecol. Prog. Ser.***472**: 1–13.

Fry, B., Brand, W., Mersch, F.J., Tholke, K., and Garritt, R. (1992) Automated analysis system for coupled $\delta^{13}C$ and $\delta^{15}N$ measurements. *Anal. Chem.***64**: 288–291.

Fuchsman, C. a, Murray, J.W., and Staley, J.T. (2012) Stimulation of autotrophic denitrification by intrusions of the bosporus plume into the anoxic black sea. *Front. Microbiol.***3**: 257.

Fuchsman, C.A., Murray, J.W., and Konovalov, S.K. (2008) Concentration and natural stable isotope profiles of nitrogen species in the Black Sea. *Mar. Chem.***111**: 90–105.

Galloway, J.N., Aber, J.D., Erisman, J.W., Seitzinger, S.P., Howarth, R.W., Cowling, E.B., and Cosby, B.J. (2003) The Nitrogen Cascade.*BioSciences*.**53**. 341-356.

Galloway, J.N., Dentener, F.J., Capone, D.G., Boyer, E.W., Howarth, R.W., Seitzinger, S.P., et al. (2004) Nitrogen cycles : past , present , and future.*Biogeochemistry.***70**. 153-226.

Gaye, B., Nagel, B., Dähnke, K., Rixen, T., and Emeis, K.-C. (2013) Evidence of parallel denitrification and nitrite oxidation in the ODZ of the Arabian Sea from paired stable isotopes of nitrate and nitrite. *Global Biogeochem. Cycles***27**: 1059–1071.

Glaubitz, S., Kießlich, K., Meeske, C., Labrenz, M., and Jürgens, K. (2013) SUP05 dominates the Gammaproteobacterial sulfur oxidizer assemblages in pelagic redoxclines of the central Baltic and Black Seas. *Appl. Environ. Microbiol.***79**: 2767–76.

Glaubitz, S., Lueders, T., Abraham, W.-R., Jost, G., Jürgens, K., and Labrenz, M. (2009) 13C-isotope analyses reveal that chemolithoautotrophic *Gamma*- and *Epsilonproteobacteria* feed a microbial food web in a pelagic redoxcline of the central Baltic Sea. *Environ. Microbiol.***11**: 326–337.

Graneli, E., Wallstrom, K., Larsson, U., Graneli, W., and Elmgren, R. (1990) Nutrient limitation of primary production in the Baltic Sea area. *Ambio***19**: 142–151.

Granger, J. and Sigman, D.M. (2009) Removal of nitrite with sulfamic acid for nitrate N and O isotope analysis with the denitrifier method. *rapid Commun. mass Spectrom.***23**: 3753–3762.

Granger, J., Sigman, D.M., Lehmann, M.F., and Tortell, P.D. (2008) Nitrogen and oxygen isotope fractionation during dissimilatory nitrate reduction by denitrifying bacteria. *Limnol. Oceanogr.***53**: 2533–2545.

Granger, J., Sigman, D.M., Needoba, J.A., and Harrison, P.J. (2004) Coupled nitrogen and oxygen isotope fractionation of nitrate during assimilation by cultures of marine phytoplankton. *Limnol. Oceanogr.***49**: 1763– 1773.

Granger, J., Sigman, D.M., Rohde, M.M., Maldonado, M.T., and Tortell, P.D. (2010) N and O isotope effects during nitrate assimilation by unicellular prokaryotic and eukaryotic plankton cultures. *Geochim. Cosmochim. Acta***74**: 1030–1040.

Grasshoff, K. (1975) The hydrochemistry of landlocked basins and fjords. Academic Press, New York.

Grasshoff, K., Ehrhardt, M., and Kremling, K. (1983) Methods of seawater analysis Verlag Chemie.

Großkopf, T., Mohr, W., Baustian, T., Schunck, H., Gill, D., Kuypers, M.M.M., et al. (2012) Doubling of marine dinitrogen-fixation rates based on direct measurements. *Nature***488**: 361–4.

Grote, J. (2009) Physiology, ecology, and genomics of facultative chemoautotrophic *Epsilonproteobacteria* in marine pelagic redoxclines. *Inst. Balt. Sea Res. Warn.* 114.

Grote, J., Jost, G., Labrenz, M., Herndl, G.J., and Juergens, K. (2008) *Epsilonproteobacteria* Represent the Major Portion of Chemoautotrophic Bacteria in Sulfidic Waters of Pelagic Redoxclines of the Baltic and Black Seas. *Appl. Environ. Microbiol.***74**: 7546–7551.

Grote, J., Labrenz, M., Pfeiffer, B., Jost, G., and Juergens, K. (2007) Quantitative Distributions of *Epsilonproteobacteria* and a Sulfurimonas Subgroup in Pelagic Redoxclines of the Central Baltic Sea . *Appl. Environ. Microbiol.***73**: 7155–7161.

Grote, J., Schott, T., Bruckner, C.G., Glöckner, F.O., Jost, G., Teeling, H., et al. (2012) Genome and physiology of a model *Epsilonproteobacterium* responsible for sulfide detoxification in marine oxygen depletion zones. *Proc. Natl. Acad. Sci.***109**: 506–510.

Gruber, N. and Galloway, J.N. (2008) An Earth-system perspective of the global nitrogen cycle. *Nature***451**: 293–296.

Gruber, N., Jorge L. Sarmiento, and Sarmiento, J.L. (1997) Global patterns of marine nitrogen fixation and denitrification. *Glob. Biogeochem. Cycles***11**: 235–266.

Gustafsson, E. (2012) Modelled long-term development of hypoxic area and nutrient pools in the Baltic Proper. *J. Mar. Syst.***94**: 120–134.

Halpern, B.S., Walbridge, S., Selkoe, K.A., Kappel, C. V, Micheli, F., D'Agrosa, C., et al. (2008) A global map of human impact on marine ecosystems. *Science* .**319**: 948–952.

Hannig, M., Braker, G., Dippner, J., and Jürgens, K. (2006) Linking denitrifier community structure and prevalent biogeochemical parameters in the pelagial of the central Baltic Proper (Baltic Sea). *FEMS Microbiol. Ecol.***57**: 260–271.

Hannig, M., Kuypers, M.M.M., Woebken, D., Martens-Habbena, W., and Jürgens, K. (2007) Shift from denitrification to anammox after inflow events in the central Baltic Sea. *Limnol. Oceanogr.***52**: 1336–1345.

HELCOM (1997) Airborne pollution load to the Baltic Sea 1991– 1995. In, *Baltic Sea Environ. Proc. 69*., p. 29.

HELCOM (2002) Fourth periodic assessment of the state of the marine environment of the Baltic Sea area 1994–1998. In, *Balt. Sea Environ. Proc. No. B 82*., p. 215 pp.

HELCOM (2013) Review of the fifth Baltic Sea pollution load compilation for the 2013 HELCOM Ministerial Meeting. 1–49.

HELCOM (1998) The third Baltic Sea pollution load compilation. In, *Baltic Sea Environment Proceedings 70*., p. 133.

Hietanen, S., Jäntti, H., Buizert, C., Jürgens, K., Labrenz, M., and Voss, M. (2012) Hypoxia and nitrogen processing in the Baltic Sea water column. *Limnol. Oceanogr.***57**: 325–337.

Hoch, M.P., Fogel, M.L., and Kirchman, D.L. (1994) Isotope fractionation during ammonium uptake by marine microbial assemblages. *Geomicrobiol. J.***12**: 113–127.

Holtermann, P.L. and Umlauf, L. (2012) The Baltic Sea tracer release experiment: 2. Mixing processes. *J. Geophys. Res.***117**: 1-17.

Hong, B., Swaney, D.P., Mörth, C.-M., Smedberg, E., Eriksson Hägg, H., Humborg, C., et al. (2012) Evaluating regional variation of net anthropogenic nitrogen and phosphorus inputs (NANI/NAPI), major drivers, nutrient retention pattern and management implications in the multinational areas of Baltic Sea basin. *Ecol. Modell.***227**: 117–135.

Horrigan, S.G., Montoya, J.P., Nevins, J.L., and McCarthy, J.J. (1990) Natural isotopic composition of dissolved inorganic nitrogen in the Chesapeake Bay. *Estuar. Coast. Shelf Sci.***30**: 393–410.

Humborg, C., Danielsson, Å., Sjöberg, B., and Green, M. (2003) Nutrient land–sea fluxes in oligothrophic and pristine estuaries of the Gulf of Bothnia, Baltic Sea. *Estuar. Coast. Shelf Sci.***56**: 781–793.

Jackson, A.L., Inger, R., Bearhop, S., and Parnell, A. (2009) Erroneous behaviour of MixSIR, a recently published Bayesian isotope mixing model: a discussion of Moore & Semmens (2008). *Ecol. Lett.***12**: E1–5.

Jäntti, H. and Hietanen, S. (2012) The effects of hypoxia on sediment nitrogen cycling in the Baltic Sea. *Ambio***41**: 161–9.

Jäntti, H., Stange, F., Leskinen, E., and Hietanen, S. (2011) Seasonal variation in nitrification and nitrate-reduction pathways in coastal sediments in the Gulf of Finland, Baltic Sea. *Aquat. Microb. Ecol.***63**: 171–181.

Jensen, Petersen, J., Dalsgaard, T., and Thamdrup, B. (2009) Pathways, rates, and regulation of N_2 production in the chemocline of an anoxic basin, Mariager Fjord, Denmark. *Mar. Chem.***113**: 102–113.

Jilbert, T., Slomp, C.P., Gustafsson, B.G., and Boer, W. (2011) Beyond the Fe-P-redox connection : preferential regeneration of phosphorus from organic matter as a key control on Baltic Sea nutrient cycles. *Biogeosciences***8**: 1699–1720.

Johannsen, A., Dähnke, K., and Emeis, K. (2008) Isotopic composition of nitrate in five German rivers discharging into the North Sea. *Org. Geochem.***39**: 1–12.

Jost, G., Zubkov, M. V, Yakushev, E., Labrenz, M., and Juergens, K. (2008) High abundance and dark CO_2 fixation of chemolithoautotrophic prokaryotes in anoxic waters of the Baltic Sea. *Limnol. Oceanogr.***53**: 14–22.

Karsh, K.L., Granger, J., Kritee, K., and Sigman, D.M. (2012) Eukaryotic assimilatory nitrate reductase fractionates N and O isotopes with a ratio near unity. *Environ. Sci. Technol.***46**: 5727–35.

Kendall, C. (1998) Tracing nitrogen sources and cycling in catchments. In, Kendall,C. and McDonnell,J.J. (eds), *Isotope tracers in catchment hydrology*. Elsevier, Amsterdam, pp. 521–576.

Kendall, C., Elliott, E., and Wankel, S. (2007) Tracing anthropogenic inputs of nitrogen to ecosystems. In, R.H. Michener,K.L. (ed), *Stable isotopes in ecologyand environmental Science* Blackwell Publishing, pp. 375–449.

Kern, M. and Simon, J. (2009) Electron transport chains and bioenergetics of respiratory nitrogen metabolism in *Wolinella succinogenes* and other *Epsilonproteobacteria*. *Biochim. Biophys. Acta***1787**: 646–56.

Kim, T.-W., Lee, K., Najjar, R.G., Jeong, H.-D., and Jeong, H.J. (2011) Increasing N abundance in the northwestern Pacific Ocean due to atmospheric nitrogen deposition. *Science***334**: 505–9.

Knapp, A.N., Sigman, D.M., and Lipschultz, F. (2005) N isotopic composition of dissolved organic nitrogen and nitrate at the Bermuda Atlantic Time-series Study site. *Global Biogeochem. Cycles***19**: 1–15.

Korth, F., Deutsch, B., Frey, C., Moros, C., and Voss, M. (2014) Nitrate source identification in the Baltic Sea using its isotopic ratios in combination with a Bayesian isotope mixing model. *Biogeosciences***11**: 4913–4924.

Korth, F., Fry, B., Liskow, I., and Voss, M. (2013) Nitrogen turnover during the spring outflows of the nitrate-rich Curonian and Szczecin lagoons using dual nitrate isotopes. *Mar. Chem.***154**: 1–11.

Koszelnik, P. and Gruca-Rokosz, R. (2013) Determination of nitrate isotopic signature in waters of different sources by analysing the nitrogen and oxygen isotopic ratio. *Environ. Sci. Process. Impacts***15**: 751.

Kritee, K., Sigman, D.M., Granger, J., Ward, B.B., Jayakumar, A., and Deutsch, C. (2012) Reduced isotope fractionation by denitrification under conditions relevant to the ocean. *Geochim. Cosmochim. Acta***92**: 243–259.

Kuypers, M.M.M., Lavik, G., Woebken, D., Schmid, M., Fuchs, B.M., Amann, R., et al. (2005) Massive nitrogen loss from the Benguela upwelling system through anaerobic ammonium oxidation. *Proc. Natl. Acad. Sci. U. S. A.***102**: 6478–6483.

Kuypers, M.M.M., Silekers, A.O., Lavik, G., Schmid, M., Jørgensen, B.B., Kuenen, J.G., et al. (2003) Anaerobic ammonium oxidation by anammox bacteria in the Black Sea. *Nature***422**: 608–611.

Lääne, A., Kraav, E., and Titova, G. (2005) Global International Waters Assessment, Baltic Sea, regional assessment 17 University of Kalmar (ed) United Nations Environment Programme, Kalmar, Sweden.

Labrenz, M., Grote, J., Mammitzsch, K., Boschker, H.T.S., Laue, M., Jost, G., et al. (2013) *Sulfurimonas gotlandica* sp. nov., a chemoautotrophic and psychrotolerant *epsilonproteobacterium* isolated from a pelagic redoxcline, and an emended description of the genus Sulfurimonas. *Int. J. Syst. Evol. Microbiol.***63**: 4141–8.

Labrenz, M., Jost, G., and Jürgens, K. (2007) Distribution of abundant prokaryotic organisms in the water column of the central Baltic Sea with an oxic-anoxic interface. *Aquat. Microb. Ecol.***46**: 177–190.

Labrenz, M., Jost, G., Pohl, C., Beckmann, S., Martens-Habbena, W., and Juergens, K. (2005) Impact of Different In Vitro Electron Donor/Acceptor Conditions on Potential Chemolithoautotrophic Communities from Marine Pelagic Redoxclines. *Appl. Environ. Microbiol.***71**: 6664–6672.

Labrenz, M., Sintes, E., Toetzke, F., Zumsteg, A., Herndl, G.J., Seidler, M., and Jürgens, K. (2010) Relevance of a crenarchaeotal subcluster related to *CandidatusNitrosopumilus maritimus* to ammonia oxidation in the suboxic zone of the central Baltic Sea. *ISME J.***4**: 1496–1508.

Lam, Lavik, G., Jensen, M.M., Vossenberg, J. van de, Schmid, M., Woebken, D., et al. (2009) Revising the nitrogen cycle in the Peruvian oxygen minimum zone. *Proc. Natl. Acad. Sci.***106**: 4752–4757.

Lam, P. and Kuypers, M.M.M. (2011) Microbial nitrogen cycling processes in Oxygen Minimum Zones. In, *Annual Review of Marine Science, Vol 3*., pp. 317–345.

Larsson, U., Elmgren, R., and Wulff, F. (1985) Eutrophication and the Baltic Sea: causes and consequences. *Ambio (Sweden)*.

Lass, H.U. (2003) Dissipation in the Baltic proper during winter stratification. *J. Geophys. Res.***108**: 3187.

Lehmann, M., Reichert, P., Bernasconi, S., Barbieri, A., and McKenzie, J.A. (2003) Modelling nitrogen and oxygen isotope fractionation during denitrification in a lacustrine redox-transition zone. *Geochim. Cosmochim. Acta***67**: 2529–2542.

Lehmann, M.F., Sigman, D.M., McCorkle, D.C., Brunelle, B.G., Hoffmann, S., Kienast, M., et al. (2005) Origin of the deep Bering Sea nitrate deficit: Constraints from the nitrogen and oxygen isotopic composition of water column nitrate and benthic nitrate fluxes. *Global Biogeochem. Cycles***19**: 1–15.

Lehmann, M.F., Sigman, D.M., McCorkle, D.C., Granger, J., Hoffmann, S., Cane, G., and Brunelle, B.G. (2007) The distribution of nitrate $^{15}N/^{14}N$ in marine sediments and the impact of benthic nitrogen loss on the isotopic composition of oceanic nitrate. *Geochim. Cosmochim. Acta***71**: 5384–5404.

Lipschultz, F., Wofsy, S.C., Ward, B.B., Codispoti, L.A., Friedrich, G., and Elkins, J.W. (1990) Bacterial transformations of inorganic nitrogen in the oxygen-deficient waters of the Eastern Tropical South Pacific Ocean. *Deep Sea Res. Part A. Oceanogr. Res. Pap.***37**: 1513–1541.

Liu, K.-K., Su, M.-J., Hsueh, C.-R., and Gong, G.-C. (1996) The nitrogen isotopic composition of nitrate in the Kuroshio Water northeast of Taiwan: evidence for nitrogen fixation as a source of isotopically light nitrate. *Mar. Chem.***54**: 273–292.

Lunau, M., Voss, M., Erickson, M., Dziallas, C., Casciotti, K., and Ducklow, H. (2012) Excess nitrate loads to coastal waters reduces nitrate removal efficiency: mechanism and implications for coastal eutrophication. *Environ. Microbiol.*

Lundberg, C. (2005) Eutrophication in the Baltic Sea from area-specific biological effects to interdisciplinary consequences.

Lundberg, C., Jakobsson, B.-M., and Bonsdorff, E. (2009) The spreading of eutrophication in the eastern coast of the Gulf of Bothnia, northern Baltic Sea – An analysis in time and space. *Estuar. Coast. Shelf Sci.***82**: 152–160.

Mammitzsch, K., Jost, G., and Jürgens, K. (2014) Impact of dissolved inorganic carbon concentrations and pH on growth of the chemolithoautotrophic epsilonproteobacterium *Sulfurimonas gotlandica* GD1(T.). *Microbiologyopen***3**: 80–8.

Mariotti, A., Germon, J.C., Hubert, P., Kaisre, P., Letolle, R., Tardieux, A., and Tardieux, P. (1981) Experimental determination of nitrogen kinetic isotope fractionation: Some principles; Illustration for the denitrification and nitrification processes. *Plant Soil***62**: 413–430.

Mariotti, A., Landreau, A., and Simon, B. (1988) 15N isotope biogeochemistry and natural denitrification process in groundwater: Application to the chalk aquifer of northern France. *Geochim. Cosmochim. Acta***52**: 1869–1878.

Matear, R.J. and Hirst, A.C. (2003) Long-term changes in dissolved oxygen concentrations in the ocean caused by protracted global warming. *Global Biogeochem. Cycles***17**: 1-24.

Matthäus, W., Nehring, D., Feistel, R., Nausch, G., Mohrholz, V., and Lass, H.-U. (2008) State and Evolution of the Baltic Sea, 1952–2005 Feistel,R., Nausch,G., and Wasmund,N. (eds) John Wiley & Sons, Inc., Hoboken, NJ, USA.

Mayer, B., Boyer, E.W., Goodale, C., Jaworski, N.A., Breemen, N. van, Howarth, R.W., et al. (2002) Sources of nitrate in rivers draining sixteen watersheds in the northeastern U.S.: Isotopic constraints. *Biogeochemistry***57/58**: 171–197.

Mengis, M., Schif, S.L., Harris, M., English, M.C., Aravena, R., Elgood, R.J., and MacLean, A. (1999) Multiple geochemical and isotopic approaches for assessing ground water NO_3^- Elimination in a riparian zone. *Ground Water***37**: 448–457.

Meyer-Harms, B., Reckermann, M., Voss, M., Siegmund, H., and von Bodungen, B. (1999) Food selection by calanoid copepods in the euphotic layer of the Gotland Sea (Baltic Proper) during mass occurrence of N_2-fixing cyanobacteria. *Mar. Ecol. Ser.***191**: 243–250.

Michaels, A.F., Siegel, D.A., Johnson, R.J., Knap, A.H., and Galloway, J.N. (1993) Episodic inputs of atmospheric nitrogen to the sargasso sea: contributions to new production and phytoplankton blooms. *Global Biogeochem. Cycles***7**: 339–351.

Miyake, Y. and Wada, E. (1971) The isotope effect on the nitrogen in biochemical, oxidation-reduction reactions. *Rec. Oceanogr. Work Japan***11**: 1–6.

Montoya, J., Carpenter, E., and Capone, D. (2002) Nitrogen fixation and nitrogen isotope abundances in zooplankton of the oligotrophic North Atlantic. *Limnol. Oceanogr.***47**: 1617–1628.

Moore, J.W. and Semmens, B.X. (2008) Incorporating uncertainty and prior information into stable isotope mixing models. *Ecol. Lett.***11**: 470–80.

Moreno-Viviàn, C., Cabello, P., Martìnez-Luque, M., Blasco, R., and Castillo, F. (1999) Prokaryotic nitrate reduction: molecular properties and functional distinction among bacterial nitrate reductases. *J. Bacteriol.***181**: 6573–6584.

Mort, H.P., Slomp, C.P., Gustafsson, B.G., and Andersen, T.J. (2010) Phosphorus recycling and burial in Baltic Sea sediments with contrasting redox conditions. *Geochim. Cosmochim. Acta***74**: 1350–1362.

Mulholland, P.J., Helton, A.M., Poole, G.C., Hall, R.O., Hamilton, S.K., Peterson, B.J., et al. (2008) Stream denitrification across biomes and its response to anthropogenic nitrate loading. *Nature***452**: 202–5.

Myrberg, K. and Andrejev, O. (2006) Modelling of the circulation, water exchange and water age properties of the Gulf of Bothnia. *Oceanologia***48**: 55–74.

Naqvi, S.W.A., Voss, M., and Montoya, J.P. (2008) Recent advances in the biogeochemistry of nitrogen in the ocean. *Biogeosciences***5**: 1033–1041.

Naqvi, S.W.A., Yoshinari, T., Jayakumar, D.A., Altabet, M.A., Narvekar, P. V., Devol, A.H., et al. (1998) Budgetary and biogeochemical implications of N_2O isotope signatures in the Arabian Sea. **394**: 462–464.

Nausch, G., Feistel, R., Naumann, M., and Mohrholz, V. (2014) Water Exchange between the Baltic Sea and the North Sea, and conditions in the Deep Basins. In, *Baltic Sea Environment Fact Sheet*., p. online.

Nausch, G., Feistel, R., Umlauf, L., Nagel, K., and Siegel, H. (2008) Hydrographisch-chemische Zustandseinschätzung der Ostsee 2007. *Mar. Sci. Reports***72**: 1–93.

Needoba, J.A., Sigman, D.M., and Harrison, P.J. (2004) The mechanism of isotope fractionation during algal nitrate assimilation as illuminated by the $^{15}N/^{14}N$ of intracellular nitrate. *J. Phycol.***40**: 517–522.

Nestler, A., Berglund, M., Accoe, F., Duta, S., Xue, D.M., Boeckx, P., and Taylor, P. (2011) Isotopes for improved management of nitrate pollution in aqueous resources: review of surface water field studies. *Environ. Sci. Pollut. Res.***18**: 519–533.

Neumann, T. (2000) Towards a 3D-ecosystem model of the Baltic Sea. *J. Mar. Syst.***25**: 405–419.

Neumann, T., Fennel, W., and Kremp, C. (2002) Experimental simulations with an ecosystem model of the Baltic Sea: A nutrient load reduction experiment. *Global Biogeochem. Cycles***16**: 7–1–7–19.

Okubo, A. (1971) Oceanic diffusion diagrams. *Deep Sea Res. Oceanogr. Abstr.***18**: 789–802.

Osterblom, H., Hansson, S., Larsson, U., Hjerne, O., Wulff, F., Elmgren, R., and Folke, C. (2007) Human-induced trophic cascades and ecological regime shifts in the Baltic Sea. *Ecosystems***10**: 877–889.

Pagenkopf W (2001) Aktuelle Nährstoffbilanzierung für Teilgebiete des Einzugsgebiets der Warnow Geodaten Integration und Analyse, Berlin.

Parnell, A.C., Inger, R., Bearhop, S., and Jackson, A.L. (2010) Source partitioning using stable isotopes: coping with too much variation. *PLoS One***5**: e9672.

Paulmier, A. and Ruiz-Pino, D. (2009) Oxygen minimum zones (OMZs) in the modern ocean. *Prog. Oceanogr.***80**: 113–128.

Peierls, B.L., Caraco, N.F., Pace, M.L., and Cole, J.J. (1991) Human influence on river nitrogen. *Nature***350**: 386–387.

Pfenning, K. and McMahon, P. (1997) Effect of nitrate, organic carbon, and temperature on potential denitrification rates in nitrate-rich riverbed sediments. *J. Hydrol.***187**: 283–295.

Philippot, L. (2002) Denitrifying genes in bacterial and Archaeal genomes. *Biochim. Biophys. Acta***1577**: 355–76.

Piker, L., Schmaljohann, R., and Imhoff, J. (1998) Dissimilatory sulfate reduction and methane production in Gotland Deep sediments (Baltic Sea) during a transition period from oxic to anoxic bottom water (1993-1996). *Aquat. Microb. Ecol.***14**: 183–193.

Pilkaitytė, R. and Razinkovas, A. (2006) Factors controlling phytoplankton blooms in a temperate estuary: nutrient limitation and physical forcing. *Hydrobiologia***555**: 41–48.

Ploug, H. (2008) Cyanobacterial surface blooms formed by *Aphanizomenon sp*. and *Nodularia spumigena* in the Baltic Sea: Small-scale fluxes, pH, and oxygen microenvironments. *Limnol. Oceanogr.***53**: 914–921.

Ploug, H., Kiihl, M., Buchholz-cleven, B., and Jergensen, B.B. (1997) Anoxic aggregates - an ephemeral phenomenon in the pelagic environment? *Aquat. Microb. Ecol.***13**: 285–294.

Price, N.M., Harrison, G.I., Hering, J.G., Hudson, R.J., Nirel, P.M. V., Palenik, B., and Morel, F.M.M. (1989) Preparation and chemistry of the artificial algal culture medium Aquil. *Biol. Oceanogr.***6**: 443–461.

Rabalais, N.N. (2002) Nitrogen in Aquatic Ecosystems. *R. Swedish Acad. Sci.***31**: 102–112.

Radtke, H., Neumann, T., Voss, M., and Fennel, W. (2012) Modeling pathways of riverine nitrogen and phosphorus in the Baltic Sea. *J. Geophys. Res.***117**: C09024.

Reißmann, J.H. (2005) An algorithm to detect isolated anomalies in three-dimensional stratified data fields with an application to density fields from four deep basins of the Baltic Sea. *J. Geophys. Res.***110**: 1-18.

Reissmann, J.H., Burchard, H., Feistel, R., Hagen, E., Lass, H.U., Mohrholz, V., et al. (2009) Vertical mixing in the Baltic Sea and consequences for eutrophication - A review. *Prog. Oceanogr.***82**: 47–80.

Revsbech, N.P., Thamdrup, B., Dalsgaard, T., and Canfield, D.E. (2011) Construction of Stox oxygen sensors and their application for determination of O_2 concentrations in oxygen minimum zones. In, *Methods in Enzymology: Research on Nitrification and Related Processes, Vol 486, Part A*., pp. 325–341.

Roache, P. (1976) Computational Fluid Dynamics Hermosa Publisher, Albuquerque.

Rolff, C., Elmgren, R., and Voss, M. (2008) Deposition of nitrogen and phosphorus on the Baltic Sea: Seasonal patterns and nitrogen isotope composition. *Biogeosciences Discuss.***5**: 3013–3044.

Rönner, U. and Sörensson, F. (1985) Denitrification rates in the low-oxygen waters of the stratified Baltic Proper. *Appl. Environ. Microbiol.***50**: 801–806.

Ryabenko, E., Kock, A., Bange, H.W., Altabet, M.A., and Wallace, D.W.R. (2012) Contrasting biogeochemistry of nitrogen in the Atlantic and Pacific oxygen minimum zones. *Biogeosciences***9**: 203–215.

Saaltink, R., van der Velde, Y., Dekker, S.C., Lyon, S.W., and Dahlke, H.E. (2014) Societal, land cover and climatic controls on river nutrient flows into the Baltic Sea. *J. Hydrol. Reg. Stud.***1**: 44–56.

Santoro, A.E., Buchwald, C., McIlvin, M.R., and Casciotti, K.L. (2011) Isotopic signature of N_2O produced by marine ammonia-oxidizing Archaea. *Science.***333**: 1282–1285.

Santoro, A.E. and Casciotti, K.L. (2011) Enrichment and characterization of ammonia-oxidizing archaea from the open ocean: phylogeny, physiology and stable isotope fractionation. *ISME J.***5**: 1796–808.

Savchuk, O.P. (2005) Resolving the Baltic Sea into seven subbasins: N and P budgets for 1991–1999. *J. Mar. Syst.***56**: 1– 15.

Savchuk, O.P., Wulff, F., Hille, S., Humborg, C., and Pollehne, F. (2008) The Baltic Sea a century ago - a reconstruction from model simulations, verified by observations. *J. Mar. Syst.***74**: 485–494.

Schernewski, G. and Neumann, T. (2005) The trophic state of the Baltic Sea a century ago: a model simulation study. *J. Mar. Syst.***53**: 109–124.

Selman, M., Greenhalgh, S., Diaz, R., and Sugg, Z. (2008) Eutrophication and hypoxia in coastal areas: A global assessment of the state of knowledge Washington DC.

Sferratore, A., Billen, G., Garnier, J., Smedberg, E., Humborg, C., and Rahm, L. (2008) Modelling nutrient fluxes from sub-arctic basins: Comparison of pristine vs. dammed rivers. *J. Mar. Syst.***73**: 236–249.

Shearer, G., Schneider, D.J., and Kohl, H.D. (1991) Separating the efflux and influx components. *J. Gen. Microbiol.***137**: 1179–1184.

Sigman, D.M., Altabet, M.A., McCorkle, D.C., Francois, R., and Fischer, G. (2000) The $\delta^{15}N$ of nitrate in the Southern Ocean: Nitrogen cycling and circulation in the ocean interior. *J. Geophys. Res.***105**: 19599–19614.

Sigman, D.M., Casciotti, K.L., Andreani, M., Barford, C., Galanter, M., and Böhlke, J.K. (2001) A bacterial method for the nitrogen isotopic analysis of nitrate in seawater and freshwater. *Anal. Chem.***73**: 4145–4153.

Sigman, D.M., Granger, J., DiFiore, P.J., Lehmann, M.M., Ho, R., Cane, G., and Geen, A. van (2005) Coupled nitrogen and oxygen isotope measurements of nitrate along the eastern North Pacific margin. *Global Biogeochem. Cycles***19**: 1–14.

Silva, S.R., Kendall, C., Wilkison, D.H., Ziegler, A.C., Chang, C.C.Y., and Avanzino, R.J. (2000) A new method for collection of nitrate from fresh water and the analysis of nitrogen and oxygen isotope ratios. *J. Hydrol.***228**: 22–36.

Smethie, J. and William, M. (1987) Nutrient regeneration and denitrification in low oxygen fjords. *Deep Sea Res. Part A. Oceanogr. Res. Pap.***34**: 983–1006.

Spokes, L., Jickells, T., Weston, K., Gustafsson, B.G., Johnsson, M., Liljebladh, B., et al. (2006) MEAD: an interdisciplinary study of the marine effects of atmospheric deposition in the Kattegat. *Environ. Pollut.***140**: 453–62.

Stal, L.J., Albertano, P., Bergman, B., Bröckel, K. von, Gallon, J.R., Hayes, P.K., et al. (2003) BASIC: Baltic Sea cyanobacteria. An investigation of the structure and dynamics of water blooms of cyanobacteria in the Baltic Sea—responses to a changing environment. *Cont. Shelf Res.***23**: 1695–1714.

Stålnacke, P., Grimvall, A., Sundblad, K., and Tonderski, A. (1999) Estimation of riverine loads of nitrogen and phosphorus to the Baltic Sea, 1970-1993. *Environ. Monit. Assess.***58**: 173–200.

Stepanauskas, R., Jorgensen, N.O.G., Eigaard, O.R., Žvikas, A., Tranvik, L.J., and Leonardson, L. (2002) Summer inputs of riverine nutrients to the Baltic Sea: Bioavailability and eutrophication relevance. *Ecol. Monogr.***72**: 579–597.

Stramma, L., Johnson, G.C., Sprintall, J., and Mohrholz, V. (2008) Expanding oxygen-minimum zones in the tropical oceans. *Science***320**: 655–8.

Suikkanen, S., Hakanen, P., Spilling, K., and Kremp, a (2011) Allelopathic effects of Baltic Sea spring bloom dinoflagellates on co-occurring phytoplankton. *Mar. Ecol. Prog. Ser.***439**: 45–55.

Thomas, K.L., Lloyd, D., and Boddy, L. (1994) Effects of oxygen, pH and nitrate concentration on denitrification by *Pseudomonas* species. *FEMS Microbiol. Lett.***118**: 181–186.

Thunell, R.C., Sigman, D.M., Muller-Karger, F., Astor, Y., and Varela, R. (2004) Nitrogen isotope dynamics of the Cariaco Basin, Venezuela. *Global Biogeochem. Cycles***18**: 1–13.

Ulloa, O., Canfield, D.E., DeLong, E.F., Letelier, R.M., and Stewart, F.J. (2012) Microbial oceanography of anoxic oxygen minimum zones. *Proc. Natl. Acad. Sci. U. S. A.***109**: 15996–6003.

Vahtera, E., Conley, D.J., Gustafsson, B.G., Kuosa, H., Pitkänen, H., Savchuk, O.P., et al. (2007) Internal ecosystem feedbacks enhance nitrogen-fixing cyanobacteria blooms and complicate management in the Baltic Sea. *Ambio***36**: 186–94.

Vahtera, E., Laanemets, J., Pavelson, J., Huttunen, M., and Kononen, K. (2005) Effect of upwelling on the pelagic environment and bloom-forming cyanobacteria in the western Gulf of Finland, Baltic Sea. *J. Mar. Syst.***58**: 67–82.

Velinsky, D.J., Pennock, J.R., Sharp, J.H., Cifuentes, L.A., and Fogel, M.L. (1989) Determination of the isotopic composition of ammonium-nitrogen at the natural abundance level from estuarine waters. *Mar. Chem.***26**: 351–361.

Villnäs, A., Norkko, J., Hietanen, S., Josefson, A., Lukkari, K., and Norkko, A. (2013) The role of recurrent disturbances for ecosystem multifunctionality. *Ecology***94**: 2275–2287.

Vitousek, P.M., Aber, J.D., Howarth, R.W., Likens, G.E., Matson, P.A., Schindler, D.W., et al. (1997) Human alteration of the global nitrogen cycle: Sources and consequences. *Ecol. Appl.***7**: 737–750.

Voss, M., Deutsch, B., Elmgren, R., Humborg, C., Kuuppo, P., Pastuszak, M., et al. (2006) Source identification of nitrate by means of isotopic tracers in the Baltic Sea catchments. *Biogeosciences***3**: 663–676.

Voss, M., Dippner, J.W., Humborg, C., Hürdler, J., Korth, F., Neumann, T., et al. (2011) History and scenarios of future development of Baltic Sea eutrophication. *Estuar. Coast. Shelf Sci.***92**: 307–322.

Voss, M., Dippner, J.W., and Montoya, J.P. (2001) Nitrogen isotope patterns in the oxygen-deficient waters of the Eastern Tropical North Pacific Ocean. *Deep. Res. I***48**: 1905–1921.

Voss, M., Emeis, K.-C., Hille, S., Neumann, T., and Dippner, J.W. (2005) Nitrogen cycle of the Baltic Sea from an isotopic perspective. *Global Biogeochem. Cycles***19**:

Wankel, S.D., Kendall, C., Francis, C.A., and Paytan, A. (2006) Nitrogen sources and cycling in the San Francisco Bay Estuary: A nitrate dual isotopic composition approach. *Limnol. Oceonography***51**: 1654–1664.

Wankel, S.D., Kendall, C., and Paytan, A. (2009) Using nitrate dual isotopic composition ($\delta^{15}N$ and $\delta^{18}O$) as a tool for exploring sources and cycling of nitrate in an estuarine system: Elkhorn Slough, California. *J. Geophys. Res.***114**: 1–15.

Wankel, S.D., Kendall, C., Pennington, J.T., Chavez, F.P., and Paytan, A. (2007) Nitrification in the euphotic zone as evidenced by nitrate dual isotopic composition: Observations from Monterey Bay, California. *Glob. Biogeochem. Cycles***21**: GB2009.

Ward, B.B. (2013) Oceans. How nitrogen is lost. *Science***341**: 352–3.

Ward, B.B., Devol, A.H., Rich, J.J., Chang, B.X., Bulow, S.E., Naik, H., et al. (2009) Denitrification as the dominant nitrogen loss process in the Arabian Sea. *Nature***461**: 78–U77.

Waser, N.A., Yin, K., Yu, Z., Tada, K., Harrison, P.J., Turpin, D.H., and Calvert, S.E. (1998) Nitrogen isotope fractionation during nitrate, ammonium and urea uptake by marine diatoms and coccolithophores under various conditions of N availability. *Mar. Ecol. Prog. Ser.***169**: 29–41.

Waser, N.A., Yu, Z., Yin, K., Nielsen, B., Harrison, P.J., Turpin, D.H., and Calvert, S.E. (1999) Nitrogen isotopic fractionation during a simulated diatomspring bloom: importance of N-starvation in controlling fractionation. *Mar. Ecol. Prog. Ser.* 291–296.

Wasmund, N., Nausch, G., and Matthäus, W. (1998) Phytoplankton spring blooms in the southern Baltic Sea—spatio-temporal development and long-term trends. *J. Plankton Res.***20**: 1099–1117.

Wasmund, N., Pollehne, F., Postel, L., Siegel, H., and Zettler, M.L. (2011) Biologische Zustandseinschätzung der Ostsee im Jahre 2010. *Mar. Sci. Reports* 1–176.

Wasmund, N., Voss, M., and Lochte, K. (2001) Evidence of nitrogen fixation by non-heterocystous cyanobacteria in the Baltic Sea and re-calculation of a budget of nitrogen fixation. **214**: 1–14.

Wellman, R.P., Cook, F.D., and Krouse, H.R. (1968) Nitrogen-15: Microbiological Alteration of Abundance. *Science.***161**: 269–270.

Wenk, C.B., Blees, J., Zopfi, J., Veronesi, M., Bourbonnais, A., Schubert, C.J., et al. (2013) Anaerobic ammonium oxidation (anammox) bacteria and sulfide-dependent denitrifiers coexist in the water column of a meromictic south-alpine lake. *Limnol. Oceanogr.***58**: 1–12.

Wenk, C.B., Zopfi, J., Blees, J., Veronesi, M., Niemann, H., and Lehmann, M.F. (2014) Community N and O isotope fractionation by sulfide-dependent denitrification and anammox in a stratified lacustrine water column. *Geochim. Cosmochim. Acta***125**: 551–563.

Widdel, F. and Bak, F. (1992) Gram-negative mesophilic sulfate-reducing bacteria. In, Balows,T.H.G., Dworkin,A.M., Harder,W., and Schleifer,K.H. (eds), *The Prokaryotes*. Springer, New York, pp. 3353–3378.

Wu, J., Calvert, S.E., and Wong, C.S. (1997) Nitrogen isotope variations in the subarctic northeast Pacific: relationships to nitrate utilization and trophic structure. *Deep Sea Res. Part I Oceanogr. Res. Pap.***44**: 287–314.

Wunderlich, A., Meckenstock, R., and Einsiedl, F. (2012) Effect of different carbon substrates on nitrate stable isotope fractionation during microbial denitrification. *Env. Sci Technol***46**: 4861–4868.

Xue, D., De Baets, B., Van Cleemput, O., Hennessy, C., Berglund, M., and Boeckx, P. (2013) Classification of nitrate polluting activities through clustering of isotope mixing model outputs. *J. Environ. Qual.***42**: 1486–97.

Xue, D., De Baets, B., Van Cleemput, O., Hennessy, C., Berglund, M., and Boeckx, P. (2012) Use of a Bayesian isotope mixing model to estimate proportional contributions of multiple nitrate sources in surface water. *Environ. Pollut.***161**: 43–9.

Yang, L., Han, J., Xue, J., Zeng, L., Shi, J., Wu, L., and Jiang, Y. (2013) Nitrate source apportionment in a subtropical watershed using Bayesian model. *Sci. Total Environ.***463-464**: 340–7.

Yoshida, N. (1988) ^{15}N-depleted N_2O as a product of nitrification. *Nature***335**: 528–529.

Zumft, W.G. (1997) Cell biology and molecular basis of denitrification. *Microbiol. Mol. Biol. Rev.***61**: 533–616.

List of figures

Introduction

Chapter 1

Chapter2

List of tables

List of Abbreviation

AMZ - **A**noxic **m**arine **z**one

Anammox - **A**naerobic **A**mmonium **O**xidation

AOA – **A**mmonium **o**xidizing **a**rchaea

AOB – **A**mmonium **o**xidizing **b**acteria

CARD - **Ca**talyzed **r**eporter **d**eposition

CTD – **C**onductivity, **T**emperature and **D**ensity

DAPI - 4',6-**D**i**A**midino-2-**P**heny**l**Indol

DIN - **D**issolved **I**norganic **N**itrogen

ETNP - **E**astern **T**ropical **N**orth **P**acific

ETSP - **E**astern **T**ropical **S**outh **P**acific

FISH - **F**luorescence **I**n **S**itu **H**ybridization

GB - **G**otland **B**asin

GC - **G**as **C**hromatography

IAEA - **I**nternational **A**tomic **E**nergy **A**gency

IRMS - **I**sotope **R**atio **M**ass **S**pectrometer

MQ - **M**illi **Q** (destilled and filtered water)

Nap - Periplasmic nitrate reductase

Nar - Membrane bound nitrate reductase

N – **N**itrogen

N_2 – Molecular **N**itrogen

N_2O - **N**itrous **o**xide

NH_4^+ - Ammonium

NO_3^- - Nitrate

NO_2^- Nitrite

ODZ - **O**xygen **d**eficient **z**one

PMF - **P**roton **M**otoric **F**orce

PON - **P**articulate **O**rganic **N**itrogen

TN – **T**otal **N**itrogen

USGS - **U**. **S**. **G**eological **S**urvey

VSMOW - **V**ienna **s**tandard **m**ean **o**cean **w**ater

Acknowledgement

I am grateful to my supervisor PD Dr. Maren Voss, who gave me the chance to do this PhD thesis at the Leibniz Institute for Baltic Sea Research. Your excellent mentoring, helpful discussions and the possibility to attend to international conferences helped me to get ideas and keep the focus. The participation in the EU+ project HYPER gave me the chance to cooperate with Dr. Susanna Hietanen, which has been a pleasure. I feel very grateful for her input, additional support and the chance to visit her and her working group at Helsinki University. I felt always welcome and Susanna, Dana Helleman and Tom Jilbert made my stay unforgettable. The collaboration with PD Dr. Joachim W. Dippner has broaden my understanding about physical oceanography and the application of numerical models. I want to thank all the members of my thesis committee for their encouraging discussions.

I am grateful to my whole working group, in its present and past configurations, for fruitful discussion, advice, assistance and the many needed breaks for coffee, chocolate and some cake. Here, special thanks is given to Iris Liskow, who instructed me in stable isotope analysis and who's technical assistance was very valuable over the years. Frederike Korth always supported me when I needed advice or just someone to talk to. I always enjoyed the train rides in the morning and our lunch breaks on the comfortable couch.

Thanks to the help of Matthias Labrenz, Klaus Jürgens and Bärbel Buck, who gave me the chance to work with the culture *Sulfurimonas gotlandica*and who were never tired giving me new advices when things did not work out the way they were supposed to.

Furthermore, I would like to thank all my co-authors of the publications which were part of this thesis: Maren Voß, Joachim Dippner, Susanna Hietanen, Klaus Jürgens, Matthias Labrenz, Frederike Korth, Barbara Deutsch, and Claudia Moros.

I thank the DAAD for sponsoring me to go to the Oceans Science Meeting in Honolulu, Hawaii.

I also want to thank all the people, who accompanied me during my studies, supporting and encouraging me.

Most importantly I want to thank my family and my partner Benni for their love, support, patience and encouragement in hard times, which made this thesis possible.

Supplemental material

Chapter 1

Table S1: Overview of the sampling stations (location and selected chemical parameters).

Area	Date	Latitude	Longitude	Salinity	$NO_3^-+NO_2^-$ [µMol]	$\delta^{15}N$ (‰)	$\delta^{18}O$ (‰)
Western Baltic Sea	11.02.2008	12,4498	54,6503	8,87	3,79	4,8	3,4
	11.02.2008	12,7056	54,6959	9,22	3,81	4,3	3,5
	11.02.2008	13,0583	54,7950	8,51	4,26	4,7	4,4
	11.02.2008	13,2770	54,8598	8,20	2,71	5,0	5,2
	12.02.2008	13,9460	54,7099	7,73	2,81	4,7	3,0
	12.02.2008	13,9886	55,0624	7,73	3,04	5,0	3,1
	12.02.2008	14,1578	54,0763	5,98	46,25	8,0	1,8
	12.02.2008	14,2827	54,6338	7,74	2,97	3,9	0,0
Baltic Proper	25.02.2009	15,5695	55,5169	7,76	2,80	3,3	4,5
	25.02.2009	17,5808	57,2238	7,1	3,44	1,5	-0,9
	26.02.2009	17,3519	57,7003	7,01	3,52	3,1	0,1
	26.02.2009	18,2335	58,5837	6,45	3,79	2,0	-0,4
	26.02.2009	19,8832	59,7502	5,65	3,70	2,5	-0,8
	12.02.2008	14,5376	55,4046	7,71	3,13	4,4	-0,8
	13.02.2008	14,7156	55,4659	7,68	3,23	3,9	0,3
	13.02.2008	15,3344	55,3835	7,51	3,07	3,6	-0,4
	13.02.2008	15,6326	55,4564	7,48	2,95	3,5	0,0
	13.02.2008	15,9834	55,2501	7,62	3,54	4,0	-1,0
	19.02.2008	15,9837	55,2498	7,64	3,27	4,3	-1,1
	19.02.2008	17,0665	55,2168	7,45	3,24	3,5	-1,0
	19.02.2008	18,2351	55,3266	7,37	2,91	3,4	-1,6
	19.02.2008	18,4013	55,5502	7,34	2,61	4,0	-1,6
	18.02.2008	18,6002	55,6339	7,37	2,76	3,8	-1,3
	18.02.2008	18,8658	55,8413	7,37	2,88	4,8	1,6
	18.02.2008	19,1677	56,0841	7,37	2,71	4,3	2,0
	18.02.2008	19,5833	56,6334	7,34	3,46	3,8	-1,7
	18.02.2008	19,8289	57,0713	7,34	3,34	3,4	-2,0
	16.02.2008	20,0506	57,3196	7,35	3,38	2,6	-2,7
Gulf of Finnland	04.03.2009	24,8500	59,8036	5,24	6,82	4,1	-0,2
	04.03.2009	25,6325	59,8659	5,09	8,12	6,4	-1,4
	04.03.2009	23,9989	59,6836	5,35	8,77	6,6	-1,4
	04.03.2009	22,9002	59,4836	6,11	6,95	6,4	-1,5
Gulf of Bothnia	27.02.2009	19,1177	60,1913	5,42	3,10	2,9	0,7
	27.02.2009	19,1464	60,6967	5,45	3,81	2,9	-1,1
	27.02.2009	19,2836	61,2265	5,54	3,96	5,8	-0,1
	27.02.2009	19,4678	61,7032	5,57	3,40	2,4	-1,1

	27.02.2009	19,7182	62,1441	5,45	3,49	3,2	-1,8
	28.02.2009	19,9682	62,5872	5,52	3,66	1,8	-2,2
	28.02.2009	20,4862	63,0417	5,54	4,31	4,0	-0,7
	20.11.2011	21,584	63,834	3,1	5,53	1,83	-2,79
Southern Rivers	15.11.2009	21,38187	55,30128	0	145,03	10,0	1,5
	01.12.2009	21,38187	55,30128	0	179,18	9,0	1,3
	07.12.2009	21,13293	55,69043	0	114,87	10,0	1,7
	22.02.2010	21,13293	55,69043	0	140,47	8,8	1,3
	17.01.2003	12,1429	54,03246	0	259,00	8,2	6,5
	13.02.2003	12,1429	54,03246	0	135,00	9,3	6,5
Northern rivers	11.11.2009	22,8415	65,9335	0	7,41	1,6	10,6

Chapter 2

Text S2. Sensitivity of Dirichlet boundary conditions

In this section we demonstrate that the isotopic enrichment factor is not sensitive to the choice of the boundary condition at x_0. The boundary is shifted to f=0.8 (f is the ratio of nitrate concentration at a given time point divided by the initial nitrate concentration) from Fig. 17b with the corresponding boundary conditions of 4.4 µmol L^{-1} for NO_3 concentration with $\delta^{15}N_{NO3}$ = 8‰. This nitrate concentration corresponds to a decrease in the upper boundary of the denitrification zone from 20 µmol L^{-1} oxygen concentration down to 10µmol L^{-1} oxygen concentration. If the initial NO_3 concentration is lower, than the actual consumption is lower for the same change in $\delta^{15}N_{NO3}$. Under these settings, the model simulation is still in good agreement with observations if the denitrification rate in the model is reduced from 14 nmol N L^{-1} d^{-1} to 11.2 nmol N L^{-1} d^{-1} (Fig. sf1). A further adjustment of eddy diffusivity and isotopic enrichment factor was not necessary probably because of the relatively narrow range of meaningful parameters. By changing this boundary condition it is not necessary to change the fractionation factor, representing how robust this assumption is.

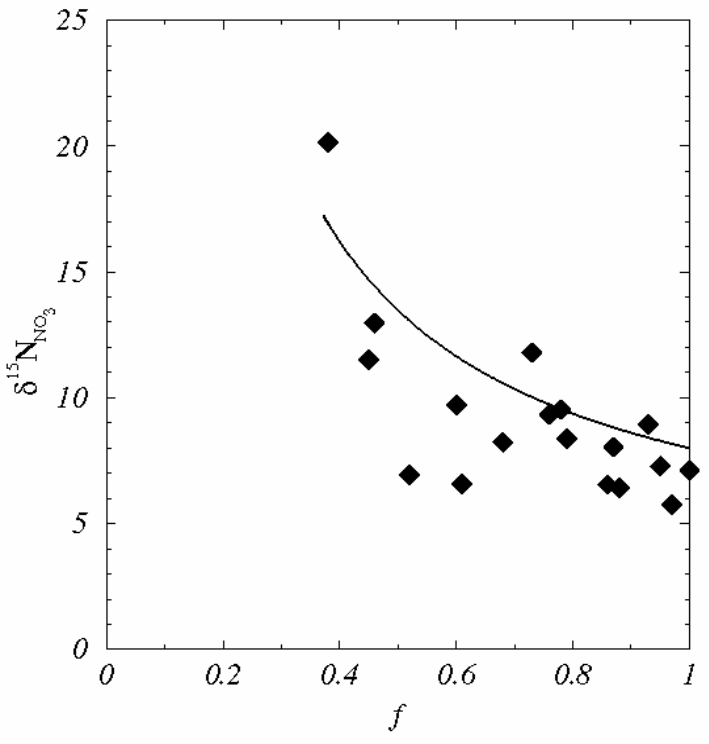

Supporting figure sf 1: Result of sensitivity test for Dirichlet boundary conditions

Text S3 Sensitivity test of model parameters

The presented model has six parameters (please see main text). Some were directly derived from observations, some were estimated. To demonstrate the response of a non-linear model for three estimated parameters a sensitivity analysis is presented for the coefficient of eddy diffusivity, the isotopic enrichment factor, and the denitrification rate.

1. Eddy diffusivity

The estimated value of the coefficient of eddy diffusivity was 600 m^2s^{-1}. A variation of ±5%, i.e. 570 m^2s^{-1} and 630 m^2s^{-1}, indicates two things: firstly, the model simulation is in good agreement with observations in a very narrow band of ±5%. Secondly, eddy diffusivity only influenced the length of the simulated curve (Fig. sf2). A test with a much higher eddy diffusivity of 900 m^2s^{-1} produced unrealistic results such that the influence of horizontal diffusion is too strong and denitrification is suppressed, which is indicated by a weak fractionation. In a further test an eddy diffusivity of 300 m^2s^{-1} was used. In this case, the model became numerically unstable.

2. Isotopic enrichment factor

The model estimate for the isotopic enrichment factor of denitrification was -1.9‰. A slight variation of this value by only ±0.5‰ indicates - similar to the eddy diffusivity - that the range of valid parameters is very narrow. In contrast to the eddy diffusivity, the variation of the isotopic enrichment factor influences the slope of the simulated curve (Fig. sf3). Another test with a much higher isotopic enrichment factor of -5‰ produced unrealistic results and the curve did not match the data points (Fig. sf3).

3. Denitrification rates

The best simulation through the data of $\delta^{15}N_{NO3}$ was used, to receive a denitrification rate from our stable isotope data. The model estimate for the denitrification rate was 14 nmol N L^{-1} d^{-1} and therefore lower than published rates of denitrification (Hietanen et al., 2012). A slight variation of the denitrification rate of ± 10% already indicated that only a small range of valid parameters exists, similar to eddy diffusivity and isotopic enrichment factors. This is because the denitrification rate is the most sensitive parameter in the model. It influences both, the length and the slope of the simulated curve (Fig. sf4). A reduction of denitrification

rate by 20% produced unrealistic model results. An increase by 20% caused numerical unstable model results.

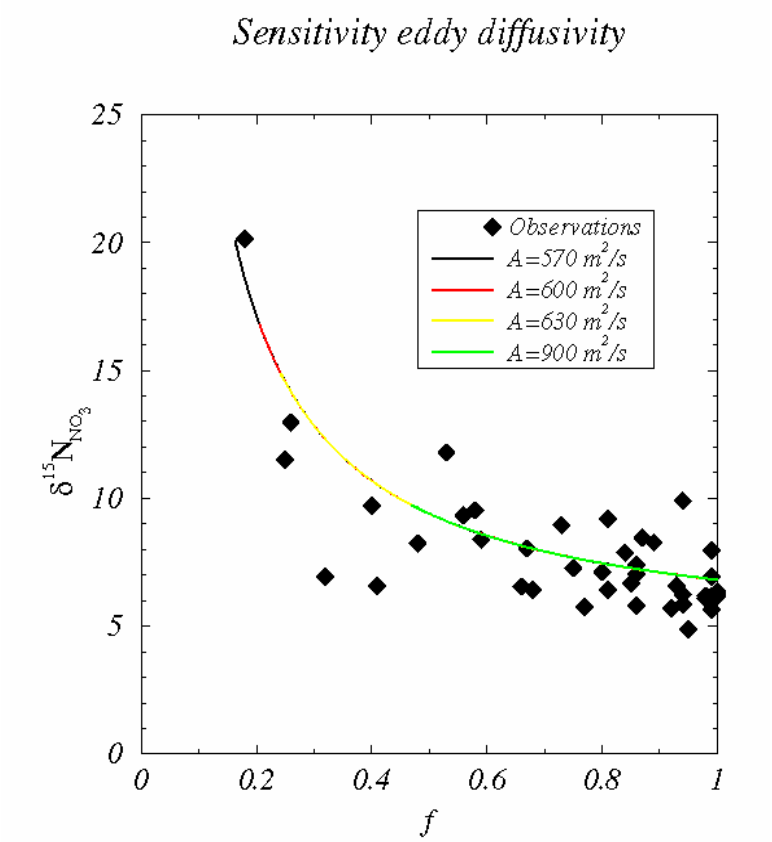

Supporting figure sf 2: Results of sensitivity test for 4 different coefficients of eddy diffusivity

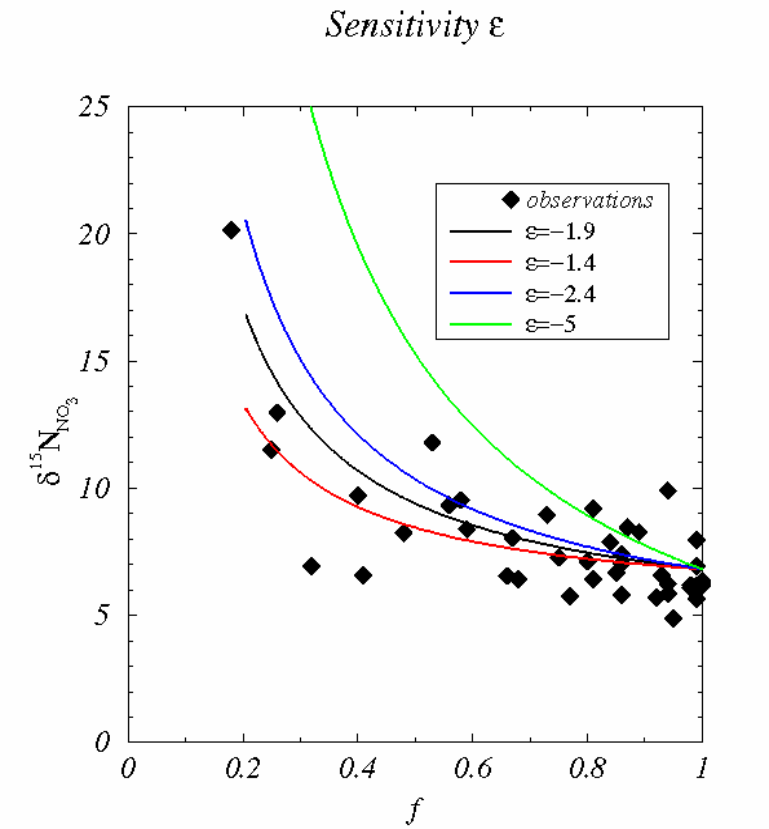

Supporting figure sf 3: Results of sensitivity test for 4 different isotopic enrichment factors

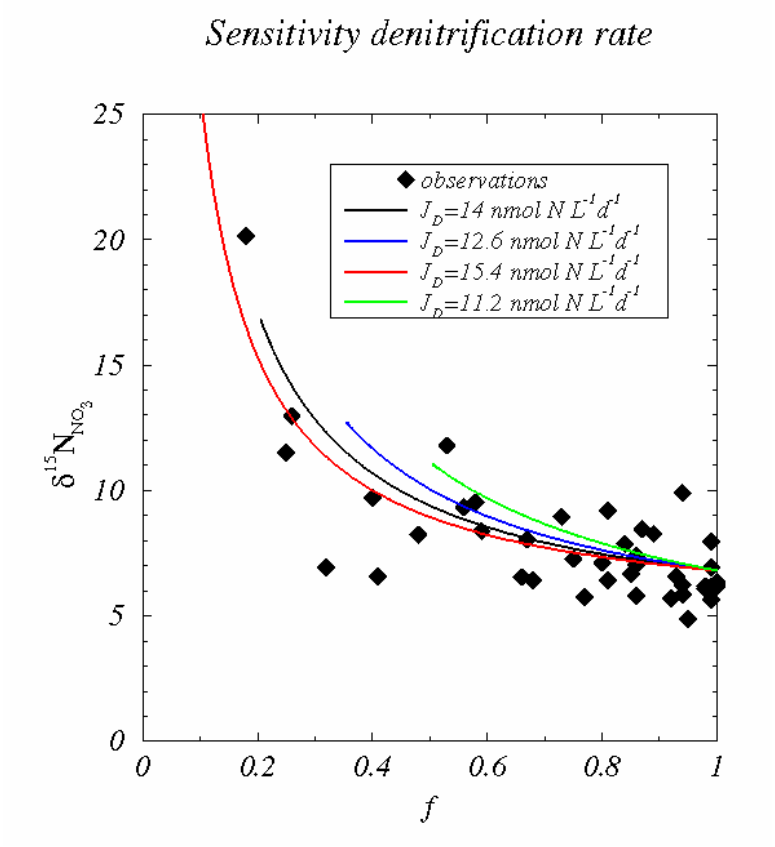

Supporting figure sf 4: Results of sensitivity test for 4 different denitrification rates

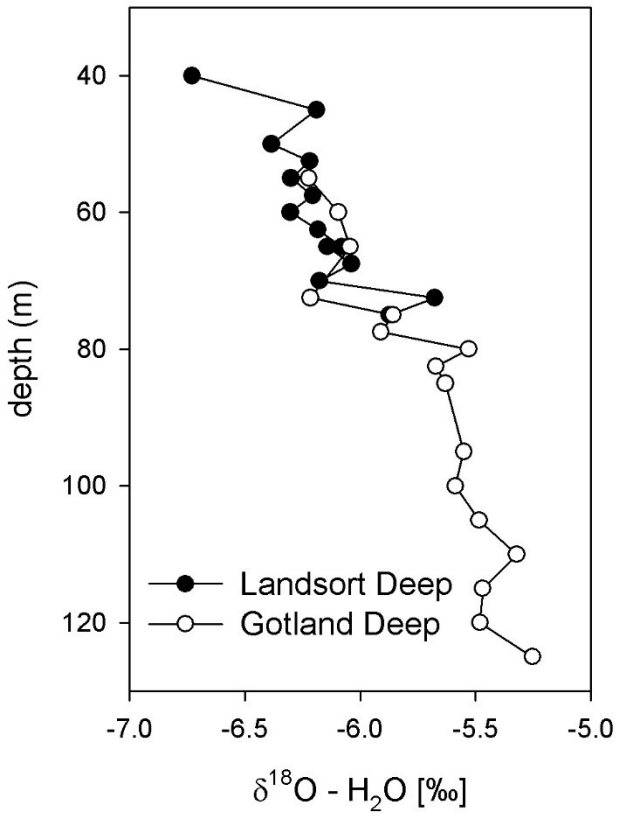

Supporting figure sf 5: Two depth profiles of $\delta^{18}O_{H2O}$ sampled in 2010 at the Landsort and Gotland Deep. 12 mL water were filtered and frozen at -20°C until analysis. The average $\delta^{18}O_{H2O}$ was -6.0 ± 0.4 ‰. Measurements were done in courtesy of U. Struck, Leibniz Institute for Research on Evolution and Biodiversity

Chapter 3

Text S4 Impact of Nap-catalyzed denitrification on the $\delta^{18}O$:$\delta^{15}N$ ratio in nitrate

Functions of the subunits of Nap

The presence and composition of the gene cluster *napAGHBFLD*, encoding the respiratory enzyme Nap, are similar in free-living denitrifying Epsilonproteobacteria(Kern and Simon, 2009). NapA and NapB are two highly conserved catalytic subunits. The former, which constitutes, the large subunit, contains a molybdenum cofactor and a [4Fe-4S] cluster. The latter is a c-type cytochrome(Moreno-Viviàn et al., 1999). In most denitrifying bacteria (e.g., *Pseudomonas sp.* strain G-179, *E. coli*, *R. spaeroides* DSM 158, *Thiosphaera pantotropha*), the structural gene *napC*, encoding a membrane-bound cytochrome C, is thought to be responsible for electron transfer from the quinol pool to the catalytic complex napAB(Bedzyk et al., 1999; Moreno-Viviàn et al., 1999; Philippot, 2002); but in all Epsilonproteobacteria, including *S. gotlandica*, napC is lacking(Kern and Simon, 2009; Grote et al., 2012). In *S. gotlandica*, proteins encoded by other structural genes may accomplish electron flow between the cell membrane and periplasm. In other Epsilonproteobacteria, the *napGH* complex is responsible for the generation of a proton-motive force (PMF) allowing ATP generation(Kern and Simon, 2009). We can only speculate that this is also the case in *S. gotlandica*.

Declaration of authorship/ Selbstständigkeitserklärung

The opportunity for this doctoral project has not been conveyed to me commercially. In particular, I did not engage an organization that, for a fee, seeks supervisors for the preparation of dissertations. Nor did I engage an organization to, in whole or in part, take care of incumbent obligations with regard to the examinations for me.

I hereby declare that I produced the present thesis independently and without external help. I did not use any auxiliary materials or sources other than the ones indicated and passages used literally or with regards to content have been declared as such.

Die Gelegenheit zum vorliegenden Promotionsvorhaben ist mir nicht kommerziell vermittelt worden. Insbesondere habe ich keine Organisation eingeschaltet, die gegen Entgelt Betreuerinnen/ Betreuer für die Anfertigung von Dissertationen sucht oder die mir obliegenden Pichten hinsichtlich der Prüfungsleistungen für mich ganz oder teilweise erledigt.

Ich versichere hiermit an Eides statt, dass ich die vorliegende Arbeit selbstständig angefertigt und ohne fremde Hilfe verfasst habe. Dazu habe ich keine außer den von mir angegebenen Hilfsmitteln und Quellen verwendet und die den benutzten Werken inhaltlich und wörtlich entnommenen Stellen habe ich als solche kenntlich gemacht.

.....

Date/ Datum Signature/ Unterschrift